JAIST Repository
https://dspace.jaist.ac.jp/

Title	チーグラー・ナッタ触媒を用いた官能基化によるポリプロピレンの物性改良
Author(s)	永井，健
Citation	
Issue Date	2017-03
Type	Thesis or Dissertation
Text version	ETD
URL	http://hdl.handle.net/10119/14261
Rights	
Description	Supervisor:寺野　稔，マテリアルサイエンス研究科，博士

JAIST
JAPAN
ADVANCED INSTITUTE OF
SCIENCE AND TECHNOLOGY

Japan Advanced Institute of Science and Technology

Improvement of physical properties of polypropylene through functionalization with Ziegler-Natta catalyst

TAKESHI NAGAI

Japan Advanced Institute of Science and Technology

Improvement of physical properties of polypropylene through functionalization with Ziegler-Natta catalyst

by

Takeshi Nagai

Submitted to

Japan Advanced Institute of Science and Technology

In partial fulfillment of the requirements

For the degree of

Doctor of Philosophy

Supervisor: Professor Dr. Minoru Terano

School of Materials Science
Japan Advanced Institute of Science and Technology

March 2017

Referee-in-chief: **Professor Dr. Minoru Terano**
Japan Advanced Institute of Science and Technology

Referees: **Professor Dr. Donglin Jiang**
Japan Advanced Institute of Science and Technology

Associate Professor Dr. Toshiaki Taniike
Japan Advanced Institute of Science and Technology

Associate Professor Dr. Kazuaki Matsumura
Japan Advanced Institute of Science and Technology

Professor Dr. Katsuhisa Tokumitsu
The University of Shiga Prefecture

Preface

The present dissertation is the result of the studies under the direction of Professor Dr. Minoru Terano during 2013-2017. The purpose of this dissertation is to investigate the effect of functionalization of polypropylene on physical properties through polymerization with Ziegler-Natta catalyst.

The first chapter shows a general introduction according to the object of this research. Chapter 2 describes the effect of a small amount of aromatic functional group on crystallization behavior of polypropylene. Chapter 3 describes improvement of physical properties of polypropylene with a small amount of reactive functional group. Chapter 3 describes physical properties of polypropylene nanocomposites prepared from polypropylene containing a small amount of reactive functional groups. The last chapter concludes this dissertation.

Takeshi Nagai

Terano Laboratory,

School of Materials Science,

Japan Advanced Institute of Science and Technology

March 2017

Contents

Chapter 1

General Introduction

1-1. Polypropylene

The demand for plastics has reached 245 million tons annually, and is continuing to grow dramatically. Figure 1 shows the demand for plastics in 2006 [1]. Commodity plastics, namely polyethylene (PE), polypropylene (PP), polyvinyl chloride (PVC), polystyrene (PS) and polyethylene terephthalate (PET) account for 90% of the total. Among those, PP is one of the plastics with the highest demand.

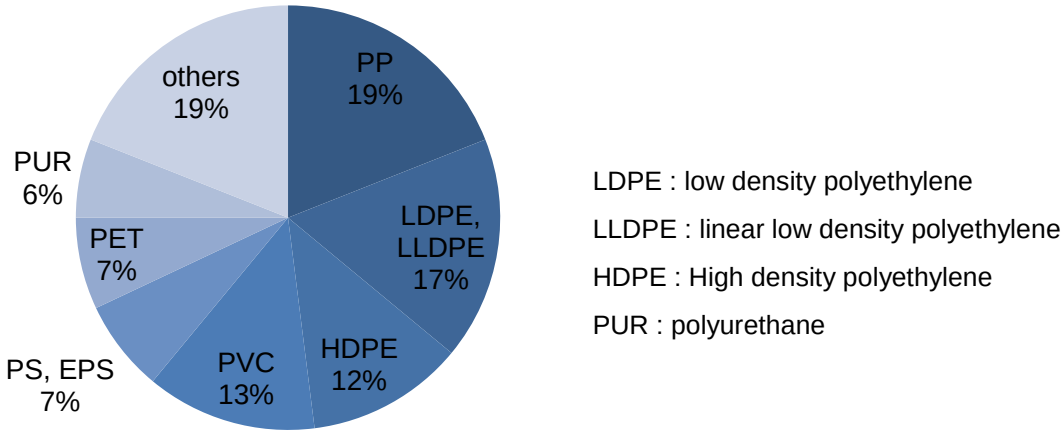

Figure 1. World plastics demand by resin types 2006 [1].

Various petrochemical products are synthesized using propylene as raw material, and as shown in Figure 2, approximately two-thirds of propylene is consumed to synthesize PP [2]. That illustrates how extensive the demand for PP is. Steam cracking of naphtha, the gasoline refining process, and propane dehydrogenation technology are the three means of obtaining propylene [3].

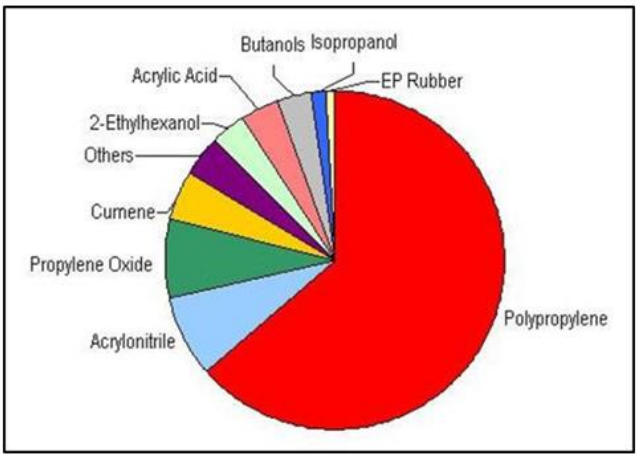

Figure 2. Global propylene consumption [1].

Polypropylene has good chemical resistance and balance of physical properties, and, at approximately 0.90 g/cm^3, the lowest density among thermoplastic resins. It also lends itself well to many molding processes, including injection molding and extrusion molding. Such excellent properties led to the rapid spread of polypropylene to many industrial applications, and it has made an especially enormous impact in the automotive field. Reducing the amount of fuel consumed by automobiles is important both from an environmental standpoint and in terms of economic benefits for users, and reducing vehicle weight is one of the most direct ways of doing so. PP is one of the lightest available materials, and automakers favor using more of it in product development. Several interior and exterior parts are made entirely of PP. Interior doors, pillars, panels and consoles are all PP molded products. PP also plays a major role in automobile exterior products, serving as the basis for bumpers. In addition, PP is used in rocker panels and the grille of some vehicles [4]. Injection molding is used to form the majority of automobile parts. As shown in Figure 3, a 2005 survey has indicated that injection molding is the most common application of polypropylene worldwide [5]. The injection

molding process involves melting the polymer pellets and then pouring them into a closed mold. After that, the polymer is cooled and solidifies in the mold. Food containers, toys, sports goods, as well as jar and bottle caps are PP products. It also has medical applications, such as disposable syringes [4].

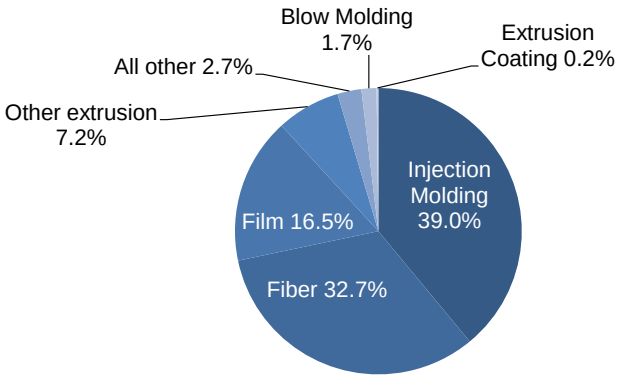

Figure 3. Global consumption of polypropylene by end use application [1].

1-2. Primary structure of polypropylene

The performance of PP based on control of the primary structure has been carried out through a considerable amount of research on synthesis catalysts, especially ZN catalysts, as well as through research on the synthesis process using ZN catalysts. This study focuses on ZN catalysts.

1-2-1. Tacticity

Stereoregularity is one of the important elements of the primary structure. Propylene contains diastereomer structures based on the absolute configuration of the tertiary carbon in the main chain. As shown in Figure 4, methyl groups can all bond in the same direction, a structure described as isotactic, where the asymmetric carbon has the same absolute configuration, in alternating directions (syndiotactic), or randomly, in a structure called atactic. The ensuing stereoregularity is known as tacticity. Two adjacent monomer units with the same absolute configuration in the asymmetric carbon are meso diads, while units with an opposite absolute configuration are racemo diads, which are represented as *m* and *r*, respectively.

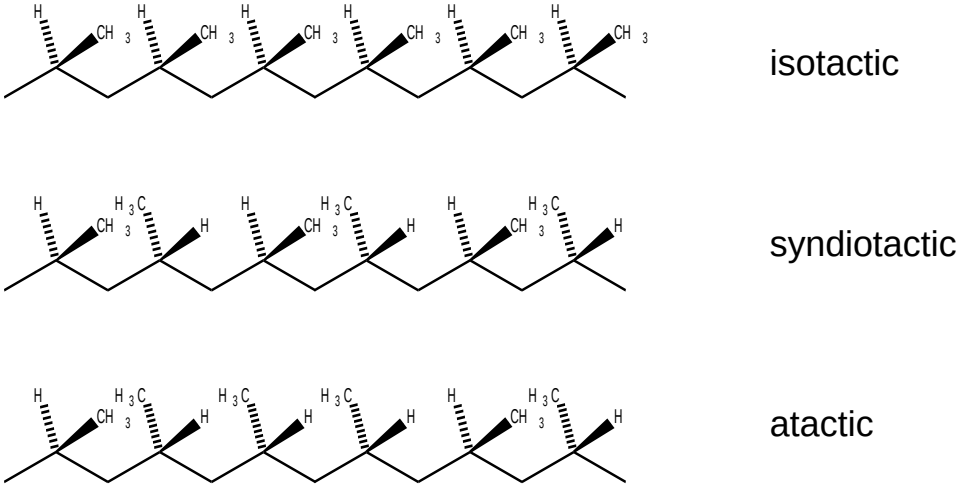

Figure 4. Stereo configuration of polypropylene.

1-2-2. Development of the primary structure

Ziegler was the first to discover that a $TiCl_4/AlR_3$ mixture had the ability to induce the polymerization ethylene [6]. In 1954, Natta used the same catalyst system and became the first to successfully synthesize PP with a 30 to 40% isotactic content [7]. After that, Natta *et al.* immediately achieved the synthesis of PP with a 90% isotactic content using a $TiCl_3/AlEt_2Cl$ catalyst [8]. However, since they were only able to synthesize a mere 1 kg of PP for each gram of catalyst and the extremely low catalytic activity, and the low stereoregularity of 90% indicated a need to remove catalyst residue and separate atactic polymers, the manufacturing of PP also involved issues of limited productivity, process complexity, and cost increases.

In 1972, Solvay succeeded at obtaining porous $TiCl_3$ with an extremely large specific surface area by causing $TiCl_4$ to react with $TiCl_3$ prepared by an aluminum reduction reaction and subsequently subjected to an ether treatment [9]. This increased $TiCl_3$

activity approximately tenfold over previous attempts while successfully raising PP stereoregularity to 95%.

A supported catalyst was developed using a simple substance featuring a large surface area and a surface that contained functional groups capable of bonding chemically with transition metal compounds, and it was found that $MgCl_2$, in particular, manifested superb activity as a simple substance [10]. The $MgCl_2$ improved both the concentration and activity of the Ti species [11]. However, the low stereoregularity of the resulting PP was a problem, and its use was originally limited to the synthesis of PE. For PP, not only productivity, but also stereoregularity are important. Further research to improve PP stereoregularity led to the development of a high activity, high stereospecificity catalyst using a Lewis base referred to as an internal donor [12]. These high activity and stereospecificity obtained by co-grinding $MgCl_2$, $TiCl_4$ and a Lewis base compound referred to as an internal donor were used in conjunction with a trialkylaluminum compound as a co-catalyst and a second Lewis base compound referred to as an external donor. In 1978, an ethyl benzoate and methyl *p*-toluate combination was used at Montedison. Despite exhibiting a high degree of catalytic activity that made it virtually unnecessary to wash the catalyst residue, in many cases it still required the removal of 6 to 10% of the generated atactic polymers [13].

High activity, high stereoselectivity catalysts were subsequently achieved through efficient catalyst preparation methods and optimal donor combinations, enabling the synthesis of sufficient polymers requiring virtually no deliming or atactic polymer removal [14,15]. A catalyst using an alkyl phthalate compound as an internal donor and an alkoxysilane compound as an external donor was reported to enable the highly efficient synthesis of PP with isotactic content of 95% or higher in the early 1980s [16].

In the latter half of that decade, a catalyst using 1,3-diether as an internal donor was developed, and this catalyst was capable of manifesting high activity and isotacticity without an external donor [17].

1-2-3. Structure of the $MgCl_2$ supported ZN catalyst

The $MgCl_2$ supported ZN catalyst has bonded $MgCl_2$ simple substance and Ti, with the structure shown in Figure 5, and is used in conjunction with an organic aluminum compound called a co-catalyst that causes a reduction in the Ti in the $TiCl_4$ to the trivalent state. The Ti species resulting from the reduction become the active species.

Donors are considered to play several different roles: 1. Activation of the $MgCl_2$ simple substance during catalyst preparation. 2. Change the Ti species distribution on the simple substance by blocking the low stereoregularity active sites on the surface of the simple substance. 3. Poison non-stereospecific sites through strong Lewis acids. 4. Enhance the electronic properties and stereospecificity of the Ti species via coadsorption. 5. Balance the active Ti species to control catalytic properties directly.

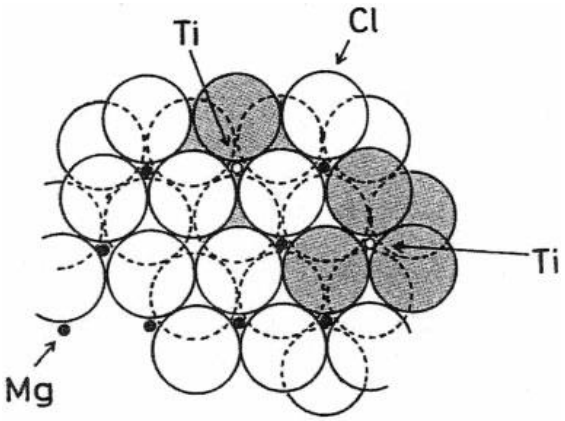

Figure 5. Model for surface of $MgCl_2$-supported $TiCl_4$ catalyst [18].

1-2-4. Propylene polymerization mechanism

The polymerization of propylene begins with the alkyl groups adding cis to propylene π-coordinated to the vacant conformations of the coordinatively unsaturated Ti atoms. The addition of polymer chains to the propylene π-coordinated to the vacant conformations advances the growth reaction. Propylene has regioselectivity, a property that determines whether Ti bonds to the carbon in the first or the second direction during insertion in Ti-C bonds, and these patterns are known as 1,2-insertion and 2,1-insertion, respectively.

1-2-5. Stereostructure control mechanism

Cossee, Arlman, Corradini *et al.* described the structure of the ZN catalyst isospecific active species shown in Figure 6 [19,20]. Direction is regulated by the steric repulsion between the *β*-carbon growing polymer chains and the Cl on the adjacent Ti (Mg) atoms, and propylene monomers are distributed in a way that minimizes the steric repulsion with the *β*-carbon. Since transfer insertion advances polymerization, the direction of the growing polymer chain changes, the two conformations are nonequivalent, and the steric repulsion at the coordination site where the growing polymer chain transferred returns the next monomer to its original direction before it is coordinated. The advance of isospecific polymerization is attributed to those factors.

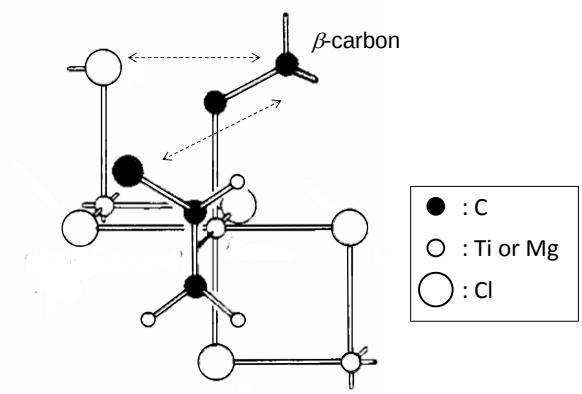

Figure 6. Isospecific active species of ZN catalyst [19].

1-2-6. Use of hydrogen and chain transfer

The substantial activation effect of hydrogen is observed in substances such as $MgCl_2/TiCl_4/AlEt_3$ [21], $MgCl_2/TiCl_4$/dialkyl phthalate-AlR_3/alkoxysilane compounds [22-25], and $MgCl_2/TiCl_4$/1,3-diether compound-AlR_3 [26,27]. Catalytic activity increases approximately threefold compared to activity without hydrogen [28]. After the regioirregular 2,1-insertion of monomers in the growth chain, inserting propylene becomes difficult. It is assumed that the inactive dormant sites are activated by the chain transfer toward the hydrogen, which controls PP molecular weight. Consequently, hydrogen is used as an industrial molecular weight modifier.

1-2-7. Metallocene catalysts

In the late 1970s, Kaminsky *et al.* discovered that homogeneous catalysts (metallocene catalysts) consisting of methylaluminoxane (MAO), which is a condensation product of water and $AlMe_3$, and group 4 metallocene compounds such as Ti or Zr exhibited high activity in olefin polymerization[29]. Since their active sites are homogeneous, these catalysts are also called single-site catalysts. Based on the unimodal distribution pattern they exhibit in a temperature rising elution fractionation (TREF) analysis, ethylene−1-alkene copolymers (linear low density polyethylene (LLDPE)) synthesized

from metallocene catalysts are homogeneous copolymers. Metallocene catalysts and other single-site catalysts are used for the industrial production of LLDPE and ethylene–propylene (EP) random copolymers. Similarly, metallocene catalysts are used for the industrial synthesis of high stereoselectivity syndiotactic PP.

1-3. Polypropylene morphology

1-3-1. Constituents of PP morphology

Polypropylene is a crystalline polymer. As shown in Figure 7, all crystalline polymers have a hierarchical structure with a different scale. The skin-core structure has a macroscopic morphology on the order of millimeters. Spherulites, whose size is on the order of a few μm, can be observed through optical microscopy. The lamellar crystals in the spherulites measure a few hundred Å and are generally observed using an electron microscope. The α-form iPP unit cells measure 6 to 20 Å. The iPP conformations are based on a 3/1 helix structure [30]. Crystal structures such as α crystal, β crystal, γ crystal and smectic phase can be taken by iPP. The α (monoclinic) crystals represents the dominant crystal structure. It is divided into α_1(C2/c) and α_2(P21/c) based on the differences between spatial groups. The α crystal lamellar structure is peculiar in that, it is likely to form a crosshatched structure where the daughter lamellae grow essentially perpendicularly in the tangential direction relative to the mother lamellae that form in the radial direction [31,32]. The trigonal lattice that constitutes the β crystals was discovered in 1959 [33]. Compared to α crystals, β crystals exhibit high impact strength and superior toughness, as well as lower tensile strength.

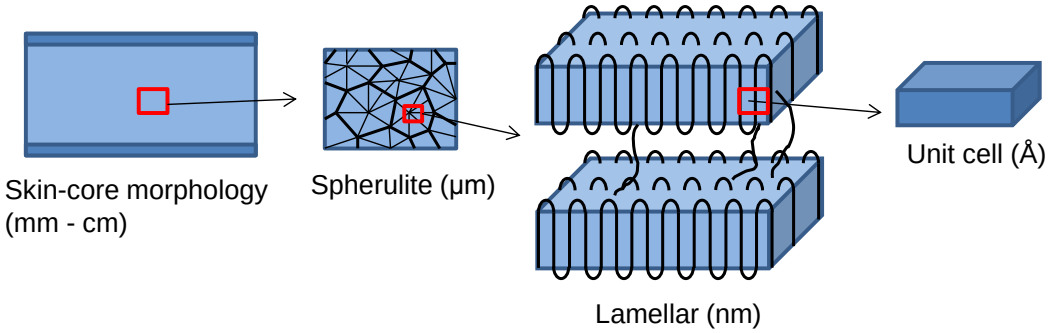

Figure 7. Higher order structure of PP.

The impact resistance and transparency of PP is affected by the size of the spherulites. Normally, PP with large spherulites is opaque and exhibits poor impact resistance. The addition of nucleating agents is widely applied [34,35] as an effective way to reduce the size of the spherulites, which also changes according to the crystallization conditions. Fast cooling produces more spherulites.

Melting temperature is affected by the size of the crystals and is strongly dependent on the thickness of the crystal along the direction of the polymer chain. Lamellae built from a certain crystal size (lamellar thickness l, width α) can be envisioned, and the energy freely generated by those lamellar crystals can be derived from the following equation.

$$\triangle \Phi_c = 2\alpha 2\sigma_e + 4\alpha l\sigma_s - \alpha 2l\triangle f$$

In typical lamellar crystals, $l << \alpha$ is assumed, and since $\Delta\Phi_c = 0$ at melting temperature T_m, the equation below is obtained.

$$T_m = T_m^0\left(1 - \frac{2\sigma_e}{l\triangle H_m}\right)$$

The lamellar thickness l and melting temperature T_m of the samples prepared according to various crystallization conditions are measured with methods such as small-angle X-ray scattering or Differential scanning calorimetry (DSC). The melting temperature dependence on crystal thickness is then plotted, and the equilibrium melting temperature T_m^0 can be derived through infinite extrapolation of lamellar thickness l. In addition, the surface free energy σ_e can be obtained from the inclination of the line.

1-3-2. Crystallization mechanism

Crystallizing random-coil high polymer chains involves first aggregating several polymer chains, resulting in the formation of a primary nucleus, whose surface is then absorbed by the polymer chain, causing the formation of secondary nuclei that lead to significant crystal growth. The crystals start to occupy the samples as a whole (overall crystallization rate constant *k*). The crystals collide with one another, and crystallization finishes when all non-crystallized portions have been fully consumed. The primary nucleation rate *I* can be derived from the number of spherulites formed per hour, while the spherulite growth rate *G* can be derived from the speed at which the spherulites increase in size. Both of those rates are strongly dependent on the crystallization temperature. The crystallization rate is determined by the primary nucleation rate *I* and the spherulite growth rate *G*.

1-4. Improvement of polypropylene properties

1-4-1. Enhancement of PP physical properties through functionalization

PP has excellent physical properties and formability, and is the most widely used plastic material. In contrast, the carbon-carbon or carbon-hydrogen single-bond structure is chemically stable and nonpolar, making it weak in areas such as adhesiveness, paintability, dyeability, compatibility with heterologous polymers, and affinity with fillers. Active and vigorous research on PP functionalization is being conducted to overcome those weak points.

Methods of functionalizing PP include copolymerization and chemical treatment of the PP (post-polymerization). The former can be either direct functionalization, where functionalized PP is obtained through the copolymerization of comonomers with functional groups and propylene, or an approach where copolymer reactive functional groups obtained through the copolymerization of reactive comonomers and propylene are converted into the desired functional groups. While the direct process is ideal because it only involves one step, chemical drawbacks such as reduced catalytic activity mean that almost all functionalization processes in the market are post-polymerization processes. However, there are also issues with those processes. To reduce its cost, functionalization is commonly performed at the same time as the molding process, which results in an extremely short time for reactions and makes it difficult to control the chemical structure and the functionalization ratio. Moreover, there is also a deterioration in physical properties due to undesired polymer chain scission. Consequently, new functionalization approaches are being sought.

1-4-1-1. Direct functionalization through copolymerization.

Polymerization using ZN or metallocene catalysts with early transition metals is the most important method of synthesizing PP. It is clear that the most direct approach to synthesizing functionalized PP is the to use those catalysts in the copolymerization of propylene and comonomers having the target functional groups. However, catalyst deactivation makes the direct process difficult. The Ti, Zr, Hf, V and Al in the catalysts are Lewis acid compounds, and their formation of complexes with the non-bonded electron pairs on N, O, and X (halides) is seen as the cause of catalyst deactivation (Scheme 1).

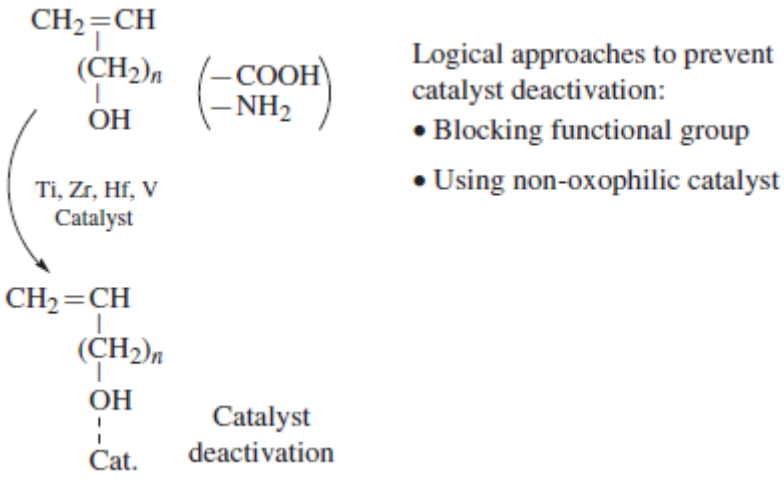

Scheme 1. Catalyst deactivation by functional group [36].

Hydrocarbon solvents such as heptane and toluene are normally used for the polymerization of propylene, but polar comonomers have poor solubility in such hydrocarbon solvents, which are nonpolar. This problem leads to decreased polymer yield and lower molecular weight. Methods such as using functional monomers that

contain neutral or acidic heteroatoms, or preventing catalyst poisoning by protecting the polar functional groups are used to circumvent the problem. Functionalization can also be achieved with less oxophilic late transition metal catalysts complexes like Fe, Ni, Co, or Pd, as exemplified by reports of functionalization based on the copolymerization of α-olefins and acrylate comonomers. Nevertheless, stereoregular polymerization remains difficult, and there of no reports concerning the functionalization of iPP.

1-4-1-1-1. PP functionalization using functional monomers that contain neutral or acidic heteroatoms

Methods using functional monomers that contain neutral or acidic heteroatoms are almost entirely limited to, respectively, borane groups [37-39,44-48] or silane groups [40-43,49,50]. Borane-containing monomers are synthesized through the reaction of a nonconjugated α, ω-diene such as 1,5-hexadiene and a dialkyl borane such as 9-borabicyclononane (9-BBN). Using either ZN [44] or metallocene [45] catalysts, Chung *et al.* reported obtaining borane-containing PP by performing copolymerization of propylene with 5-hexenyl-9-BBN [44,46-48]. PP-OH copolymers with high polarity hydroxyl groups can be obtained by oxidizing borane (Table 1), and conversion to various functional groups described later is also possible.

Table 1. Results of copolymerization of propylene and borane monomer by continuous reaction

Polymer	Mol% 5-hexenyl-9-BBN in feed	Mol% OH in Polymer	Reaction time	Yield (%)	η^2	M_v (g/mol)
PP	0	0	2	93	2.07	230×10^3
PP-OH	10	3	3	62	1.78	183×10^3
PP-OH	13	5	5	35	1.71	174×10^3

η = intrinsic viscosity.

The copolymerization of propylene with vinylsilane or allylsilane results in silane-containing PP [49,50]. Matsuyama *et al.* used an Mg supported ZN catalyst to perform copolymerization of propylene with vinylsilane [50]. Silane groups are not polar to the extent of affecting polymer characteristics. Polarity can be assigned to the PP by triggering a reaction between the compounds that contain OH, NH_2, or C=O and the Si-H bond in the side chains of the obtained polymer. In addition, the reactive silane groups introduced in the PP chains induce crosslinking.

1-4-1-1-2. PP functionalization through the protection of polar functional groups

Polar monomers such as -OH, -COOH and -NH_2 cause a drastic decrease in catalytic activity when they react directly with propylene during polymerization. In the copolymerization of monomers that contain amino groups, the length of the spacers between the vinyl and amino groups, and the bulkiness of the amino group (-NR_2) R substituent have a significant effect on the progress of the polymerization. Long spacers and bulky R substituents clearly weaken the interaction between the catalyst and the

functional groups. Steric [51-56] or electronic [57-63] protection of the functional groups is effective at preventing contact between high polarity functional groups and the catalyst. Electronic protection causes the solubility of the propagating polymer chain to deteriorate, which reduces molecular weight and decreases the polymer yield. Steric protection prevents catalyst poisoning, but also requires the availability of effective deprotection. Langer *et al.* used a ZN catalyst to perform copolymerization of propylene with steric protected 6-N, N-diisopropylamino-1-hexene [51]. Similarly, Nasman *et al.* carried out the copolymerization of propylene and 1-hexene containing 2,2,6,6-tetramethyl piperidine using a ZN catalyst [52]. Collette *et al.*, as well as Kresge, used a ZN catalyst to perform terpolymerization of a third norbornene monomer having ethylene, propylene, and primary amino groups [64,65]. Electronic protection using an alkylaluminum compound (R_3Al) was applied to the amino groups. The formation of N-AlR_2 reduces the nucleophilicity of the primary amines. As with the steric protection of the amino groups based on alkylaluminum, this is due to the strong electronic back-donation from N to Al caused by the dπ-dπ bond.

It is known that, even among α-olefins that contain OH groups, the use of a ZN or metallocene catalyst makes the copolymerization α-olefins with long methylene spacers between the vinyl and functional groups, such as comonomers like 5-hexene-1-ol [66] or 10-undecen-1-ol [67] with propylene possible. In such systems, alkylaluminum is necessary to prevent catalyst inactivation caused by the polar functional groups. Improved adhesive properties were observed in propylene-co-10-undecen-1-ol copolymers compared to homo-polymers.

1-4-1-2. PP functionalization through post-polymerization

PP is inactive and does not have reactive sites that can be easily chemically modified. Degrading the stable C-H bonds and forming free radicals in the PP chain activates the PP and is also the most practical method of chemical modification. Molecular radicals [68-71], radiation [72,73] and plasma [74-78] can be used as high energy sources to extract H atoms from the PP chains. Due to the stability of the tertiary carbon radicals, the free radicals attack the PP, easily extracting the H atoms. The functionalization of the PP chains can be achieved by inducing a reaction between the tertiary carbon radicals and the vinyl monomers that contain functional groups. However, functionalization causes the tertiary carbon radicals formed in the PP chains to promote a β-cleavage reaction, which presents the issue of a significant degradation in physical properties.

Maleic anhydride (MA) is the monomer subject to the most research [79-82]. PP functionalized with MA (MAPP) is one of the most important functionalized PPs on the market. The MA double bonds react to free radicals. In contrast, homopolymerization is difficult to perform on MA due to its low steric effect and ceiling temperature. The importance of MAPP in the market stems from its low cost and its usability as a coupling agent for fillers [83-88].

Surface modification based on triggering functionalization reactions in solids such as PP films, sheets, fibers and membranes is carried out to enhance characteristics such as adhesiveness, colorability and wettability. Oxidation reactions using chromium trioxide in sulfuric acid and potassium permanganate in sulfuric acid are known examples of chemical processes. Although it is possible to cause the formation of -COOH or other acids on the surface, the need to use toxic reagents is a drawback in terms of use in the market. The surface of PP films and fibers is modified by the free radical grafting reaction

in the solution phase, and products such as MA-modified PP film are prepared [89]. Surface modification based on a free radical grafting reaction can also be achieved through high energy radiation such as electron beam or gamma ray radiation. There are reports of surface modifications based on the addition of acrylonitrile to γ-radiated PP film [72] or of methacrylates to fibers [73]. Surface modification of PP films using low energy UV radiation has also been reported [90].

In the market, the corona treatment is used to perform surface modification of PP biaxially stretched film. This makes it possible to improve adhesiveness. Plasma treatment is another method that excels at making surface improvements [78,91,92]. The contact angle in distilled water is wider for plasma-treated samples than for non-treated samples (Table 2). Plasma treatment for automobile PP bumpers was studied by Toyota Motor Corporation in 1985 as a promising means of improving paintability [93,94], and the process is currently in industrial use.

Table 2. Effects of plasma treatments on hydrophilcity of PP surfaces

Plasma	Contact angle in distilled water (°)	
	Before treatment	After treatment
CF_4	104	123
SF_6	104	117
N_2	94	50
CO_2	94	45
O_2	95	23

PP functionalization through post-polymerization requires high temperature, high energy radiation due to C-H bond breaking. Consequently, rather than functionalization alone, polymer chain cleavage occurs as a side reaction, and there is a simultaneous undesirable deterioration in physical properties. There is a need for more controllable reactions in PP functionalization.

1-4-1-3. Functionalization through PP copolymers that contain reactive functional groups

Copolymerization with a ZN or metallocene catalyst can be used to introduce borane groups [37-39,95], *p*-methylstyrene (*p*-MS) [96-100], or divinylbenzene [101], which are reactive functional groups, in the PP chains [102].

Borane groups introduced in the polyolefin can be converted to OH, NH_2 or halides (Scheme 2). For example, C-B bonds are easily oxidized by H_2O_2/NaOH, introducing OH groups in the PP chains. In addition, PP graft copolymers can be prepared by conversion into living radical initiators. Chung *et al*. successfully grafted PMMA by adding MMA after using oxygen oxidation to turn the C-B bonds into oxides [95].

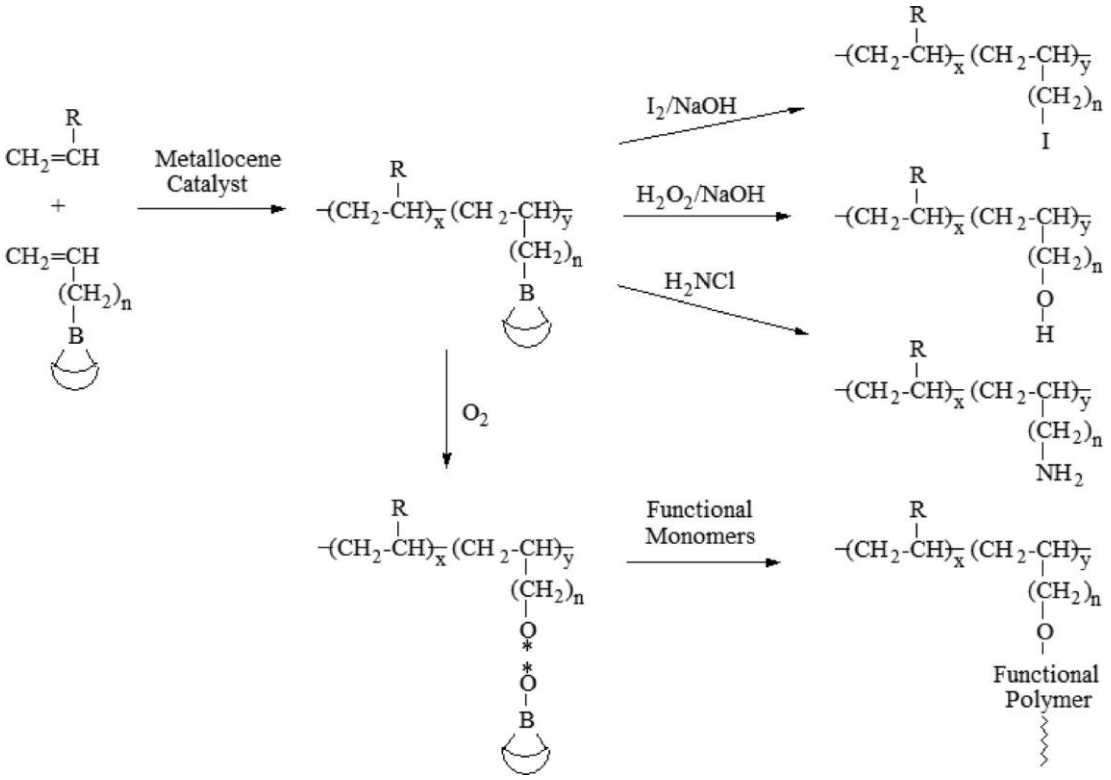

Scheme 2. Functionalization of polyolefin using reactive borane groups [36].

The copolymerization of *p*-MS with propylene produces a polymer regardless of whether a metallocene or ZN catalyst is used. The *p*-CH_3 groups are interconverted into functional groups such as -OH, -NH_2, -COOH, anhydrides, or halides. PP graft copolymers can be prepared by conversion into anionic initiators (Scheme 3) [98-100]. Metallocene catalysts exhibit poor catalytic activity and low introduced *p*-MS content. In contrast, no decrease in catalytic activity was observed when *p*-MS comonomers were added during the polymerization uing ZN catalyst (Table 3). Interestingly, the molecular weight of the PP-*p*-MS copolymer was observed to increase as the concentration of *p*-MS rose. The reason for this unexpected phenomenon is unclear.

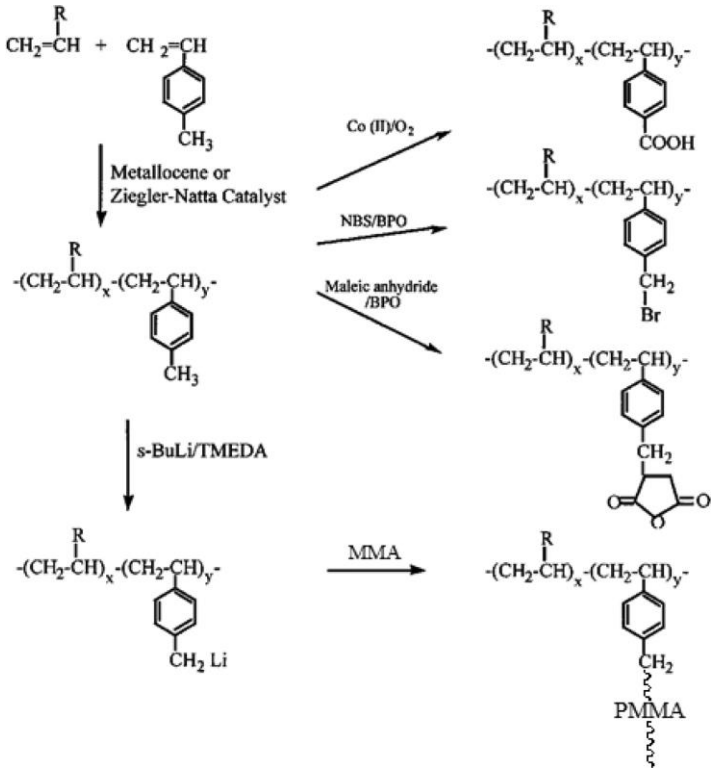

Scheme 3. Functionalization of polyolefin using *p*-MS [36].

Table 3. Summary of copolymerization reactions between propylene (m_1) and *p*-MS (m_2) in the presence of ($MgCl_2/TiCl_4/ED/AlEt_3$) catalyst[1]

		Copolymer properties				
m_1/m_2 (psi)/(mmol)	Cat. activity (kg/(mol-Ti·atm·h)	*p*-MS (mol%)	M_w (10^3 g/mol)	M_w/M_n	T_m (C°)	H_r (J/g)
29/0	658	0	109.9	4.41	158.4	59.9
29/33.9	645	0.4	168.2	5.54	154.9	57.1
29/68.6	650	0.6	202.2	202.2	154.3	56.2

[1]Polymerization conditions: catalyst = 17.4 µmol Ti. Al/Ti = 90, ED (electron donor) /Ti = 6, 50°C, 100 mL toluene.

Copolymerization with dienes introduces C=C double bonds in the side chains. Kitagawa *et al.* studied copolymerization with propylene using methyl-1,4-hexadiene [103]. A $TiCl_3/AlEt_2Cl$ catalyst produced random copolymers. The double bonds introduced in the polymer chains facilitated the formation of crosslinking in the polymers. In addition, conversion to OH, NH_2, anhydrides, or halogens is possible.

Since it serves a building block for the construction of multisegment polymers, polypropylene that contains reactive functional groups at its ends is particularly interesting. The preparation of polyolefin block copolymers, graft copolymers and long-chain branched polymers is difficult, and end-functionalization represents a challenge for many researchers. The chemical modification of PP with unsaturated ends is one way to synthesize end-functionalized PP. There are two types of methods to prepare chain end unsaturated PP. The first is the thermal degradation process, which is performed through a degradation reaction of oxides in the melt. The degradation of physical properties that accompanies the polymer chain cleavage cannot be avoided. The other method uses a metallocene catalyst, which involves manipulation based on a termination reaction caused by β-hydrogen elimination. Neither method results in a large conversion to unsaturated PP. A lot of research on the hydroboration, hydroalumination, and hydrosiliration of PP end vinylidene has been conducted. However, the low concentration of unsaturated end functional groups and the poor dissolution of polymers relative to the organic solvents that can dissolve the reagents used in functionalization reactions make it difficult to introduce large numbers of functional groups. In contrast, the chain transfer that occurs during the polymerization reaction allows for the convenient introduction of reactive functional groups at the ends of the polymers. It has been reported that zinc-alkyl and aluminum-alkyl act as chain transfer agents in

propylene polymerization using ZN catalysts. Marks *et al.* later discovered that in metallocene catalyst-based polymerization, organosilanes having Si-H groups worked as effective chain transfer agents and produced silane-terminated PP (Scheme 4) [104]. Chung *et al.* have reported on the synthesis of end-functionalized PP through B-H chain transfer using a metallocene catalyst [48]. The fact that these end functional groups can be converted into the earlier-described functional groups presents many advantages.

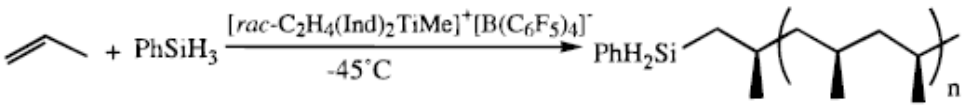

Scheme 4. Synthesis of silane-terminated PP [104].

Hagahara *et al.* carried out the copolymerization of propylene with 1-butene-1-ol based on a zirconocene catalyst system combined with MAO. The polar comonomers acted as chain transfer reagents and produced terminally hydroxylated PP [105].

1-4-2 Enhancement of PP physical properties through composites

1-4-2-1. PP composites

The possibility of enhancing crystallization behavior or mechanical properties, and of providing new functions, by adding organic or inorganic substances to polymers is an extremely important point. These additions include polymer alloys and composites. Recently, the engineering plastics that have been used in products are gradually being replaced by PP compounds prepared through the addition of random copolymers or inorganic fillers to the PP (Figure 8). Compared to other plastics, PP has various strong points such as lightness, high moldability, and excellent recyclability, making it

extremely desirable to further expand the fields where PP is used by substituting it for other plastics.

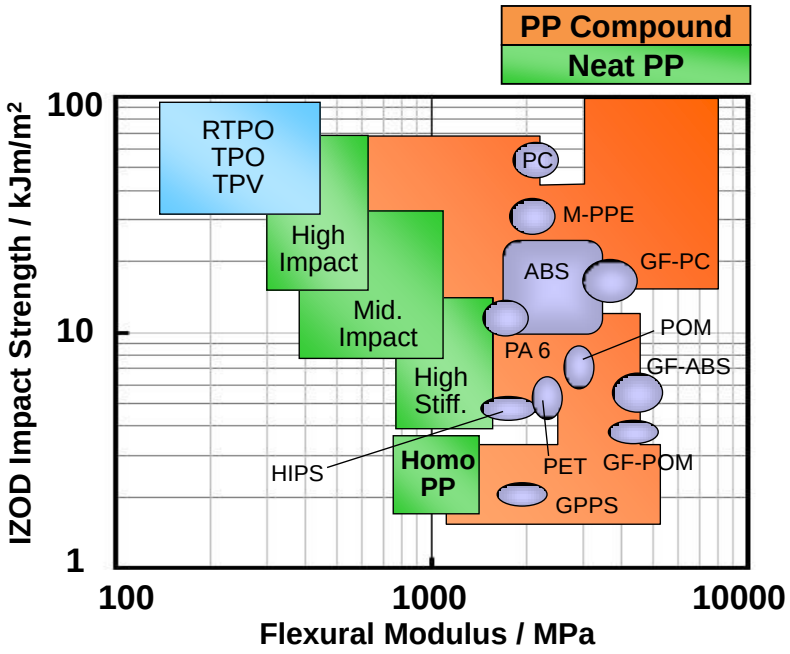

Figure 8. Mechanical properties of PP, PP compounds and other plastics.

Along with the demand for PP, filler consumption is increasing year after year (Figure 9) [106]. Talc, calcium carbonate and glass fiber are typical fillers for PP, and talc is the most commonly used filler. The introduction of talc improves the heat deflection temperature and shrinkage rate of PP. Both reinforcement and low cost are important. In contrast, rubber is added to compensate for the decrease in impact strength. The Super Olefin Polymer, which is composed of PP homopolymer, ethylene-propylene rubber (EPR), and talc is widely used as an automotive material [107].

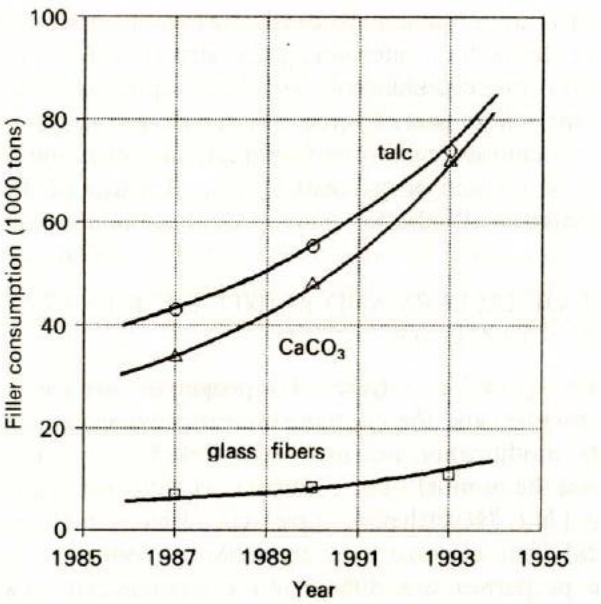

Figure 9. Amount of filler consumption in Western Europe for fillers (talc, $CaCO_3$ and glass fiber) used as reinforcing agents for PP [106].

Glass fiber added to PP in a compound generally exhibits a greater reinforcement than talc, calcium carbonate, mica, or other fillers because of its large aspect ratio (Figure 10) [108]. Coupling agents such as maleic anhydride modified-PP or acrylic acid grafted PP are added to provide good adhesion between the glass fiber and PP. Shearing during compounding or molding breaks the fibers. The length and length distribution of the fibers has a considerable effect on physical properties, making it necessary to optimize screw designs, as well as compounding and molding conditions.

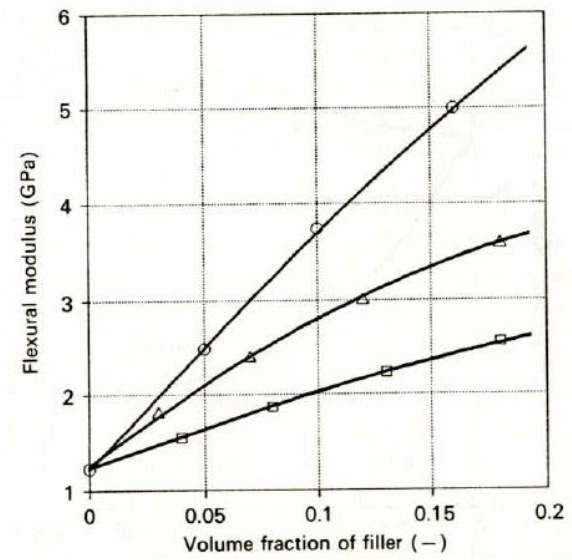

Figure 10. Effect of filler anisotropy on the flexural modulus of PP composites

: (○) glass fiber, (Δ) talc, and (□) $CaCO_3$ [108].

1-4-2-2. PP nanocomposites

Polymer-based nanocomposites have been the subject of greater attention since Usuki *et al.* succeeded at achieving high clay dispersion in polyamides in 1988 [109]. Compared to micro-sized particles, nanoparticles have a large surface area, and remarkably stronger interaction between the polymers and the fillers, or between different fillers. This results in a dramatically greater reinforcement effect. Given the importance of PP in the market, considerable research is being devoted to PP-based nanocomposites. This research spans a broad spectrum that extends beyond investigating the addition compatibilizer and the chemical modification of fillers to also cover topics such as functionalized PP and polymer grafted PP. In addition to reinforcement effects, there are also reports about providing functions such as electro conductivity, thermal conductivity, and heat resistance.

1-5. Objective

This research studied the functionalization of PP aimed at enhancing its physical properties. Maleic anhydride grafted PP, the current representative functionalized PP on the market, is prepared through a chemical treatment that uses peroxide. Since the functionalization process advances the scission of the main chain, a dramatic degradation of physical properties is unavoidable. The use of maleic anhydride grafted PP is typically limited to additives, and applying in injection molded products, where demand is the strongest, is difficult. Therefore, the use of functionalization through copolymerization is considered important to enhance the physical properties of PP. Metallocene catalysts have been researched extensively since they can be introduced in functional groups more efficiently than ZN catalysts, and have a uniform atactic site structure. However, PP synthesized with ZN catalysts rather than metallocene catalysts form thicker lamellae, and exhibits higher melting points and crystallinity. The broad molecular weight distribution of PP synthesized with ZN catalysts also provides good moldability. The low cost of ZN catalysts also makes them attractive from an industrial point of view. This research therefore sought to enhance PP physical properties by functionalizing PP through copolymerization that used ZN catalysts, which can synthesize PP with good physical properties and moldability.

Chapter 2 describes research involving the small-scale introduction of functional groups through copolymerization using ZN catalysts aimed at enhancing the physical properties of PP without disrupting its crystalline structure. The physical properties of the resulting polymers were investigated. Normally, functional groups introduced in the polymer chains disrupt the crystallization of PP, lowering its melting temperature and degrading its mechanical properties. If the functional groups are introduced in the PP

chains on a small scale, crystallization is not disrupted. In contrast, even a small-scale introduction of functional groups into the PP chains is expected to have significant effects in the areas of nucleation or grafting. Given that small-scale functionalization can also prevent the dramatic decrease in catalytic activity, it is also expected to present advantages in terms of the synthesis of functionalized PP.

The research presented in Chapter 3 studied the introduction of reactive functional groups in the polymer chains for the purpose of enhancing the physical properties of PP. This involved attempting to trigger crosslinking reactions between the reactive functional groups introduced in the PP chains through the post-polymerization of the obtained polymers. Analyses of the polymer structure, crystallization behavior, and mechanical properties were performed.

In Chapter 4, efforts to induce graft formation onto the nanosilica in the PP polymer chains using reactive functional groups introduced on a small scale in the PP chains are described. The results of investigations of the crystallization behavior and mechanical properties of the obtained nanocomposites are presented. Chapter 5 summarizes the findings of this research on enhancing PP physical properties using small-scale functionalization through ZN catalysts.

The small-scale introduction of functional groups into the PP chains studied in this research is expected to avoid impairing the excellent physical properties of PP, and even improve them. The fact that catalytic activity does not decrease is also deemed to make this study extremely valuable in terms of polymer synthesis.

References

[1] H. A. Maddah, *American Journal of Polymer Science*, **6**, 1 (2016).

[2] Chemical Prices, *News and Analysis Chemical Market Intelligence*, ICIS.com., N.p., n.d. Web. 16. Aug. (2011).

[3] Q.T.H. Shubhra, Quazi, A.K.M.M. Alam, M.A. Quaiyyum, *Journal of thermoplastic composite materials*, 0892705711428659 (2011).

[4] H.G. Karian, *Handbook of Polypropylene and Polypropylene Composites.* New York: Marcel Dekker (1999).

[5] Pre-feasibikity study for PDH/CAN/PP complex, Vol. I, Al-Zamil & Brothers Company, Oct. (2004).

[6] K. Ziegler, H. Breil, H. Martin, E. Holzkamp, German Patent 973 626 (1953).

[7] Montecatini, Italian Patent 535 712 (1954).

[8] Montecatini, Italian Patent 526 101 (1954).

[9] Solvay, U.S. Patent 3 769 233 (1973).

[10] Montedison , British Patent 1 286 867 (1968).

[11] K. Czaja, B. Król, *Polimery*, **43**, 287 (1998).

[12] Montedison , Belgian Patent 785 332 (1972).

[13] Montedison and Mitsui P. C., German Patent 2 643 143 (1977).

[14] Shell Oil, U.S. Patent 4 414 132 (1979),

[15] Shell Oil, U.S. Patent 4 393 182 (1979).

[16] Montedison , European Patent 45 977 (1982).

[17] HIMONT Inc., U.S. Patent 4 971 937 (1990).

[18] N. Kashiwa, *J. Polym. Sci. Part A: Polym. Chem.*, **42**, 1 (2004).

[19] P.Corradini, V. Borane, R. Fusco, G. Guerra, *J. Catal.*, **77**, 32 (1982).

[20] P. Corradini, G. Guerra, *Prog. Polym. Sci*., **16**, 239 (1991).

[21] G. Gaustalla, U. Giannini, *Macromol. Chem. Rapid Commun.*, **4**, 519 (1983).

[22] J.C. Chadwick, A. Miedema, O. Sudmeijer, *Macromol. Chem*., **195**, 167 (1994).

[23] J.C. Chadwick, G.M.M. van Kessel, O. Sudmeijer, *Macromol. Chem. Phys.*, **196**, 1431 (1995).

[24] R. Spitz, P. Masson, C. Bobichon, A. Guyot, *Macromol. Chem.*, **190**, 717 (1989).

[25] J.C.W. Chien, T. Nozaki, *J. Polym. Sci. Part A: Polym. Chem.*, **29**, 205 (1991).

[26] E. Albizzati, U. Giannini, G. Morini, M. Galimberti, L. Barino, R. Scordamaglia, *Macromol. Symp.* **89**, 73 (1995).

[27] J.C. Chadwick, G. Morini, E. Albizzati, G. Balbontin, I. Mingozzi, A. Cristofori, O. Sudmeijer, G.M.M. van Kessel, *Macromol. Chem. Phys.*, **197**, 2501 (1996).

[28] E. Albizzati, M. Galimberti, U. Giannini, G. Morini, *Makromol. Chem., Macromol. Symp*., **48/49**, 223 (1991).

[29] H.J. Sinn, W. Kaminsky, *Adv. Organomet. Chem*., **18**, 99 (1980).

[30] G. Natta, P. Corradini, C. *del Nuovo Cimento*, **15**, 40 (1960).

[31] F.J. Khoury, *Res. Nat. Bur. St.*, **70A**, 29 (1966).

[32] B. Lotz, S. Graff, S. Straupe, J.C. Wittman. *Polymer*, **32**, 2902 (1991).

[33] H.D. Keith, Padden Jr FJ, N.M. Walker, H.W. Wyckoff. *J. Appl. Phys.*, **30**, 1485 (1959).

[34] H.N. Beck, *J. Appl. Polym. Sci.*, **9**, 2131 (1965).

[35] D.R. Morrow, *J. Macromol. Sci. Phys.*, **B3**, 53 (1965).

[36] T.C.M. Chung, *Academic Press* (2002).

[37] T.C. Chung, U.S. Patent 4734472 (1989).

[38] T. C. Chung, U.S. Patent 4812529 (1989).

[39] S. Ramakrishnan, E. Berluche, T.C. Chung, *Macromolecules*, **23**, 378 (1990).

[40] G. Natta, G. Mazzanti, P. Longi, F. Bernardini, *J. Polym. Sci*., **31**, *181* (1958).

[41] N.S. Nametkin, A.V. Topchiev, S.G. Dourgarian, I.M. Tolchinski, *Vysokomol. Soedin.*, **1**, 1739 (1959).

[42] U. Giannini, G. Bruckner, E. Pellono, A. Cassata, *Polym. Lett*., **5**, 527 (1967).

[43] A. Carbonaro, A. Greco, I.W. Bassi, *Eur. Polym. J.*, **4**, 445 (1968).

[44] T.C. Chung, D. Rhubright, *Macromolecules*, **26**, 3019 (1993).

[45] W. Lin, J. Dong, T.C.M. Chung, *Macromolecules*, **41**, 8452 (2008).

[46] T.C. Chung, W. Janvikul, *J. Organometallic Chemistry* **581,** 176 (1999).

[47] T.C. Chung, D. Rhubright, *Macromolecules*, **24**, 970 (1991).

[48] T.C. Chung, G. Xu, Y. Lu, Y. Hu, *Macromolecules*, **34,** 8040 (2001).

[49] N.S. Nametkin, A.V. Topchiev, S.G. Dourgarian, I.M. Tolchinski, *Polym. Sci. (USSR)*, **2**, 133 (1961).

[50] T. Asanuma, T. Matsuyama, *Polymer Bulletin*, **26**, 205 (1991).

[51] A.W. Langer, R.R. Haynes, U.S. Patent 3755279 (1973).

[52] M.R. Kesti, G.W. Coates, R.M. Waymouth, *J. Am. Chem. Soc*., **114**, 9679 (1992).

[53] C.E. Wilen, M. Auer, J.H. Nasman, *J. Polym. Sci. A: Polym. Chem.*, **30**, 1163 (1992).

[54] G. Bertolini, L. Lanzini, L. Marchese, A. Roggero, A. Lezzi, S. Costanzi, *J. Polym. Sci. A: Polym. Chem*., **32**, 961 (1994).

[55] M.J. Schneider, R. Schafer, R. Mulhaupt, *Polymer*, **38**, 2455 (1997).

[56] U. M. Stehling, K.M. Stein, M.R. Kesti, R.M. Waymouth, *Macromolecules*, **31**, 2019 (1998).

[57] K.J. Clark, W.G. City, U.S. Patent 3949277 (1970).

[58] D.N. Schulz, K. Kitano, T.J. Burkhardt, A.W. Langer, U.S. Patent 4518757 (1984).

[59] P. Aaltonen, B. Lofgren, *Macromolecules*, **28**, 5353 (1995).

[60] P. Aaltonen, G. Fink, B. Lofgren, J. Seppala, *Macromolecules*, **29**, 5255 (1996).

[61] S. Bruzaud, H. Cramail, L. Duvignac, A. Deffieux, *Macromol. Chem. Phys.*, **198**, 291 (1997).

[62] C.E. Wilen, J.H. Nasman, *Macromolecules*, **27**, 4051 (1994).

[63] M.M. Marques, S.G. Correia, J.R. Ascenso, A.F.G. Ribeiro, P.T. Gomes, A.R. Dias, P. Foster, M.D. Rausch, J.C.W, Chien, *J. Polym. Sci. A: Polym. Chem.*, **37**, 2457 (1999).

[64] J.W. Collette, R. Ro, F.M. Sonnenburg, U.S. Patent 3901860 (1975).

[65] S. Datta, E.N. Kresge, U.S. Patent 4987200 (1991).

[66] K. Hakala, B. Lofgren, T. Helaja, *Eur. Polym. J.*, **34**, 1093 (1998).

[67] Santeri Paavola, Barbro Lo¨ fgren, Jukka V. Seppala, *European Polymer Journal*, **41**, 2861 (2005).

[68] M.F. Diop, J.M. Torkelson, *Macromolecules*, **46**, 7834 (2013).

[69] M. Saule, S. Navarre, O. Babot, W. Maslow, L. Vertommen, B. Maillard, *Macromolecules*, **36**, 7469 (2003).

[70] M. Saule, L. Moine, M. Degueil-Castaing, B. Maillard, *Macromolecules*, **38**, 77 (2005).

[71] L. Assoun, S.C. Manning, R.B. Moore, *Polymer*, **39**, 2571 (1998).

[72] M. Miura, S. Kamamatsu, *Kobunshi Kagaku*, **19**, 175 (1962).

[73] K. Kawase, K. Hayakawa, *Radiat. Res.*, **30**, 116 (1967).

[74] R. Singh, *Prog. Polym. Sci.*, **17**, 251 (1992).

[75] J. Jagur-Grodzinski, *Prog. Polym. Sci.*, **17**, 361 (1992).

[76] T. Yagi, A.E. Pavlath, A.G. Pittman, *J. Apply. Polym. Sci*., **27**, 4019 (1982).

[77] D.E.J. Bergbreiter, *Prog. Polym. Sci*., **19**, 529 (1994).

[78] J.C. Brosse, G. Legeay, F. Poncin-Epaillard, *Functional Polymers: Synthesis and Applications*, ACS, Washington, DC, 201 (1996).

[79] A. Hogt, *ANTEC*, 1478 (1988).

[80] M. Xanthos, *Reactive Extrusion: Principles and Practice*, Hanser, Munich, 33 (1992).

[81] H.G. Fritz, B. Stoehrer, *Int. Polym. Proc.*, **1**, 31 (1986).

[82] K. Ebner, J.L. White, *Int. Polym. Proc.*, **9**, 233 (1994).

[83] A.R. Bunsell, *Fiber Reinforcement of Composite Materials* (1998).

[84] R.C. Constable, *ANTEC*, 127 (1994).

[85] H.G. Karian, *ANTEC*, 1665 (1995).

[86] J.B. Herater, E.M. Lacey, *Mod. Plast.*, **41**, 123 (1964).

[87] E.A. Flexman, Jr., *Polym. Eng, Sci*., **19**, 564 (1979).

[88] B.E. Epstein, U.S. Patent 4 174 358 (1979).

[89] F. Severini, M. Pegoraro, L. Yuan, G. Ricca, N. Fanti, *Polymer*, **40**, 7059 (1999).

[90] S. Tazuke, H. Kimura, *Macromol. Chem.*, **179**, 2603 (1978).

[91] F. Leroux, C. Campagne, A. Perwuelz, Leon, Gengembre, *J. Colloid and Interface Sci*. **328**, 412 (2008).

[92] K.N. Pandiyaraj, V. Selvarajan, R.R. Deshmukh, C. Gao, *Appl. Surface Sci*. **255**, 3965 (2009).

[93] Y. Takahashi, K. Fukuda, T. Kaneko, *Toyota Eng.*, **35**, 65 (1985).

[94] D.L. Cho, K.H. Shin, W.-J. Lee, D.-H. Kim, *J. Adhesion Sci. Technol.*, **15**, 653 (2001).

[95] T.C. Chung, D. Rhubright, G.J. Jiang, *Macromolecules*, **26**, 3467 (1993).

[96] T.C. Chung, H.L. Lu, R.D. Ding, *Macromolecules*, **30**, 1272 (1997).

[97] H.L. Lu, S. Hong, T.C. Chung, *J. Polym. Sci. Pol. Chem.*, **37**, 2795 (1999).

[98] H.L. Lu, T.C. Chung, *J. Polym. Sci. Pol. Chem.*, **37**, 4176 (1999).

[99] T.C. Chung, *Prog. Polym. Sci*., **27**, 39 (2002).

[100] L. Wang, D. Wan, Z.J. Zhang, F. Liu, H.P. Xing, Y.H. Wang, T. Tang, *Macromolecules*, **44**, 4167 (2011).

[101] J.Y. Dong, H. Hong, T.C. Chung, *Macromolecules*, **36**, 6000 (2003).

[102] G. Moad, *Prog. Polym. Sci*, **24**, 81 (1999).

[103] S. Kitagawa, I. Okada, *Polym. Bull.*, **10**, 109 (1983).

[104] K. Koo, T.J. Marks, *J. Am. Chem. Soc.*, **120**, 4019, (**1998)**.

[105] H. Hagihara, K. Tsuchihara, J. Sugiyama, K. Takeuchi, T. Shiono, *J. Polym. Sci. Pol. Chem.* **42**, 5600 (2004).

[106] H. A. Maddah, *American Journal of Polymer Science*, **6**, 1 (2016).

[107] Yutaka Obata, Takashi Sumitomo, Toshikazu Ijitsu, Masatoshi Matsuda, Takao Nomura, *Polym. Eng. Sci*, **41**, 408 (2001).

[108] H.P. Schlumpf, *Kunststoffe*, **73**, 511 (1983).

[109] A. Usuki, Y. Kawasumi, Y. Kojima, A. Okada, T. Kurauchi, O. Kamigaito, *J. Mater*. **8**, 1174 (1993).

Chapter 2

Polypropylene crystallization behavior after introducing small amount of aromatic functional groups

2-1. Introduction

Polypropylene (PP) is one of the most widely used commodity plastics that possesses well-balanced physical properties featured with excellent characteristics such as good moldability, lightweight, recyclability, halogen-free and low cost. Researches on PP have continued since the discovery of the $TiCl_3$ catalyst in 1954. Compared to catalysts in those days, current industrial $MgCl_2$-supported $TiCl_4$ catalysts with the addition of donors exhibit a hundred fold increase in catalytic activity as well as high stereospecificity, resulting in a great improvement of polymer properties [1,2]. The melt blending of PP with fillers and the development of molding technology have further enhanced the physical properties to explore a broader application field.

The inclusion of comonomers or functional groups into polyolefin is also an important approach to expand polymer properties. With a significant progress in the field, the direct copolymerization to produce copolymers with short chain branches randomly placed on the main chain [3-20] or via reactive intermediate approach to introduce reactive groups followed by converting the reactive sites into a variety of functional groups [21-27] offers a versatile and effective way to incorporate a variety of properties into polyolefins. The size and the content of these side chains were reported to greatly impact physical properties and crystallization characteristics [6-20]. For example, Henschke *et al.* polymerized propylene with 1-butene, 1-hexene, 1-octene, 1-dodecene and 1-hexadecene to produce copolymers with comonomer contents ranging from 1.0 to 90.4 mol% [12]. They reported that the melting temperature and the glass transition temperature decreased as the length and the number of side chains increased. Coutinho *et al.* copolymerized propylene with 1-hexene and 1-octene [13]. They found that the copolymer with 1-hexene content up to 15.7 mol% enabled the crystallization

from a molten state, while the 1-octene copolymer already failed to crystallize at a content of 7.0 mol% and remained as an amorphous polymer. These results demonstrated that a random introduction of side chains in the main chain inhibits the crystallization, in which a longer side chain offers a stronger inhibitory effect. Functional groups introduced into PP chains also change the physical properties of PP. Using a Ziegler-Natta catalyst, Weiss *et al.* introduced a hydroxyl group into PP, aiming at enhancing the dielectric constant [19]. They found that the introduction of hydroxyl groups increased the dielectric constant, while decreased the crystal growth rate due to a larger viscosity arising from an attractive force between hydroxyl groups. In addition, the increase of hydroxyl groups on side chains further inhibited the crystallization and decreased the crystallinity and the melting temperature. Similarly, Chung *et al.* copolymerized propylene with *p*-methylstyrene and reported a great drop of the melting temperature from 158°C for homo PP to 128°C for the copolymer containing 2.3 mol% of comonomer with the decrease of crystallinity into half [20]. This is attributed to the disruption of the continuity of PP chains in the presence of randomly distributed side chains as like the case of α-olefin comonomers. On the contrary, the introduction of functional groups into PP chains without disrupting continuity has expanded the application into different areas. For example, Taniike and coworkers selectively introduced hydroxyl group into PP only at the chain end by a chain transfer control technique using metallocene catalyzed polymerization [28,29]. The synthesized polymer was utilized as a grafted chain for PP nanocomposites using SiO_2 as nanofillers. They found that the grafting of PP to SiO_2 at hydroxyl chain ends allowed an excellent dispersion of nanofillers in PP matrix and the great enhancement of reinforcement due to the physical crosslinkage and the co-crystallization between PP matrix and the

grafted chain. Accordingly, a small introduction of functional groups that manifest theirs effect even at a small amount without deteriorating the base properties of PP is therefore an interesting area of research, while only limited works have been done for such polymer design.

In the present research, aromatic functional groups were introduced into PP chains at a small amount by copolymerization of propylene with styrene and 1-allylnaphthalene comonomers. The physical properties and the crystallization behavior at different comonomer contents were examined. We found that the presence of aromatic functional groups can trigger the nucleation in the crystallization of PP even at a small addition amount without changing the physical properties of PP.

2-2. Experiments

2-2-1. Materials

Propylene of research grade was donated by Japan Polypropylene Co., Ltd. and used without further purification. *n*-Heptane (purchased from Kanto Chemical Co., Inc.) was dried by passing through a column of molecular sieve 4A followed by N_2 bubbling for 2 h prior to use. A fifth generation Ziegler-Natta catalyst ($TiCl_4$/diether/$MgCl_2$) was prepared using diether as an internal donor based on a patent [30]. Triethylaluminum (TEA) was donated from Tosoh Finechem Co. Styrene (Sty) and 1-allylnaphthalene (Naph) (purchased from Kanto Chemical Co., Inc.) were used as delivered. Octadecyl 3-(3,5-di-*tert*-butyl-4-hydroxyphenyl) propionate (AO-50) was donated by ADEKA Co. and used as a stabiliser.

2-2-2. Polymerization

Polymerization was conducted in a 1 L stainless steel reactor using the $TiCl_4$/diether/$MgCl_2$ catalyst. After sufficient N_2 replacement, 200 mL of heptane was introduced into the reactor. The solvent was saturated with 0.5 MPa of propylene at 50°C for 15 min. Thereafter, 2.0 mmol of TEA as an activator and 0-10 mmol of Sty or Naph as a comonomer were added prior to the addition of 10 mg of the catalyst and 8.0 mmol of hydrogen. Polymerization was conducted at 50°C under the total pressure of 0.5 MPa for 30 min. PP powder was repetitively washed with acidic ethanol and water, and reprecipitated from xylene into acetone followed by drying in *vacuo*.

2-2-3. Polymer characterization

The polymer structure was analyzed by NMR (Bruker 400 MHz) operated at 120°C. The comonomer content was determined based on ^{1}H NMR with the scan number of 1000 using hexachloro-1,3-butadiene as a diluent and 1,1,2,2-tetrachloroethane-d2 as an internal lock and reference. The stereostructure of PP was determined by ^{13}C NMR with the scan number of 5000 using 1,2,4-trichlorobenzene as a diluent, 1,1,2,2-tetrachloroethane-d2 as an internal lock and reference, and dibutylhydroxytoluene (BHT) as a stabilizer. The molecular weight and molecular weight distribution of the copolymer were measured by a gel-permeation chromatography (GPC, Waters ALC 150C) at 140°C and a flow rate of 1 mL/min using *o*-dichlorobenzene as an eluent. Polystyrene standards were used for calibration.

Differential scanning calorimetry (DSC) was acquired under N_2 on a Mettler Toledo DSC 822 analyzer to evaluate the crystallization behavior. After impregnating 1.0 wt% of AO-50 to PP powder using acetone as a solvent, PP powder was hot pressed into a

film with the thickness of 200 μm at 230°C under 20 MPa for 5 min followed by a stepwise quenching at 100°C for 5 min and at 0°C for 1 min. A film sample was heated in an aluminum pan at 230°C for 10 min to erase a thermal history, and then cooled down at the cooling rate of 5 °C/min to 132°C for isothermal crystallization. Both of the cooling rate and the crystallization temperature were carefully selected to evaluate reliable crystallization rates, which were defined as the inverse of the half time of the crystallization (denoted as $t_{1/2}^{-1}$). Subsequently, the sample was cooled down at the cooling rate of 20 °C/min to 50°C, and kept for 5 min. The melting temperature and the crystallinity were determined from the melting endotherm in the second heating, where the sample was heated to 200°C at the heating rate of 20 °C/min. The lamellar thickness distribution was calculated based on the following Gibbs -Thomson equation:

$$T_m = T_m^0 \left(1 - \frac{2\sigma_e}{l\Delta H_f}\right) \quad (1)$$

where T_m is the melting temperature of polymer, l is the lamellar thickness, T_m^0 is the equilibrium melting temperature of an infinite crystal, σ_e is the surface free energy of the basal plane and ΔH_f is the melting enthalpy of perfect crystal. Following values were used for the calculation: T_m^0 = 464.0 K, ΔH_f = 209 J/cm^3 and σ_e = 102.9 J/cm^2 [31].

The spherulite growth was observed using a polarized optical microscope (POM, Leica DMLP) equipped with an automated hot-stage (Mettler Toledo FP82HT). The retardation plate was used during POM observation. A film sample with the thickness of 50 μm was prepared in a similar way to the aforementioned method. The spherulite growth was observed at 135°C after heating the sample at 230°C for 10 min and subsequently cooling it to 135°C at 20 °C/min. The spherulite growth rate was

evaluated from POM images by measuring the diameter of each spherulite along the isothermal crystallization time. The rate of the nucleation was evaluated by counting the number of spherulites in a 1 mm^2 region of POM images at 1080 sec after reaching the isothermal crystallization temperature. The reproduction was confirmed by two independent measurements for each sample.

Tensile properties were measured at a crosshead speed of 1 mm/min at room temperature using a tensile tester (Abecks Inc., Dat-100). Film samples with the thickness of 200 μm were cut into a dumbbell shape specimen. The stress-strain curve for tensile properties was chosen as a representative of five independent measurements.

2-3. Results and Discussion

Propylene copolymerization in the presence of styrene (Sty) and 1-allylnaphthalene (Naph) was performed using a Ziegler-Natta catalyst. The amount of comonomers was varied as summarized along polymerization results in Table 1. No obvious effect of comonomer addition on the polymerization activity was observed for both of the Sty and Naph comonomers due to an extremely low concentration in the polymerization system (Figure 1). The ^1H NMR spectra for PP-Sty and PP-Naph are shown in Figure 2. The main peaks observed between 0.90 to 1.96 ppm are assigned to CH, CH_2 and CH_3 in the PP backbone, and both of the PP-Sty and PP-Naph polymers are presumed to have nearly the same structure as PP. Magnification of NMR spectra for a proton of a tertiary carbon at the branch point of the PP backbone and a proton in the aromatic region are shown in insets of Figure 2a,b. Despite being extremely small peaks, they are sufficiently strong to endorse the incorporation of comonomers. In the case of PP-Sty, the quantitative analysis of comonomer content was obtained from the ratio between the

peak area for a tertiary carbon proton at the branch point located at the chemical shift of δ = 2.84 ppm and the peak area for methine protons of the PP backbone at the chemical shift of δ = 1.72 ppm. It should be noted that the peaks assigned to aromatic protons in the benzene ring were not used in this case due to an overlap with impurity peaks originated from the NMR solvent. The comonomer content of PP-Naph was calculated using the peak area for aromatic protons of the naphthyl group detected at the chemical shift of δ = 8.15 ppm relative to the peak area of methine protons of the PP backbone.

Table 1. Summary of reaction conditions and results for the copolymerization.

Sample	Amount of comonomer addition (mmol)	Activity (kg-polymer /mol-Ti·h)	Comonomer Content[a] (mol%)	M_n (g/mol)	M_w/M_n	Number of functional groups per polymer chain	*mmmm*[b] (mol%)
homo-PP	0	6.1×10^3	-	6.60×10^4	5.17	0	93
PP-Sty1.5	1.5	5.7×10^3	1.2×10^{-2}	4.72×10^4	6.99	0.13	93
PP-Sty2.0	2.0	7.0×10^3	1.6×10^{-2}	6.58×10^4	5.41	0.25	93
PP-Sty2.5	2.5	4.7×10^3	1.8×10^{-2}	5.84×10^4	5.60	0.25	93
PP-Sty10	10	6.6×10^3	5.6×10^{-2}	6.87×10^4	5.09	0.92	93
PP-Naph1.0	1.0	6.5×10^3	5.0×10^{-3}	6.46×10^4	5.43	0.08	94
PP-Naph1.4	1.4	4.1×10^3	7.0×10^{-3}	-	-	-	94
PP-Naph1.5	1.5	6.0×10^3	8.0×10^{-3}	6.68×10^4	5.10	0.13	94
PP-Naph2.0	2.0	6.1×10^3	1.0×10^{-2}	6.73×10^4	5.07	0.16	94
PP-Naph2.5	2.5	5.0×10^3	1.4×10^{-2}	6.46×10^4	5.20	0.22	94
PP-Naph3.0	3.0	6.7×10^3	1.7×10^{-2}	5.85×10^4	5.88	0.24	94
PP-Naph10	10	5.2×10^3	4.2×10^{-2}	6.13×10^4	5.40	0.61	94

[a] Analyzed by ^{1}H NMR. [b] Analyzed by ^{13}C NMR.

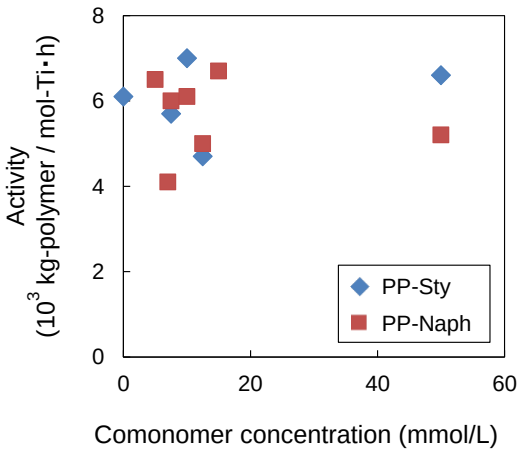

Figure 1. Effect of the comonomer concentration on the catalytic activity.

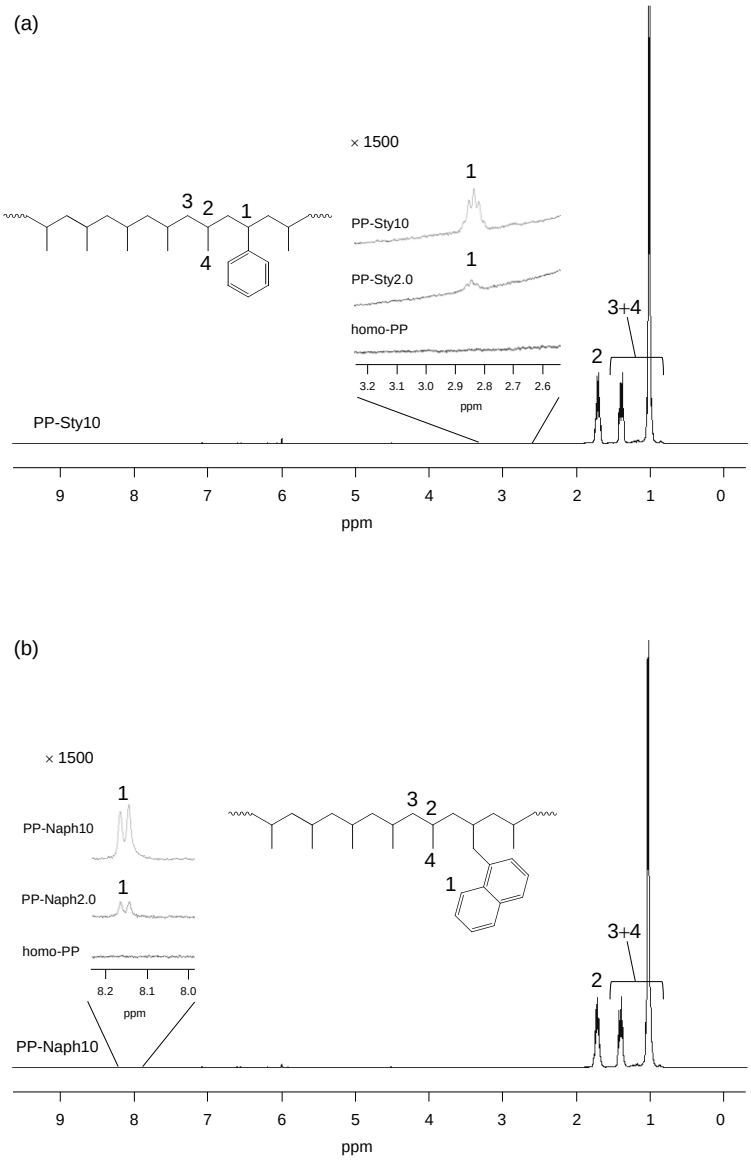

Figure 2. ^{1}H NMR spectra: (**a**) PP-Sty and (**b**) PP-Naph.

In order to confirm the incorporation of comonomers into the PP backbone, ^{13}C NMR analysis was conducted. However, the peaks of comonomer units could not be detected due to an extremely low content in both of the PP-Sty and PP-Naph copolymers. Consequently, additional polymerization was performed using the same catalyst system with the addition amount of comonomer of 100 mmol to confirm the incorporation.

Nonetheless, it was still unable to detect the peaks of Naph units by ^{13}C NMR, while the further increase of the comonomer addition amount led to the loss of the catalyst activity. On the other hand, the detection of comonomer units was successfully obtained in the case of Sty as a comonomer due to the higher incorporation amount (denoted as PP-Sty100). ^{13}C NMR spectra of PP-Sty100 and polystyrene homopolymer obtained by homopolymerization of Sty using the same catalyst are compared in Figure 3. It was clearly observed that the peak of methine carbons of Sty units in the copolymer shifted to downfield (42.2 ppm) with respect to methines of Sty units in the homopolymer (41.5 ppm), evidencing the incorporation of comonomer into the PP backbone without forming homopolymer. This fact let us believe that Sty and Naph comonomers with much lower reactivity hardly form its homopolymer in the presence of propylene.

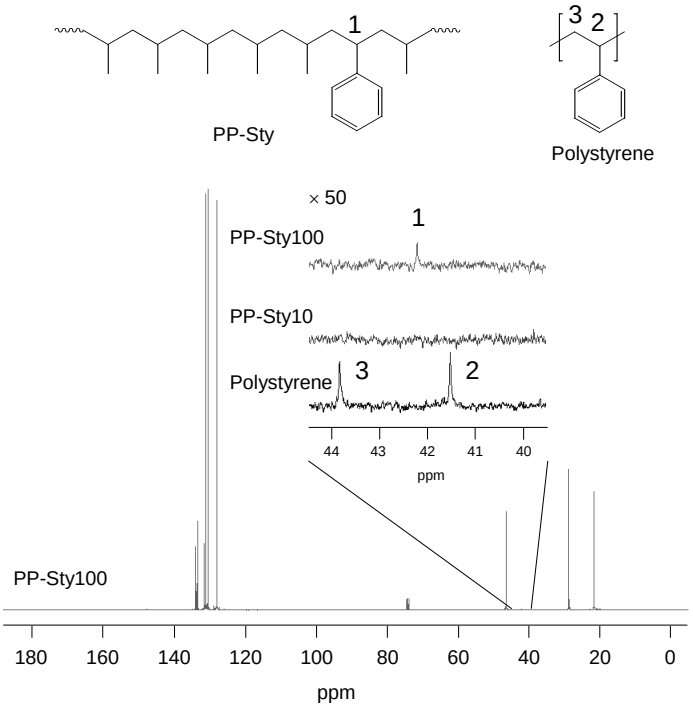

Figure 3. ^{13}C NMR spectra of PP-Sty and polystyrene homopolymer.

Figure 4 shows the relationship between the comonomer concentration in the polymerization medium and the amount of comonomer incorporated into PP chains. The increase of the comonomer concentration in the polymerization medium resulted in a monotonic increase of the comonomer incorporation for both of the Sty and Naph comonomers.

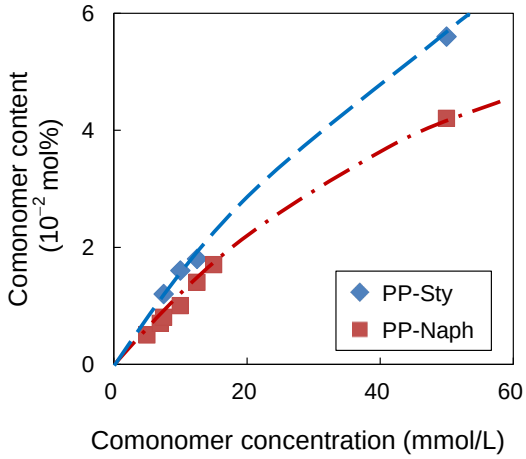

Figure 4. Relationship between the comonomer concentration and comonomer content.

The molecular weight and molecular distribution analyzed by GPC for all PP-Sty and PP-Naph polymers were found to be similar, and there was no obvious reduction in molecular weight due to the addition of comonomers (Table 1). The degree of polymerization calculated from the number average molecular weight (M_n) and the comonomer content obtained from ^{1}H NMR were used to estimate the average number of functional groups per polymer chain (Table 1). Since this value was less than 1 for all polymer samples, it is likely that there is existence of polymer chains without comonomer incorporation. The meso pentad (*mmmm*) for homo-PP, PP-Sty and

PP-Naph analyzed by ^{13}C NMR was almost the same at 93 to 94%, indicating that the stereoregularity was not affected by the presence of a small amount of comonomers.

Isothermal crystallization at 132°C was performed using DSC, and the results are shown in Table 2 and Figure 5. The crystallization rate ($t_{1/2}^{-1}$) was found to decrease gradually with the increase of the comonomer content, which is a typical tendency for the introduction of comonomers into side chains. However, an improvement in the crystallization rate was clearly evident when a very small amount of comonomer (*i.e.* less than 2×10^{-2} mol%) was incorporated for both of the PP-Sty and PP-Naph polymers. This behavior is an unusual for the introduction of comonomers at a normal content and has never been reported so far. For PP-Sty, the fastest crystallization rate was observed at a comonomer content of 1.6×10^{-2} mol% (PP-Sty2.0). In the case of PP-Naph, the fastest crystallization rate was observed at a comonomer content of 1.0×10^{-2} mol% (PP-Naph2.0). For both of the cases, the enhancement of the crystallization rate was also confirmed at 128°C. Although catalytic residues could potentially affect the crystallization behavior of the polymer, it must not be the case since the catalytic activity was essentially equal in all cases and the purification of polymer samples was similarly applied. In addition, ^{1}H NMR measurements confirmed that comonomer residues were completely removed from all polymer samples.

Table 2. Results of DSC measurements.

Sample	$t_{1/2}^{-1}$ [a] (s^{-1})	T_m [b] (°C)	X_c [b] (%)
homo-PP	$1.82 \pm 0.06 \times 10^{-3}$	168	49
PP-Sty1.5	1.8×10^{-3}	167	48
PP-Sty2.0	$2.20 \pm 0.06 \times 10^{-3}$	167	47
PP-Sty2.5	1.8×10^{-3}	167	47
PP-Sty10	1.7×10^{-3}	166	47
PP-Naph1.0	1.9×10^{-3}	167	48
PP-Naph1.4	2.1×10^{-3}	167	48
PP-Naph1.5	$2.20 \pm 0.09 \times 10^{-3}$	167	48
PP-Naph2.0	$2.50 \pm 0.07 \times 10^{-3}$	167	48
PP-Naph2.5	2.1×10^{-3}	167	48
PP-Naph3.0	1.9×10^{-3}	167	48
PP-Naph10	1.7×10^{-3}	167	47

[a] Isothermal crystallization rate at 132°C. [b] Obtained from the melting endotherm in the second heating cycle at the heating rate of 20 °C/min.

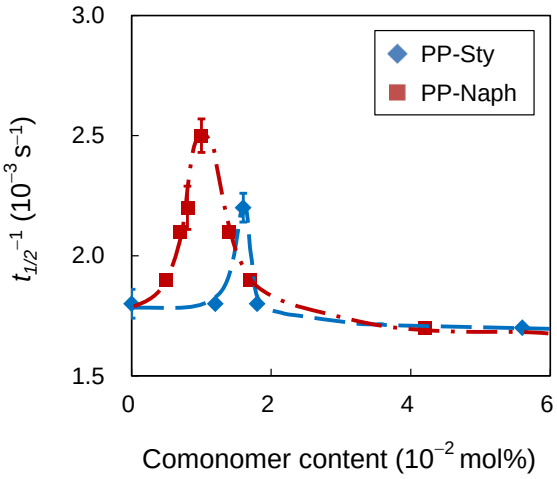

Figure 5. Effect of the comonomer content on the crystallization rate.

The melting temperature and the crystallinity were calculated using the endothermic peak observed during the second heating to 230°C after isothermal crystallization (Table 2). The lamellar thickness distribution was calculated from the melting endotherm using Gibbs-Thomson equation (Figure 6). It was found that the melting temperature, the

crystallinity and the lamellar thickness distribution were similar for all samples. The tensile properties were also evaluated for homo-PP and PP-Naph10 samples. Figure 7 shows that there is almost no difference for the tensile properties for both of the samples. These results confirmed that the incorporation of functional comonomers into PP chains at a small amount has no effect on the base properties of PP, in contrast to the crystallization behavior. Compared at the same comonomer content, the crystallization rate was faster for PP-Naph than for PP-Sty, demonstrating that Naph groups introduced in PP chains affected the crystallization behavior more effectively than Sty groups. It is speculated that intermolecular interaction of PP chains through aromatic rings and/or the presence of the heterogeneous structures induced the crystallization of PP. In contrast, introducing a relatively high comonomer content exhibited the typical effects for the introduction of side chains (*i.e.* When the comonomer content was increased over some level, the enhancement in the crystallization rate rather disappeared plausibly due to the said side-chain effects.).

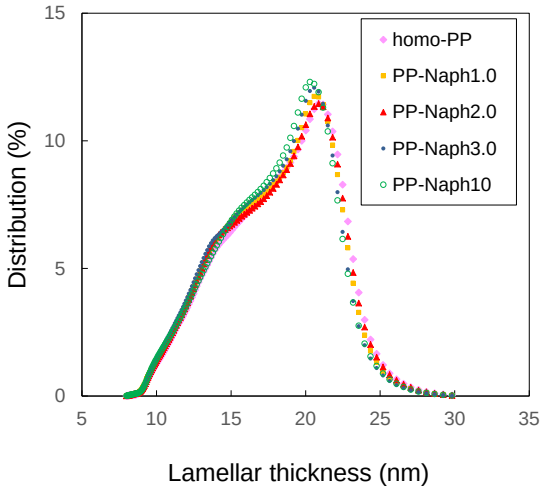

Figure 6. Lamellar thickness distribution of homo-PP and PP-Naph.

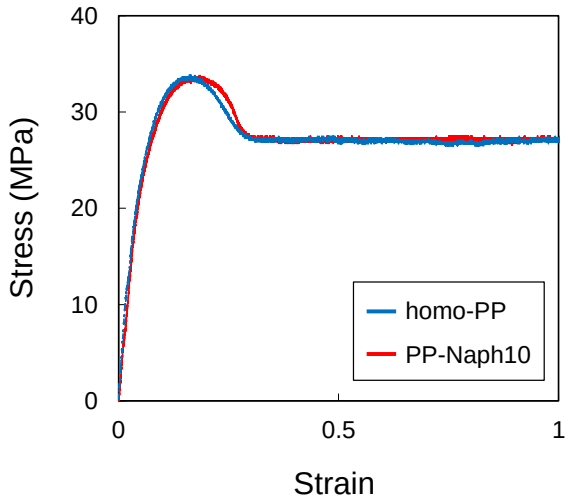

Figure 7. Stress-strain curves of homo-PP and PP-Naph10.

To understand the origin of the crystallization rate enhancement, the spherulite formation was observed by POM during isothermal crystallization at 135°C (Figure 8). The obtained POM images were used to calculate the nucleation and spherulite growth rates. The results showed a clear difference for the nucleation rate calculated based on the number of spherulites at 1080 sec after reaching the isothermal crystallization temperature. PP-Naph2.0, which possessed the greatest crystallization rate enhancement, exhibited the largest nucleation rate (Figure 9a). On the other hand, almost no difference was observed for the spherulite growth rate for all samples (Figure 9b). These results demonstrated that the enhancement of the crystallization rate was caused by nucleation. POM observation was also performed for PP-Sty2.0, which exhibited the greatest enhancement of the crystallization rate among PP-Sty samples. The result showed the increment of spherulite density and nucleation rate similarly to PP-Naph system, indicating nucleation accelerated crystallization.

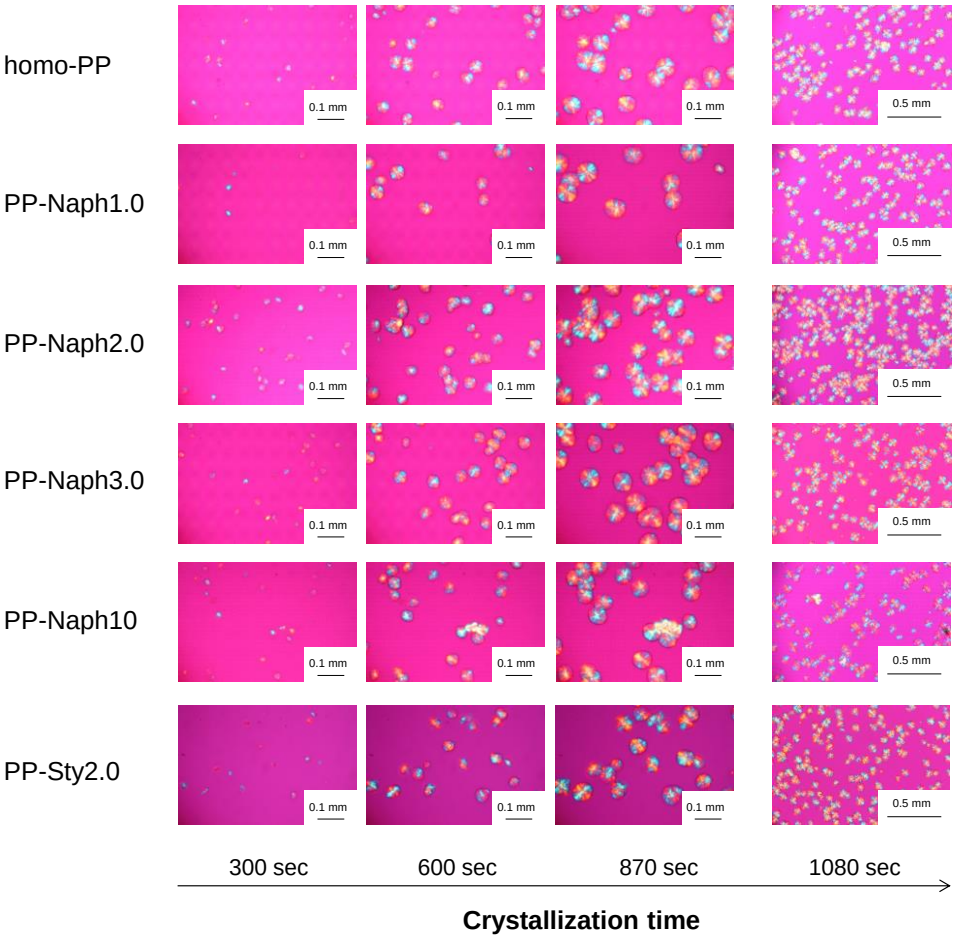

Figure 8. POM images during isothermal crystallization at 135°C.

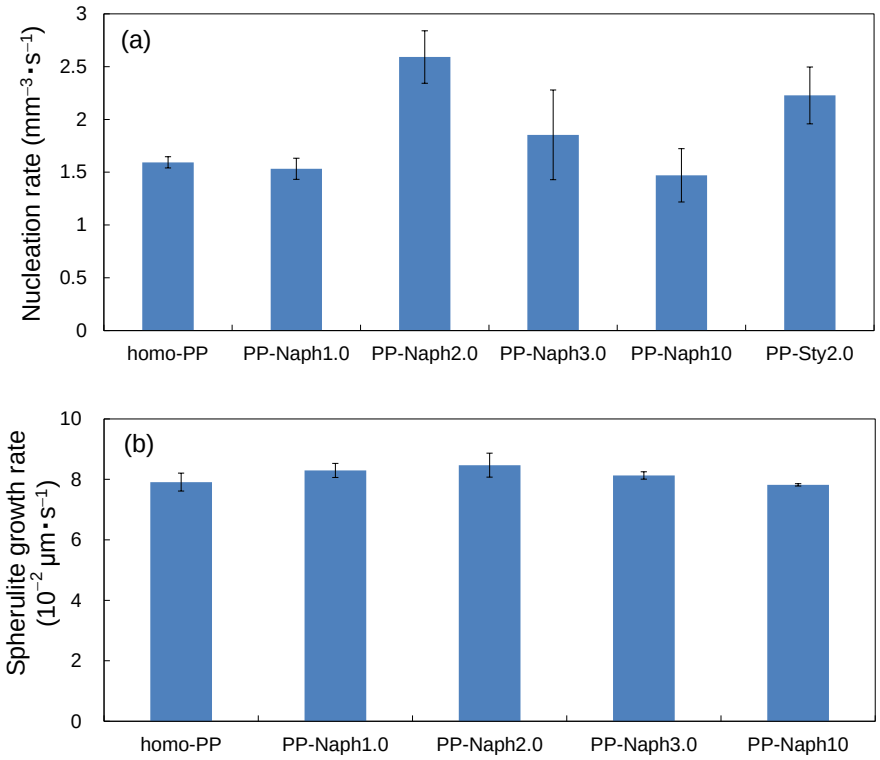

Figure 9. Crystallization behavior of homo-PP and copolymers:

(a) nucleation and (b) spherulite growth rates.

2-4. Conclusions

A small amount of aromatic functional groups was introduced into polypropylene by copolymerization with styrene or 1-allylnaphthalene using a Ziegler-Natta catalyst. The synthesized polymers contained less than 0.1 mol% of the comonomer content. The addition of comonomers at a small amount in polymerization not only suppressed unfavorable effects during polymerization such as a decrement in catalytic activity, but also preserved the base properties of PP such as the melting temperature, the crystallinity and the tensile properties. On the contrary, an enhanced crystallization rate was observed even at a small amount of comonomer incorporation due to an accelerated nucleation, which probably originated from the polymer chain aggregation or restrictions on the movement of the polymer chains. This feature is expected to be useful for improving the polymer properties.

References

[1] N. Kashiwa, *J. Polym. Sci. Pol. Chem.*, **42**, 1 (2004).

[2] T. Taniike, M. Terano, *Adv. Polym. Sci.*, **257**, 81 (2013).

[3] W. Kaminsky, *J. Chem. Soc., Dalton Trans.*, 1413 (1998).

[4] L.S. Boffa, B.M. Novak, *Chem. Rev.*, **100**, 1479 (2000).

[5] K. Soga, H. Yanagihara, *Macromolecules*, ***22***, 2875 (1989).

[6] A.G. Simanke, G.B. Galland, L. Freitas, J.A.H. Da Jornada, R. Quijada, R.S. Mauler, *Polymer*, **40**, 5489 (1999).

[7] M.A. Villar, M.D. Failla, R. Quijada, R.S. Mauler, E.M. Vallés, G.B. Galland, L.M. Quinzani, *Polymer*, **42**, 9269 (2001).

[8] P. Starck, K. Rajanen, B. Löfgren, *Thermochim. Acta*, **395**, 169 (2003).

[9] C. Piel, P. Starck, J.V. Seppälä, W. Kaminsky, *J. Polym. Sci. Pol. Chem.*, **44**, 1600 (2006).

[10] D. Mäder, J. Heinemann, P. Walter, R. Mülhaupt, *Macromolecules*, **33**, 1254 (2000).

[11] M. Gahleitner, P. Jääskeläinen, E. Ratajski, C. Pailik, J. Reussner, J. Wolfschwenger, W. Neißl, *J. Appl. Polym. Sci.*, **95**, 1073 (2005).

[12] M. Arnold, O. Henschke, J. Knorr, *Macromol. Chem. Phys.*, **197**, 563 (1996).

[13] H. Lovisi, M.I.B. Tavares, N.M. Da Silva, S.M.C. De Menezes, L.C. De Santa Maria, F.M.B. Coutinho, *Polymer*, **42**, 9791 (2001).

[14] S. Hosoda, H. Hori, K. Yada, S. Nakahara, M. Tsuji, *Polymer*, **43**, 7451 (2002).

[15] B. Poon, M. Rogunova, A. Hiltner, E. Baer, S.P. Chum, A. Galeski, E. Piorkowska, *Macromolecules*, **38**, 1232 (2005).

[16] C. De Rosa, F. Auriemma, O.R. De Ballesteros, L. Resconi, I. Camurati, *Macromolecules*, **40**, 6600 (2007).

[17] F. Machado, E.L. Lima, J.C. Pinto, T.F. McKenna, *Eur. Polym. J.*, **44**, 1102 (2008).

[18] F. Bi, A. He, H. Li, Y. Hu, Z. He, C.C. Han, *Polym. Int.*, **60**, 1167 (2011).

[19] S. Gupta X. Yuan, T.C.M. Chung, M. Cakmak, R.A. Weiss, *Polymer*, **55**, 924 (2014).

[20] H.L. Lu, S. Hong, T.C. Chung, *J. Polym. Sci. Pol. Chem.*, **37**, 2795 (1999).

[21] M.J. Yanjarappa, S. Sivaram, *Prog. Polym. Sci*., **27**, 1347 (2002).

[22] T.C. Chung, *Prog. Polym. Sci*., **27**, 39 (2002).

[23] J.-Y. Dong, Y. Hu, *Coordin. Chem. Rev.*, **250**, 47 (2006).

[24] T.C.M. Chung, *Macromolecules*, **46**, 6671 (2013).

[25] X.-Y. Wang, Y.-X. Wang, Y.-S. Li, L. Pan, *Macromolecules*, **48**, 1991 (2015).

[26] X.-Y. Wang, Y.-G. Li, H.-L. Mu, L. Pan, Y.-S. Li, *Royal Society of Chemistry Polymer Chemistry*, **6**, 1150 (2015).

[27] T.C.M. Chung, *Adv. Polym. Sci.*, **258**, 233 (2013).

[28] T. Taniike, M. Toyonaga, M. Terano, *Polymer*, **55**, 1012 (2014).

[29] M. Toyonaga, P. Chammingkwan, M. Terano, T. Taniike, *Polymers*, **8**, 300 (2016).

[30] M. Kioka, H. Kitani, N. Kashiwa, U.S. Patent US4330649A, 18, May, (1982).

[31] A. Romankiewicz, T. Sterzynski, *Macromol. Symp*., **180**, 241 (2002).

Chapter 3

Improvement of physical properties of polypropylene with a small amount of reactive functional group

3-1. Introduction

Polypropylene (PP) is inexpensive, has well-balanced physical properties, and features excellent characteristics such as good moldability, currently making it the most common plastic with diverse uses that include packaging film, food containers, automobile parts, and electronic components. In addition, it has low environmental impact due to being lightweight, easy-to-recycle, and halogen-free, and its use is therefore expected to expand to even more fields.

Due to the fact that control of PP tacticity, i.e., of the primary structure, is crucial to obtaining excellent PP physical properties, research on propylene polymerization catalysts has mainly focused on improving catalytic activity and enhancing PP tacticity since the titanium trichloride catalyst was discovered through the work Natta *et al.* in 1954. Through the addition of an optimal donor, current $MgCl_2$-supported catalysts exhibit a several hundred fold increase in catalytic activity, as well as high stereoselectivity that makes the removal of atactic PP virtually unnecessary, compared to the catalysts in the days of Natta and his peers. The physical properties of PP were also further enhanced by developments such as impact copolymers that achieve high dispersion of rubber particles through preparation via reactor alloys using multi-stage polymerization, glass fiber and other PP compounds with blended inorganic filler, PP crystal orientation control achieved through molding technology refinements, or morphology control.

In contrast, since PP is a nonpolar polymer composed of carbon and hydrogen, it has extremely poor compatibility and bondability with other polymers. Research on the functionalization of PP to improve those properties has been actively pursued, and it is possible that the strong interaction between functional groups could improve the

mechanical properties of functionalized PP itself. A compound with ureidopyrimidinone units at both ends of the hexamethylene forms hydrogen bonds has been reported to produce very stable long polymer chains by the intermolecular interaction between its two quadruple hydrogen bonding both in solution and in the bulk [1]. Although this compound consists of small molecules, it exhibits low concentration and high viscosity in chloroform. It is therefore known that substances exhibiting sufficient interaction to change the physical properties of compounds through functional groups exist. Similarly, functional groups introduced in PP chains are expected to play an important role in improving the physical properties of PP.

Functionalizing PP can be performed through copolymerization using a catalyst [2-5], or through the post-treatment of the PP [6-9]. The most prevalent industrial functionalization process is currently functionalization through post-treatment (post-polymerization). Maleic anhydride modified PP (MAPP), the most commonly used functionalized PP on the market, is prepared by causing peroxide to act on the PP, forming free radicals in the polymer chains by extruding H radicals from the C-H bonds in the main chain, and initiating a reaction between those free radicals and maleic anhydride. However, since the tertiary macroradicals formed in the main chain due to the addition of peroxide simultaneously advance the β-scission of the PP main chain, a decrease in the molecular weight of the PP is unavoidable. As a result, the application of MAPP is currently limited to additives, such as dispersants used to achieve high dispersion of inorganic fillers in the polymer or compatibilizers in alloying with other polymers. There are also reports concerning the introduction of reactive functional groups in the PP chains through post-polymerization. In other research, silane grafting is performed by causing interaction between a peroxide and PP through melt-mixing

with vinylalkoxysilane, followed silane crosslinking [10]. Silane-grafted moisture curable polyethylene has been in wide commercial use since the 1970s, with many papers and patents concerning the silane grafting of polyolefin issued since then [11-13]. There are a few reports regarding silane crosslinking of PP. The hydrolysis and condensation reaction of alkoxysilane advances the crosslinking reaction and produces gels, but in PP, β-scission of the PP chains occurs in conjunction with the silane grafting of functional groups in the PP chains and the crosslinking reaction. The high temperature melt-mixing performed to reduce cost is tends to advance the β-scission of the PP chains extremely rapidly, making silane grafting and crosslinking difficult to obtain. The decomposition has a significant impact on the physical properties, preventing sufficiently effective enhancement of those properties during the formation of a crosslinking structure.

In contrast, reactive functional groups can also be introduced through copolymerization. Chung and his team performed propylene copolymerization using a metallocene catalyst to synthesize a linear poly(propylene-co-*p*-(3-butenylstyrene))copolymer (PP-BSt), followed by a heat treatment that triggered a Diels-Alder [2+4] interchain cycloaddition reaction between the pendent styrene groups to synthesize a crosslinked polymer [14]. They compared it to a poly(propylene-co-*p*-divinylbenzene)copolymer (PP-DVB) synthesized with the same metallocene catalyst and deduced, based on the fact that the presence of small quantities of functional group content in the PP-BSt copolymer facilitated the cycloaddition reaction between polymer chains, that having a flexible spacer effectively accelerated the formation of a three-dimensional crosslinked network [15]. Moreover, at a pendent styrene reactive functional group content of 0.16 mol%, the PP-BSt

copolymer had melting temperature of 154°C, before crosslinking, and exhibited a gel content of approximately 75% and a melting temperature of 153°C after crosslinking. At a pendent styrene content of 0.73 mol%, the melting temperature dropped to 142°C, and after crosslinking, the gel content rose to 95% or higher while the melting temperature dropped to 135°C. The greater number of crosslinked structures was observed to reduce crystallinity. The physical properties of PP can therefore be enhanced through the introduction of reactive functional groups in the PP chains via copolymerization and the subsequent crosslinking reaction. Even with a small quantity of reactive functional groups, triggering reactions such as crosslinking can notably be expected to have a significant effect on enhancing the physical properties of PP. Almost all research on the introduction of reactive functional groups via copolymerization involves the use of metallocene catalysts. There are almost no examples of studies of polymer physical properties where reactive functional groups are introduced in the PP chains using ZN catalysts, which are the most commonly used in industrial applications. The main reason for this is the poisoning of the ZN catalyst by the polar reactive functional groups. With small-scale functionalization using a ZN catalyst, the fact that comonomers are added on a small-scale means it should be possible to introduce reactive functional groups in the polymerization reaction with minimal concern about the poisoning of the catalyst.

This research studied the small-scale introduction of reactive functional groups in the PP chains and also tested the post-polymerization reaction between functional group, with the objective of enhancing the physical properties of PP. The copolymerization of propylene and comonomers having alkoxysilyl groups using a ZN catalyst was performed. After polymerization, the formation of crosslinks through the reaction

between alkoxysilyl groups was tested by melt-mixing the polymers. The functional group content in the obtained functionalized PP was analyzed by ^{1}H NMR. Differential scanning calorimetry (DSC) was used to measure the melting temperature, crystallinity, and the crystallization rate based on isothermal crystallization at 144°C. Similarly, the spherulites were observed through polarized optical microscopy (POM) and a tensile test was performed to evaluate their mechanical properties.

3-2. Experiments

3-2-1. Materials

Propylene of research grade was donated by Japan Polypropylene Co., Ltd. and used without further purification. *n*-Heptane (purchased from Kanto Chemical Co., Inc.) was dried by passing through a column of molecular sieve 4A followed by N_2 bubbling for 2 h prior to use. A 5th-generation Ziegler-Natta catalyst ($TiCl_4$/diether/$MgCl_2$) was prepared using diether as an internal donor based on a patent [16]. Triethylaluminum (TEA) was donated from Tosoh Finechem Co. Trimethoxy(7-octen-1-yl)silane (purchased from Aldrich Chemical Inc.) was used as delivered. Octadecyl 3-(3,5-di-tert-butyl-4-hydroxyphenyl) propionate (AO-50) was donated by ADEKA Co. and used as a stabiliser.

3-2-2. Polymerization

Polymerization was conducted in a 1 L stainless steel reactor using the $TiCl_4$/diether/$MgCl_2$ catalyst. After sufficient N_2 replacement, 200 mL of heptane was introduced into the reactor. The solvent was saturated with 0.5 MPa of propylene at 50°C for 15 min. Thereafter, 2.0 -7.0 mmol of TEA and 0-5.0 mmol of

Trimethoxy(7-octen-1-yl)silane comonomer were added prior to the addition of 30 mg of catalyst and 8.0 mmol of hydrogen. Polymerization was conducted at 50°C under the total pressure of 0.5 MPa for 30 min. PP powder was repetitively washed with acidic ethanol and water, and reprecipitated from xylene into acetone followed by drying in *vacuo*.

3-2-3. Post-polymerization

A twin screw extruder (Xplore Instruments, Micro Compounder IM5) was used to mix 3.5 g of polymer at 185°C under nitrogen at a mixing rate of 100 rpm. The polymer was previously impregnated in 1.0 wt% AO-50 in acetone, and the mixing force during mixing was monitored.

3-2-4. Sample film preparation

Polymer was hot pressed into a film with the thickness of 200 μm at 230°C under 20 MPa for 5 min followed by stepwise quenching at 100°C for 5 min and at 0°C for 1 min.

3-2-5. Polymer characterization

The gel content was measured to estimate the degree of crosslinking in the samples. After melt-mixing, the samples were finely cut, wrapped in a stainless steel net with a 150 μm mesh, and their initial weight was measured. The above samples were soaked in 200 mL of xylene, which was boiled for 6.5 h. The samples wrapped in the net were washed with acetone and dried in vacuo at 60°C for 1.5 h, and their weight after drying was measured. The gel content (wt%) was calculated based on the weight after the test

relative to the initial weight.

The polymer structure was analyzed by NMR (Bruker 400 MHz) operated at 120°C. The comonomer content was determined based on ^{1}H NMR with the scan number of 1000 using hexachloro-1,3-butadiene as a diluent, 1,1,2,2-tetrachloroethane-d2 as an internal lock and reference. The stereostructure of PP was determined by ^{13}C NMR with the scan number of 5000 using 1,2,4-trichlorobenzene as a diluent, 1,1,2,2-tetrachloroethane-d2 as an internal lock and reference, and dibutylhydroxytoluene (BHT) as a stabilizer.

Molecular weight and molecular weight distribution of the copolymer were measured by gel-permeation chromatography (GPC) using a Waters ALC/GPC 150C at 140°C and a flow rate of 1 mL/min using *o*-dichlorobenzene as an eluent. Polystyrene standards were used for calibration.

Differential scanning calorimetry (DSC) was acquired under N_2 on a Mettler Toledo DSC 822 analyzer to evaluate the crystallization behavior. The melting temperature (T_m) and the crystallinity (X_c) were determined from the melting endotherm in the first heating, where a sample was heated to 230°C at the heating rate of 20°C/min. A film sample was heated in an aluminum pan at 230°C for 10 min to erase a thermal history, and then cooled down at the cooling rate of 50°C/min to 144°C for isothermal crystallization. Both of the cooling rate and the crystallization temperature were carefully selected to evaluate reliable crystallization rates, which were defined as the inverse of the half time of the crystallization (denoted as $t_{1/2}^{-1}$). The crystallization temperature (T_c) was determined from the exothermic peak observed after heating the samples at 230°C for 10 min and cooling them at a rate of 20°C/min.

Spherulite growth was observed using a polarized optical microscope (POM) (Leica DMLP) equipped with an automated hot-stage (Mettler Toledo FP82HT). A film sample

with the thickness of 50 μm was prepared based on the aforementioned method. The spherulite growth was observed at 144°C after heating a sample at 230°C for 10 min. The temperature was decreased up to 144°C at 20°C/min.

Tensile properties were measured at a crosshead speed of 1 mm/min at room temperature using a tensile tester (Abecks Inc., Dat-100). Film samples were cut into a dumbbell shape for use as tensile test specimens. The Young's modulus and tensile strength values represent the average of the values obtained in tensile tests on five or more specimens.

3-3. Results and discussion

Allyltriethoxysilane (ATES) was used as a comonomer to perform copolymerization of propylene with a Ziegler-Natta (ZN) catalyst, and the introduction of reactive functional groups in the PP chains was studied. Polymerization where 2.0 mmol of ATES was added yielded approximately 30 g of polymer. ^{1}H NMR measurements were taken to analyze the polymer structure, but no peaks belonging to the comonomers could be identified. The added ATES content used in the reactions was therefore increased to 10 mmol, and copolymerization with propylene was performed again. The resulting quantity of obtained polymer decreased to approximately 11 g. Although the quantity of added comonomer content during polymerization was increased, the ^{1}H NMR spectrum only showed peaks originating in the PP, and no peaks originating in the comonomers were detected. This led to the conclusion that the copolymerization of ATES and propylene is exceedingly difficult. Consequently, trimethoxy(7-octen-1-yl)silane (OTMS), which has longer spacers between the double bonds and the functional groups, was used as a comonomer (Scheme 1).

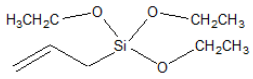

Allyltriethoxysilane (ATES)

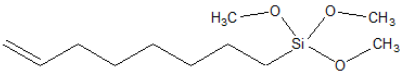

Trimethoxy(7-octen-1-yl)silane (OTMS)

Comonomer structure

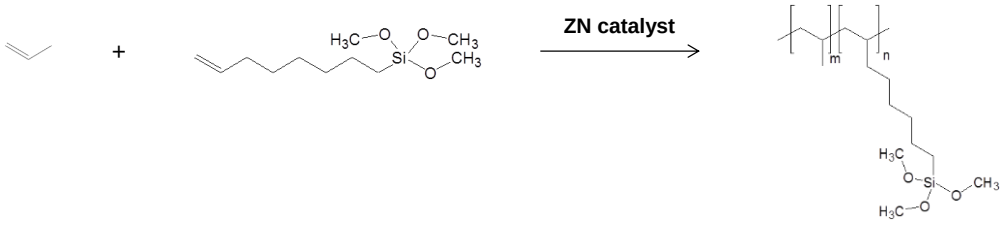

Poly(propylene-co- trimethoxy(7-octen-1-yl)silane)
(PP-OTMS)

Scheme 1

Table 1 summarizes the polymerization results. Catalytic activity was observed to decrease as the introduced comonomer content increased (Figure 1). However, at extremely low comonomer concentrations, there was almost no effect on catalytic activity. This clearly indicates that small-scale functionalization is effective in terms of synthesizing functionalized PP. ^{1}H NMR measurements were taken to analyze the polymer structure (Figure 2). Even for the PP-OTMS5 copolymer, which is expected to have the highest introduced comonomer content, the spectrum showed the main chain structure of PP in almost all respects. A peak assigned to the methoxy group were observed around $\delta = 3.7$ ppm in the expanded spectrum for the region from the $\delta = 3.5$ ppm to 6.0 ppm. Since no H^4 or H^5 peaks assigned to the protons of the vinyl end group originating from the comonomer were observed in the ^{1}H NMR spectrum for the OTMS copolymer, it is clear that all comonomer residues in the samples were completely removed. Although no copolymerization process with propylene was observed for the

ATES comonomer, the longer spacers in the OTMS comonomer prevented poisoning of the ZN catalyst and enabled copolymerization. The comonomer content introduced in the copolymer chains was calculated from ^{1}H NMR using to the equation below, based on the methine protons found in the PP main chain at δ = 1.72 ppm and the strength of the peak assigned to the protons of the methoxy group found at the chemical shift of δ = 3.7 ppm.

$$\text{Comonomer content (mol\%)} = \frac{\underline{H^{8}}/9}{\underline{H^{3}}} \times 100$$

The calculation yielded a comonomer content of 1.3×10^{-3} to 4.4×10^{-3} mol% incorporated into the PP chains. As the comonomer concentration in the polymerization system rose, the comonomer content increased (Figure 3). The added comonomer content increased the molecular weight observed by GPC (Table 1). It is conceivable that the alkoxysilane used as an external donor accelerated the growth rate of the PP chains. The degree of polymerization calculated from the number average molecular weight M_n and the comonomer content calculated with ^{1}H NMR were used to deduce the average number of functional groups per polymer chain (Table 1). Since this value was much lower than 1 for all polymers, it is likely that the polymers obtained contain a mix of polymer chains in which functional groups were introduced and chains in which they were not. The *mmmm* calculated using ^{13}C NMR exhibited a tendency to increase as comonomers were added (Table 1). It is possible that the polar comonomers selectively poisoned the atactic sites.

Table 1. Summary of reaction conditions and results for the copolymerization

Sample	Amount of comonomer addition (mmol)	Activity (kg-polymer / mol-Ti·h)	Comonomer content[a] (mol%)	M_n (g/mol)	M_w (g/mol)	M_w/M_n	Number of functional groups per polymer chain	*mmmm*[b] (mol%)
homo-PP	0	3450	-	4.84×10^4	2.06×10^5	4.26	0	92
PP-OTMS1	1	3500	1.3×10^{-3}	5.18×10^4	2.30×10^5	4.44	0.02	93
PP-OTMS2	2	2950	2.2×10^{-3}	5.65×10^4	2.32×10^5	4.11	0.03	95
PP-OTMS3	3	2650	2.9×10^{-3}	6.40×10^4	2.59×10^5	4.05	0.04	96
PP-OTMS5	5	1350	4.4×10^{-3}	-	-	-	-	96

[a] Analyzed by ^{1}H NMR. [b] Analyzed by ^{13}C NMR.

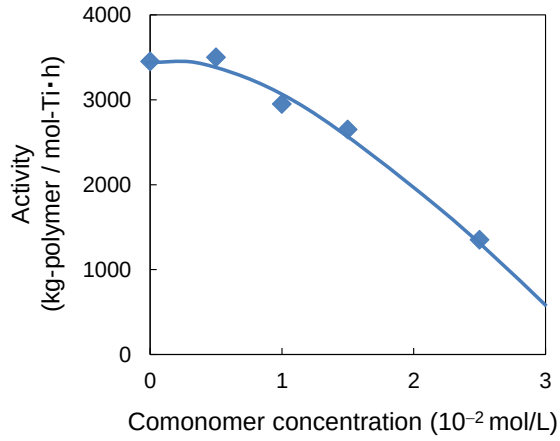

Figure 1. Effect of comonomer concentration on the catalytic activity.

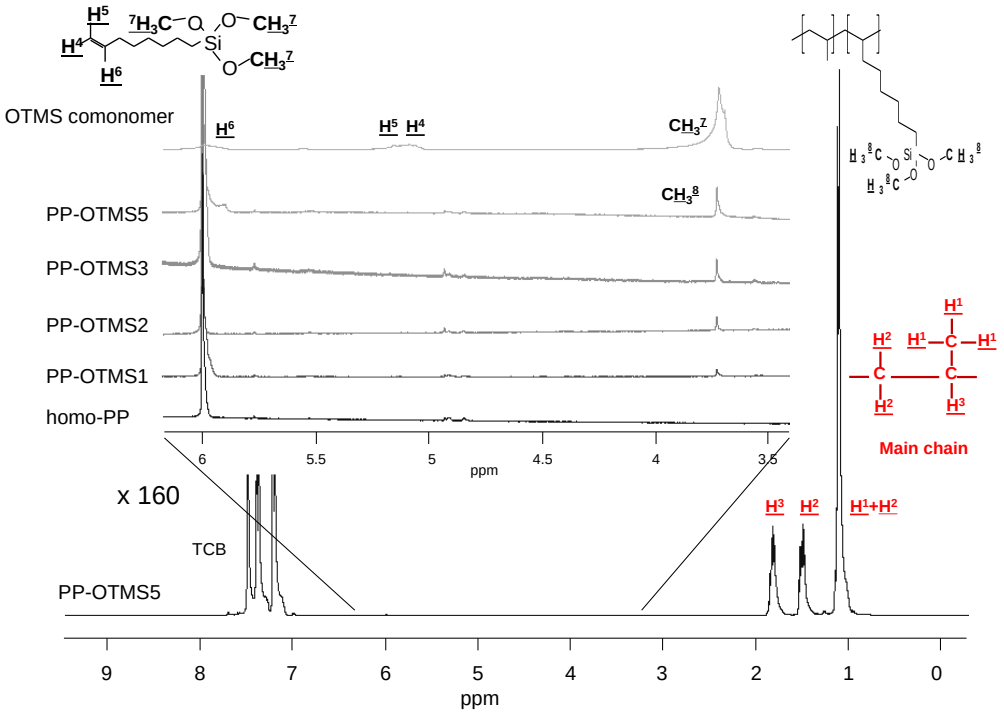

Figure 2. ^{1}H NMR spectra of homo-PP and PP-OTMS.

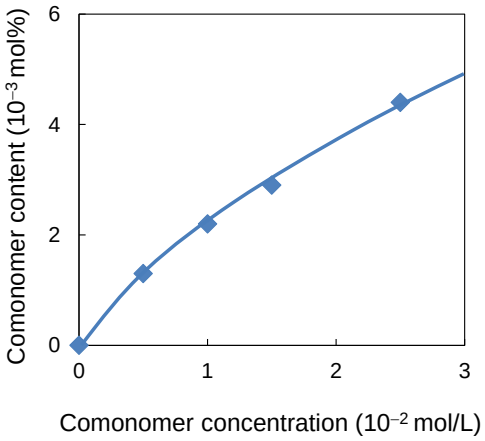

Figure 3. Relationship between comonomer concentration and comonomer content.

Melt-mixing of the PP-OTMS copolymers was applied as a post-polymerization process to induce crosslinkage through a dehydrative condensation reaction between the

methoxysilyl groups, which are reactive functional groups, incorporated into the PP chains (Scheme 2). Measuring the mixing force showed that it tended to increase in proportion with a higher comonomer content in the polymer chains (Figure 4). A condensation reaction occurring between the functional groups could increase mixing force. However, molecular weight increased as the numbers of functional groups rose. Consequently, the possibility that the higher mixing force resulted from the increase in molecular weight precluded a judgment on the functional group reactions. GPC measurements were made to observe functional group reactions due to melt-mixing arising from changes in molecular weight, and the results showed almost no such changes due to melt-mixing (Table 2). Crosslink formation due to functional group reactions could not be clearly identified from molecular weight measurements either. It is possible that molecular weight is not subject to significant change even if the functional groups introduced on a small scale triggered a crosslinking reaction. The interaction of the functional groups is also a probable cause of the increase in mixing force. Weiss *et al.* have reported that hydrogen bonding causes a greater viscosity increase in PP-OH than in PP [17]. However, in this research, the effect of hydrogen bonding on viscosity is expected to be minor due to the small scale of the functional group content.

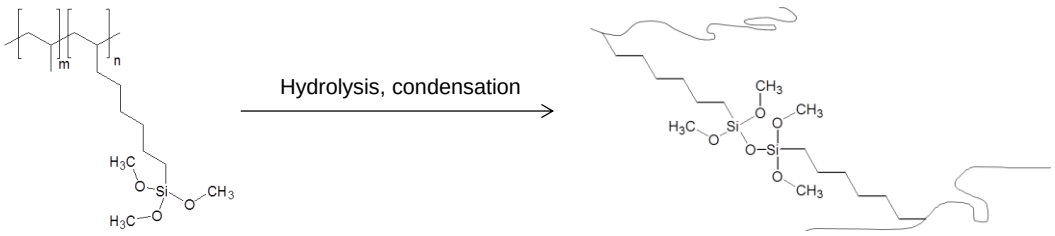

Scheme 2

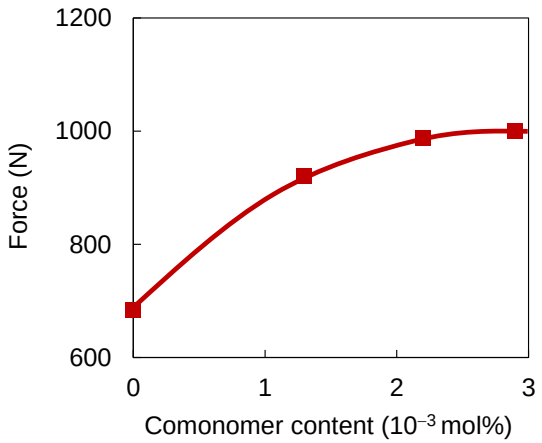

Figure 4. Relationship between comonomer content and mixing force.

Table 2. Results of GPC measurements of polymer after melt-mixing

Sample	M_n (g/mol)	M_w (g/mol)	M_w/M_n
homo-PP	4.58×10^4	1.90×10^5	4.15
PP-OTMS1	5.39×10^4	2.22×10^5	4.12
PP-OTMS2	5.68×10^4	2.27×10^5	4.00
PP-OTMS3	5.49×10^4	2.44×10^5	4.44

In order to investigate the progress of the reaction of functional groups during post-polymerization, ^{1}H NMR measurements were used to analyze the structure of the PP OTMS copolymer. The OMe content in the copolymer calculated from the ^{1}H NMR spectrum after melt-mixing became lower (Figure 5). This decrease in OMe content suggests the possibility that melt-mixing induced PP chain crosslinking via dehydrative condensation after the hydrolysis of the OMe groups. Figure 6 shows the relationship between the OMe content before melting and the reacted amount of the OMe groups during melt-mixing. While the amount of reacted functional groups rose as their

contents in the polymer increased, the amounts of reacted OMe groups were approximately constant for PP OTMS2 and PP OTMS3.

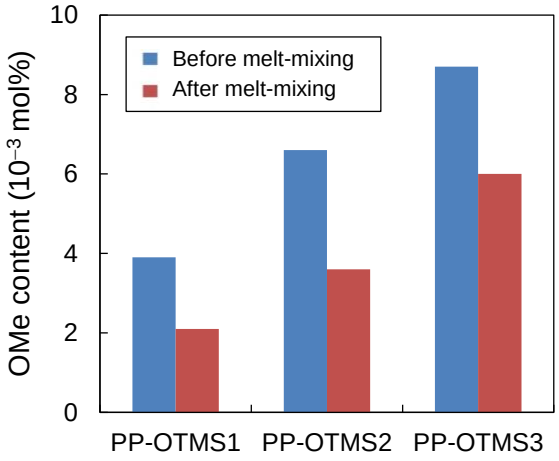

Figure 5. OMe content of PP-OTMS before and after melt-mxing.

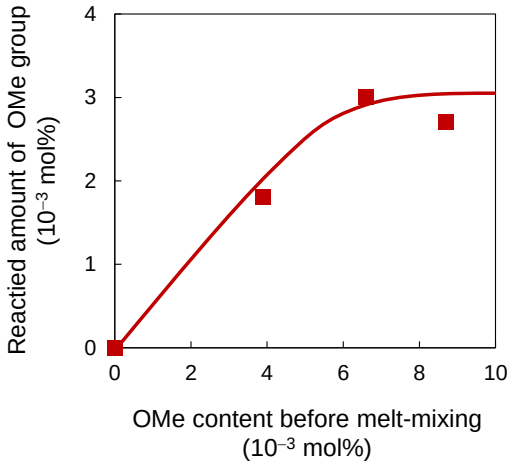

Figure 6. Relationship between OMe content and reacted amount of OMe group.

The gel content in the polymers was also calculated (Figure 7). Since 99% of each polymer dissolved in xylene, it was deduced that three-dimensional crosslinking structures did not form in the majority of the polymers, and the clear presence of xylene-insoluble matter in the PP-OTMS2 and PP-OTMS3 suggests the formation of three-dimensional crosslinking structures. Despite the almost identical reacted amounts of OMe group during melt-mixing in PP-OTMS2 and PP-OTMS3, the latter exhibited a higher gel content than the former. The higher gel content in PP-OTMS3 is attributed to additional three-dimensional crosslinkage due to intermolecular reactions arising from the higher number of functional groups in the polymer chain compared to PP-OTMS2. In contrast, the fact that the PP-OTMS1 gel content was the same 0 wt% as homo-PP indicates that three-dimensional crosslinking did not occur to an extent sufficient to form gel because there were exceedingly few functional groups, but it does not negate the possibility of functional group reactions progress.

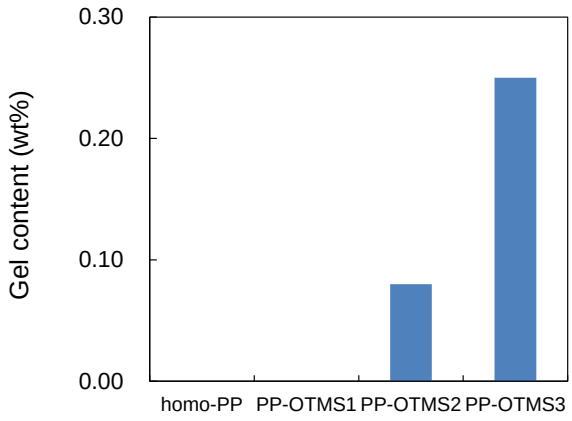

Figure 7. Gel content of PP-OTMS copolymer.

DSC measurement was conducted to investigate the crystallization behavior of PP-OTMS after the post-polymerization process (Table 3). The melting temperature and crystallinity almost maintain their values of homo-PP, regardless of the difference of the number of functional groups. In contrast, the crystallization temperature of PP OTMS copolymer measured for the non-isothermal crystallization rose by about 10°C above that for homo PP. The crystallization rate was calculated from the isothermal crystallization measurements at 144°C. At this temperature, homo-PP shows no clear exothermic peak for crystallization even after extending the crystallization to 40 min (Figure 8). In the PP-OTMS copolymers, crystallization was much faster than in the homo-PP, and was almost complete within a retention time of approximately 10 min. Figure 9 shows the relationship between OMe content before melt-mixing and the crystallization rate after that process. The crystallization rate improved as the OMe content increased, and eventually reaches saturation at a point that matches the saturation of the reacted amount of OMe group shown in Figure 6. Simply put, it is likely that the reacted amount of the OMe groups strongly affects the rise in crystallization temperature and enhancement of the crystallization rate of the polymers. As with homo-PP, no exothermic peak due to crystallization was observed in isothermal crystallization measurements at 144°C for PP-OTMS3 copolymers, which are not subjected to melt-mixing, and there was no enhancement of the crystallization rate. This suggests that, in terms of enhancing crystallization, polymer chain bonding due to the reaction between functional groups is more important than the amount of functional groups introduced in the PP chain.

Table 3. Results of DSC measurements

Sample	T_m[a] (°C)	X_c[a] (%)	T_c[b] (°C)	$t_{1/2}^{-1}$[c] (s^{-1})
homo-PP	163	43	113	n. d.[d]
PP-OTMS1	165	41	124	3.2×10^{-3}
PP-OTMS2	164	43	126	3.9×10^{-3}
PP-OTMS3	164	43	125	3.8×10^{-3}

[a] Obtained from an endotherm when 100°C quenched sample was heated at 20°C/min.

[b] Crystallization temperature was determined from a non-isothermal crystallization measurement after heating at 230 °C at the cooling rate of 20°C/min.

[c] Isothermal crystallization rate at 144°C.

[d] n. d.; not detected.

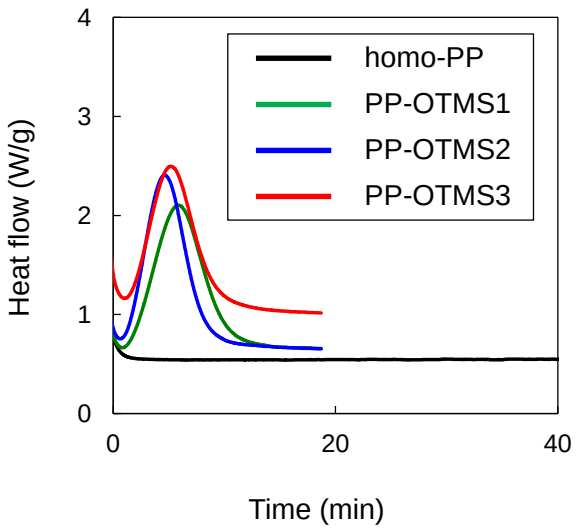

Figure 8. Exotherms of isothermal crystallization at 144°C.

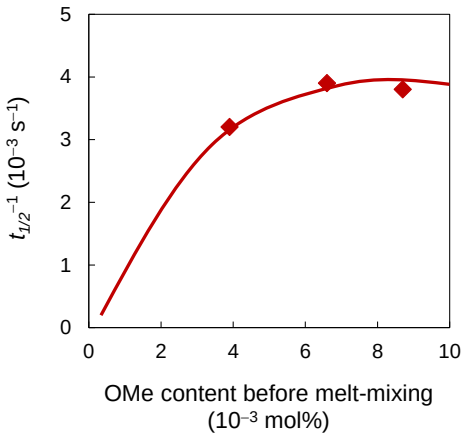

Figure 9. Effect of OMe content on crystallization rate.

The spherulites in the isothermal crystallization process at 144°C were observed using POM (Figure 10). In the PP-OTMS copolymers, crystallization was almost completed by 15 min after the start of the isothermal process, and many spherulites were observed. Only a few spherulites were observed in the homo-PP even after 80 min, and crystallization was not completed. Compared to homo-PP, a clear increase in the number of nuclei was observed in the PP-OTMS copolymers, which indicates the improvement of crystallization rate owing to the nucleation effect.

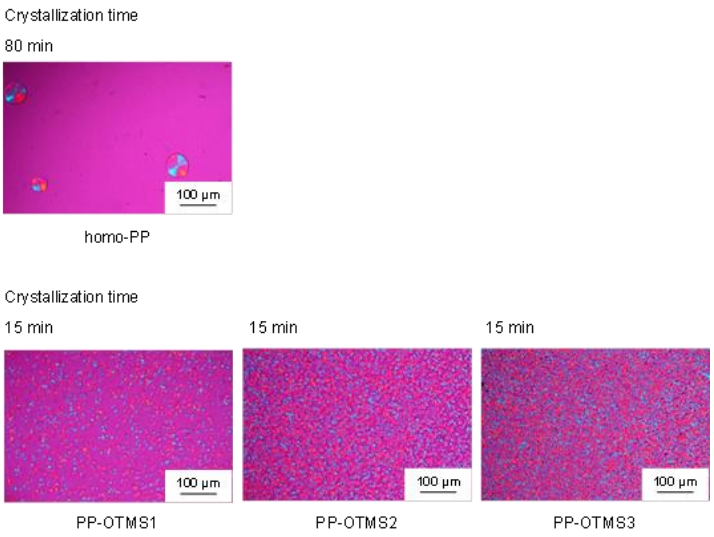

Figure 10. POM images during isothermal crystallization at 144°C.

Given that the number of functional groups introduced in the PP chains was exceedingly small and that the gel content was extremely small, it is possible that even in PP-OTMS3 the majority of the structure was similar to that of long-chain branching PP (LCB-PP) rather than a three-dimensional crosslinking structure. It is widely accepted that LCB-PP acts as a nucleating agent and enhances crystallization rate. Wang *et al.* found that the number of crystal nuclei increased and crystallization temperature rose as a result of blending LCB-PP with PP [18], while Su *et al.* found that LCB-PP crystallizes from the melt as a mixture of α crystals and γ crystals [19]. Based on those findings it is conceivable that, in this research as well, a nucleation effect manifested itself through the introduction of reactive functional groups in the PP chains causing the formation of a long-chain branching structure after the dehydrative condensation reaction due to melt-mixing. Alternatively, it is possible that the intermolecular bond formed between the PP chains through the reactive functional groups led to restricting the movement of the polymer chains and resulted in the nucleation effect.

The film samples of homo-PP and PP-OTMS after post-polymerization were treated at 130°C and 140°C for isothermal crystallization and their POM observation is shown in figure 11. The spherulite size became smaller as more functional groups were introduced in the PP chains.

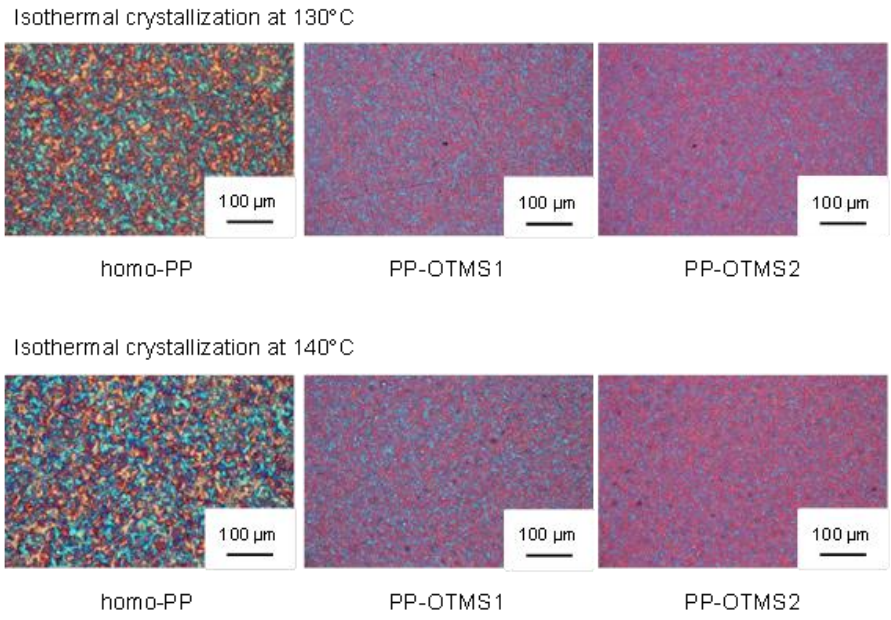

Figure 11. POM images of the isothermal crystallization samples at 130°C, 140°C.

Tensile tests were conducted to evaluate the mechanical properties of the polymers. Both Young's modulus and tensile strength rose as the number of functional groups increased, and the mechanical properties saturated in tandem with the saturation of the reacted amount of the functional groups (Figure 12). The improvement in tensile strength is attributed to the increased intermolecular interaction resulting from the formation of crosslinking or other structures through the functional group reactions. Similarly, spherulite size also has a significant effect on mechanical properties [20]. The interface between larger spherulites are weaker. It has been reported that, voids are prone to forming at the spherulite interfaces when the spherulites are generated during the process of cooling from the melt are large [21]. The reduction in spherulite size is seen as another reason for the improvement in mechanical properties.

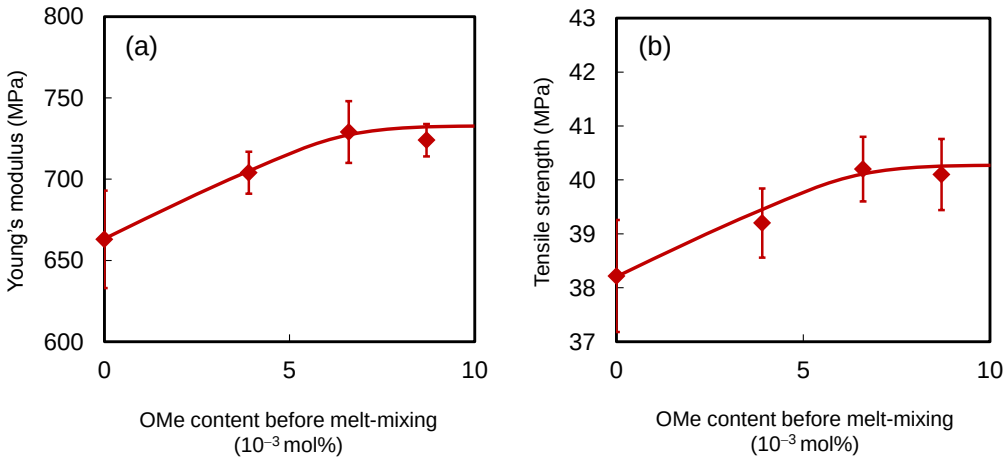

Figure 12. Effects of OMe content on mechanical properties:

(a) Young's modulus and (b) tensile strength.

As described above, the copolymerization of propylene and OTMS using a ZN catalyst was performed to introduce a small amount of functional group in the PP chain. The obtained copolymers exhibited an improved crystallization behavior and mechanical properties, which might be attributed to the crosslinking structure obtained through the condensation reaction of the functional groups introduced in the PP chains.

3-4. Conclusions

This research studied the small-scale introduction of reactive functional groups into the PP chains through the copolymerization of propylene and comonomers with alkoxysilane using a ZN catalyst. The reduction in catalytic activity was mitigated, and copolymers with an extremely low trimethoxysilyl group content of 1.3×10^{-3} to 4.4×10^{-3} mol% were synthesized, through the small-scale use of comonomers. Performing a ^{1}H NMR analysis after melt-mixing the copolymer identified a reduction in the strength of the peaks originating in the methoxysilyl groups, and the observed presence of gel suggested the possibility that the reactions between the OMe groups created PP chain crosslinkage. Moreover, a drastic enhancement of crystallization was indicated through the isothermal crystallization measurements of the functionalized PP after melt-mixing, and the POM observation results clearly showed a significant improvement in nucleation ability. Similarly, considerable improvements were observed for mechanical properties. Given the number of functional groups thought to have been consumed by the reactions and their correlation with the improvements in the crystallization rate and mechanical properties, it was deduced that rather than the interaction of the reactive functional groups themselves, the crosslinking or bonding of the polymer chains formed by the reactions had a considerable effect on the crystallization rate and mechanical properties.

No prior research has achieved enhanced crystallization or improved physical properties through functional group reactions by introducing alkoxysilyl groups in the PP chains on a small scale using a ZN catalyst. Through the introduction of polar functional group in the PP chains using the industrially effective ZN catalyst, this research mitigated decreased catalytic activity, which is a major problem, and prevented the decrease in

melting temperature and crystallinity seen in random copolymers. In addition, the reactivity of functional groups introduced in the PP chains even on a small scale, was demonstrated to be effective at considerably enhancing crystallization and significantly improving mechanical properties. This research suggests that functionalization on a small scale is an extremely effective way to enhance the physical properties of PP.

References

[1] L. Brunsveld, B.J.B. Folmer, E.W. Meijer, R.P. Sijbesma, *Chem. Rev.*, **101**, 4071 (2001).

[2] T.C. Chung, D. Rhubright, *Macromolecules*, **26**, 3019 (1993).

[3] W. Lin, J. Dong, T.C.M. Chung, *Macromolecules*, **41**, 8452 (2008).

[4] H. Hagihara, K. Tsuchihara, J. Sugiyama, K. Takeuchi, T. Shiono, *J. Polym. Sci. Pol. Chem.* **42**, 5600 (2004).

[5] S. Ramakrishnan, E. Berluche, T. C. Chung, Macromolecules, 23, 378 (1990).

[6] M. Xanthos, *Reactive Extrusion: Principles and Practice*, Hanser, Munich, 33 (1992).

[7] H.G. Fritz, B. Stoehrer, *Int. Polym. Proc.*, **1**, 31 (1986).

[8] K. Ebner, J.L. White, *Int. Polym. Proc.*, **9**, 233 (1994).

[9] Y. Seo, J. Kim, K. U. Kim, Y. C. Kim, *Polymer*, **41**, 2639 (2000).

[10] N.C. Liu, G.P. Yao, H. Huang, *Polymer*, **41**,4537 (2000).

[11] A.K. Sen, B. Mukherjee, A.S. Bhattacharyya, P.P. De, A.K. Bhowmick, *J. Appl. Pol. Sci.*, **44**, 1153 (1992).

[12] Y.-T. Shieh, H.-C. Chuang, *J. Appl. Pol. Sci.*, **81**, 1808 (2001).

[13] K. Adachi, T. Hirano, *Ind. Eng. Chem. Res*., **47**, 1812 (2008).

[14] W. Lin, Z. Shao, J. Dong, T.C.M. Chung, *Macromolecules*, **42**, 3750 (2009).

[15] J.Y. Dong, H. Hong, T.C. Chung, *Macromolecules*, **36**, 6000 (2003).

[16] M. Kioka, H. Kitani, N. Kashiwa, U.S. Patent US4330649A, 18, May, (1982).

[17] S. Gupta X. Yuan, T.C.M. Chung, M. Cakmak, R.A. Weiss, *Polymer*, **55**, 924 (2014).

[18] X.D. Wang, Y.X. Zhang, B.G. Liu, Z.J. Du, H.Q. Li, *Polym. J.*, **40**, 450 (2008).

[19] Z. Q. Su, H. Y. Wang, J. Y. Dong, X. Q. Zhang, X. Dong, Y. Zhao, J. Yu, C. C. Han, D. F. Xu, D. J. Wang, *Polymer*, **48**, 870 (2007).

[20] C. Deshmane, Q. Yuan, R. S. Perkins, R. D. K. Misra, *Mater. Sci. Eng.*, **458**, 150 (2007).

[21] J. L. Way, J. R. Atkinson, J.Nutting, *J. Mater. Sci.*, **9**, 293 (1974).

Chapter 4

Physical properties of polypropylene nanocomposites prepared from polypropylene containing a small amount of reactive functional groups

4-1. Introduction

As higher quality becomes expected of the plastic molded products used in automobiles and appliances year after year, organic and inorganic material composites are now indispensable to achieving such quality. Due to superb characteristics such as its light weight, high moldability, and excellent recyclability, PP, and PP compounds in particular, are crucial materials.

The mechanical properties of PP can be enhanced by adding inorganic fillers such as talc, silica, maica, or calcium carbonate. Polymer nanocomposites started garnering attention over ten years ago. Nanoparticles are more effective than microparticles since they have a greater surface area, higher number density, and shorter distance between particles when dispersed. A major issue concerning PP-based nanocomposites was the decreased reinforcement from the nanocomposite caused by the difficulty of obtaining high dispersion in the inorganic nanoparticles within the nonpolar PP. One of the most widely used methods of enhancing the poor dispersion of nanoparticles is the addition of a compatibilizer [1,2]. Functionalized PP such as maleic anhydride grafted PP (MAPP), for example, is often used as a compatibilizer in the market. The PP/clay nanocomposite prepared by Kawasumi *et al.* achieves high dispersion of the clay within the PP by intercalating maleic anhydride grafted PP oligomers between the silicate layers in the clay [3]. Another commonly employed approach is the chemical surface modification of the nanoparticles by short alkyl chains using a silane coupling agent [4].

In recent years, there have been many reports regarding the improvement of physical properties through the formation of networks between fillers or the filler-polymer interaction. It is possible to synthesize the inorganic filler in-situ in the polymer matrix in the melt, a reaction known as “sol-gel”, based on the hydrolysis–condensation

reactions of metal alkoxide precursors [5-12]. Polymer grafting not only enhances dispersion of nanoparticles via the organic modification, but also forms stronger interface bonds through the entanglement and mutual diffusion of the polymer chains between the matrix-and the grafted chains. This method is very versatile since it can be directly applied in the conventional melt-mixing process.

Spherical SiO_2 nanoparticles come in various sizes, are not anisotropic, and can easily be subjected to chemical modification. Consequently, there are numerous research reports concerning PP-based nanocomposites using spherical SiO_2 nanoparticles[13-22,25]. There is also a case where Young's modulus improved by approximately 30% after the addition of MAPP as a compatibilizer[17]. However, tensile strength only improved by 5%. All cases of significant improvements in tensile strength have been observed in research involving grafting polymer chains on to the SiO_2 nanoparticles [18-22]. For example, a 30% improvement in Young's modulus and a 13% improvement in tensile strength was achieved in a poly(glycidyl methacrylate)-grafted SiO_2 nanocomposite prepared by grafting glycidyl methacrylate onto SiO_2 via radical polymerization [18]. Similarly, a polystyrene-grafted SiO_2 nanocomposite obtained through the grafting of styrene onto SiO_2 by radical polymerization exhibited an 18% improvement in tensile strength [19]. Using a metallocene catalyst, Taniike *et al.* synthesized terminally hydroxylated PP (PP-OH) and grafted it onto nanosilica through a dehydrative condensation reaction [22]. They then prepared a PP/PP-grafted SiO_2 nanocomposite through melt-mixing with the PP matrix. Both the Young's modulus and tensile strength of nanocomposite improved by 30% over the base PP, which represents the greatest reinforcement observed in PP-based SiO_2 nanocomposites. The enhanced compatibility of the silica surface with

PP matrix due to organic modification not only improved silica dispersion, but also appears, through the grafting of nanosilica onto the same PP chains as in the PP matrix, to have induced physical crosslinking via co-crystallization between the grafted chains and the matrix, leading to a significant improvement in tensile strength. At the same time, a considerable improvement of the crystallization rate was also observed. This kind of strong interface bonding between the matrix and the nanofiller expands the reinforcement produced by the filler.

Direct grafting of matrix PP onto the nanoparticles is seen as an effective way to enhance physical properties. However, since PP does not contain functional groups, it is necessary to introduce functional groups that can react with the filler. The typical PP functionalization method involving the use of peroxide to form radicals in the main chain leads to the scission of the polymer chain that causes a drastic drop in physical properties [23]. In terms of physical properties, using functionalized PP as matrix is complicated. Weicheng *et al.* grafted polyethylene onto montmorillonite using functional groups incorporated into the PE [24]. They considered it likely that the chemical bond between the filler surface and the polymer matrix improved thermal-oxidative stability. However, they did not report the effects on physical properties. In contrast, through copolymerization using a metallocene catalyst, Hagihara *et al.* synthesized poly(5-hexene-1-ol-co-propylene) containing hydroxyl groups and used it as a matrix to prepare an SiO_2 nanocomposite [25]. Interaction between the hydroxyl groups introduced into the PP and the SiO_2 resulted in a high dispersion of SiO_2 in the matrix. The poly(5-hexene-1-ol-co-propylene)-based SiO_2 nanocomposite exhibited higher ductility than the PP-based SiO_2 nanocomposite. However, both Young's modulus and tensile strength were lower than those of the PP matrix. In

general, large quantities of hydroxyl groups introduced in PP side chains disrupt crystallinity, which is likely to have led to the decrease in physical properties.

In Chapter 3, PP‑OTMS was synthesized through propylene copolymerization, using a ZN catalyst and trimethoxy(7-octen-1-yl)silane (OTMS) as a comonomer. Accordingly, in Chapter 4, the reactions between the reactive functional groups contained in the PP-OTMS and the hydroxyl groups on the SiO_2 surface were used in order to study the grafting of the matrix onto the silica. Small-scale functionalization through copolymerization based on a ZN catalyst involves almost no deterioration of factors such as crystallization behavior or mechanical properties. After the hydrolysis of the trimethoxysilyl groups, which are reactive functional groups introduced in the PP chains through small-scale functionalization, triggering a condensation reaction with the SiO_2 enables the preparation of a PP-grafted SiO_2 nanocomposite where the matrix and SiO_2 are directly grafted. An improvement of the crystallization rate can be expected from the nucleation effect of the PP-grafted SiO_2, the improvement in Young's modulus due to the enhanced SiO_2 dispersion, and the improvement in tensile strength from the filler-polymer interface reinforcement brought about by the polymer chains grafted onto the SiO_2. Melt-mixing was performed using PP-OTMS as a matrix polymer with 5 wt% of SiO_2 nanoparticles. Differential scanning calorimetry (DSC) was used to measure the melting temperature, crystallinity, and the crystallization rate based on isothermal crystallization at 144°C for the prepared PP-OTMS+SiO_2. Finally, the spherulites were observed through polarized optical microscopy (POM). Young's modulus and tensile strength were measured through tensile tests to evaluate the mechanical properties.

4-2. Experiments

4-2-1. Materials

The homo-PP and PP-OTMS copolymers were prepared in accordance with the method described in Chapter 3. SiO_2 (average diameter: 26 nm, surface area: 110 $m^{2/}g$) purchased from Kanto Chemical Co., Inc. was used. Octadecyl 3-(3,5-di-tert-butyl-4-hydroxyphenyl) propionate (AO-50) was donated by ADEKA Co. and used as a stabiliser.

4-2-2. Nano-composite preparation

A twin screw extruder (Xplore Instruments, Micro Compounder IM5) was used to mix 3.5 g of polymer and its corresponding 5 wt% of SiO_2 at 185°C under nitrogen at a mixing rate of 10 rpm. The polymer was previously impregnated in 1.0 wt% AO-50 in acetone, and the mixing force during mixing was monitored every 5 min.

4-2-3. Sample film preparation

Polymer was hot pressed into a film with the thickness of 200 μm at 230°C under 20 MPa for 5 min followed by stepwise quenching at 100°C for 5 min and at 0°C for 1 min.

4-2-4. Polymer characterization

The polymer structure was analyzed by NMR (Bruker 400 MHz) operated at 120°C. The comonomer content was determined based on ^{1}H NMR with the scan number of 1000 using hexachloro-1,3-butadiene as a diluent, 1,1,2,2-tetrachloroethane-d2 as an internal lock and reference. The stereostructure of PP was determined by ^{13}C NMR with the scan number of 5000 using 1,2,4-trichlorobenzene as a diluent,

1,1,2,2-tetrachloroethane-d2 as an internal lock and reference, and dibutylhydroxytoluene (BHT) as a stabilizer.

A thin specimen obtained through cutting with a microtome (Reichert Ultracut S with a FC-S cryo attachment) was observed with a transmission electron microscope (TEM, Hitachi H-7100) to observe the dispersion of the silica nanoparticles in the matrix.

Differential scanning calorimetry (DSC) was acquired under N_2 on a Mettler Toledo DSC 822 analyzer to evaluate the crystallization behavior. The melting temperature (T_m) and the crystallinity (X_c) were determined from the melting endotherm in the first heating, where a sample was heated to 230°C at the heating rate of 20°C/min. A film sample was heated in an aluminum pan at 230°C for 10 min to erase a thermal history, and then cooled down at the cooling rate of 50°C/min to 144°C for isothermal crystallization. Both of the cooling rate and the crystallization temperature were carefully selected to evaluate reliable crystallization rates, which were defined as the inverse of the half time of the crystallization (denoted as $t_{1/2}^{-1}$). The crystallization temperature (T_c) was determined from the exothermic peak observed after heating the samples at 230°C for 10 min and cooling them at a rate of 20 °C/min.

Spherulite growth was observed using a polarized optical microscope (POM) (Leica DMLP) equipped with an automated hot-stage (Mettler Toledo FP82HT). A film sample with the thickness of 50 μm was prepared based on the aforementioned method. The spherulite growth was observed at 144°C after heating a sample at 230°C for 10 min. The temperature was decreased up to 144°C at 20°C/min.

Tensile properties were measured at a crosshead speed of 1 mm/min at room temperature using a tensile tester (Abecks Inc., Dat-100). Film samples were cut into a

dumbbell shape for use as tensile test specimens. The Young's modulus and tensile strength values represent the average of the values obtained in tensile tests on five or more specimens.

4-3. Results and discussion

Graft formation through the reactions between the reactive methoxysilyl groups introduced in the PP chains and the SiO_2 surface hydroxyl groups was studied. Melt-mixing of the PP-OTMS copolymers and SiO_2 at 185°C was applied as a post-polymerization process to obtain PP-OTMS+SiO_2 (Scheme 1). Measuring the mixing force showed that it tended to increase in proportion with a higher comonomer content in the polymer chains (Figure 1). Melt-mixing with SiO_2 exhibited higher force than without it.

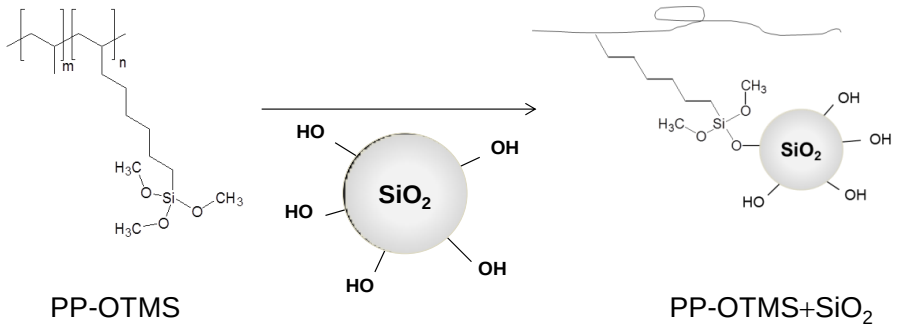

Scheme 1

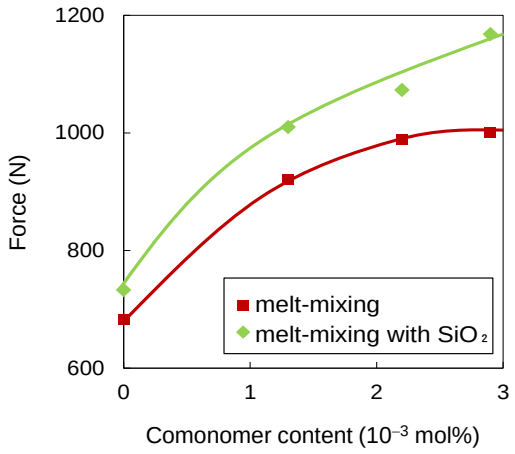

Figure 1. Relationship between comonomer content and mixing force.

To investigate the progress of functional group reactions due to post-polymerization, ^{1}H NMR measurements were used to calculate the OMe group content after melting. Based on the methine protons found in the PP main chain at δ = 1.72 ppm and the strength of the peak belonging to the protons of the OMe groups found in the vicinity of δ = 3.7 ppm, the equation (1) below was used to calculate the OMe group content.

$$\text{OMe content (mol\%)} = \frac{\underline{H^{8}}/3}{\underline{H^{3}}} \times 100 \qquad (1)$$

The OMe content after melt-mixing decreased in line with the silica compared to the same content before melt-mixing. Furthermore, a significant decrease in the OMe content was observed in comparison with cases where no silica was added (Figure 2). In particular, melt-mixing with SiO_2 left no OMe content in PP-OTMS1. Figure 3 shows the relationship between the OMe content before melting and the reacted amount of the OMe groups caused by melt-mixing. The number of reacting functional groups rose as the content of functional group in the polymer increased. Interestingly, the saturation seen

without the addition of SiO_2 was not observed. The extremely small number of functional groups makes it difficult for the functional groups in the polymers to react with one another, resulting in a small decrease of the OMe content. In contrast, it is thought that adding SiO_2 nanoparticles, which contain an extremely high number of hydroxyl groups (approximately 3 hydroxyl groups per 1 nm^2 in a 110 m^2/g of surface area) can lead to more reaction points with the functional groups, increasing the reacted amount of OMe group.

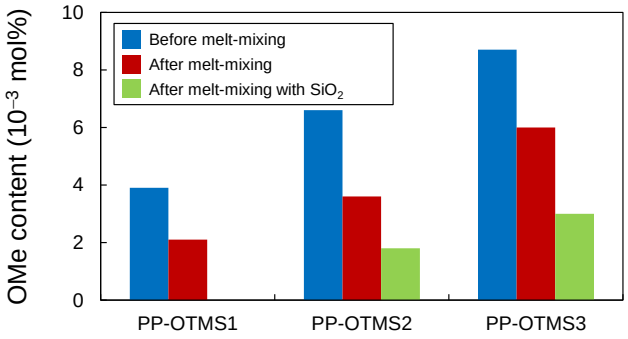

Figure 2. OMe content of PP-OTMS before and after melt-mxing.

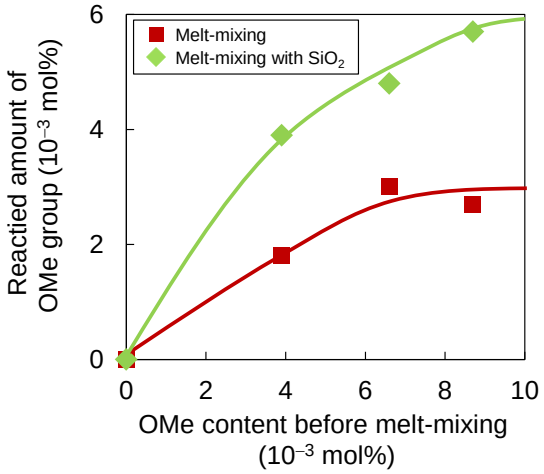

Figure 3. Relationship between OMe content and reacted amount of OMe group.

TEM observations were made to verify the dispersion of SiO_2 (Figure 4). An improvement in that dispersion was observed as there was less SiO_2 aggregation in PP-OTMS+SiO_2 than in homo-PP+SiO_2. Better dispersion was observed in the following order: homo-PP+SiO_2 < PP-OTMS1+SiO_2 < PP-OTMS2+SiO_2 < PP-OTMS3+SiO_2, and may have been the result of introducing polar functional groups in the PP chains. Another possibility is that the PP chains grafted to the SiO_2. Research by Taniike *et al.* showed that grafting PP to nano-SiO_2 and adding it to the matrix PP resulted in a major improvement of SiO_2 dispersion in the PP matrix [22].

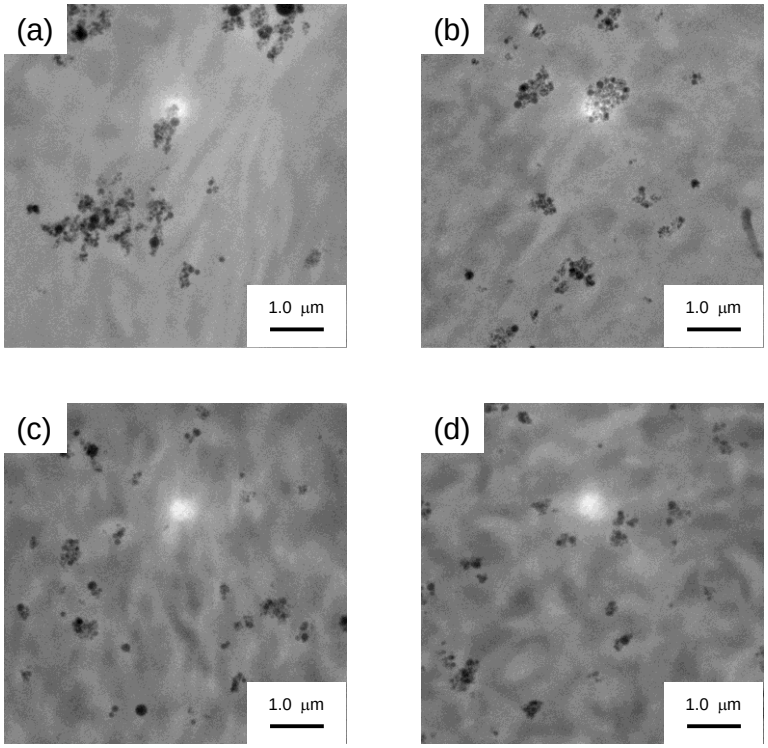

Figure 4. TEM images: (a) homo-PP+SiO_2, (b) PP-OTMS1+SiO_2, (c) PP-OTMS2+SiO_2 and (d) PP-OTMS3+SiO_2.

DSC was used to investigate the crystallization behavior of PP-OTMS+SiO_2 (Table 1). The melting temperature exhibited virtually no change as the number of functional groups rose, but there was an increase in crystallinity. The crystallization temperature of homo-PP measured for the non-isothermal crystallization remained almost unaffected by the addition of silica. PP-OTMS exhibited a crystallization temperature approximately 10°C higher than homo-PP, and PP-OTMS+SiO_2, which contained silica, exhibited an even higher crystallization temperature. Rong *et al.* have reported that grafting polymer onto silica surfaces and adding surface-grafted nanoparticles had a significant effect on crystallization of PP and led to high crystallization temperatures in non-isothermal crystallization measurements [19].

Table 1. Results of DSC measurements

Sample	T_m[a] (°C)	X_c[a] (%)	T_c[b] (°C)	$t_{1/2}^{-1}$[c] (s^{-1})
homo-PP	163	43	113	n. d.[d]
PP-OTMS1	165	41	124	3.2×10^{-3}
PP-OTMS2	164	43	126	3.9×10^{-3}
PP-OTMS3	164	43	125	3.8×10^{-3}
homo-PP+SiO_2	164	44	114	n. d.[d]
PP-OTMS1+SiO_2	164	41	127	5.4×10^{-3}
PP-OTMS2+SiO_2	164	43	128	6.2×10^{-3}
PP-OTMS3+SiO_2	164	48	128	6.4×10^{-3}

[a] Obtained from an endotherm when 100°C quenched sample was heated at 20°C/min.

[b] Crystallization temperature was determined from a non-isothermal crystallization measurement after heating at 230 °C at the cooling rate of 20°C/min.

[c] Isothermal crystallization rate at 144°C. [d] n. d.; not detected.

Figure 5 shows the DSC curve for the isothermal crystallization measured at 144°C, for which no clear exothermic peak accompanying crystallization was observed in homo-PP+SiO_2 within a maximum retention time of 40 min. This matches the results for homo-PP measured under the same conditions. Both homo-PP and homo-PP+SiO_2 had a crystallization rate of 1.8×10^{-3} s^{-1} for isothermal crystallization measured at 132°C. A general result that the addition of silica does not change the crystallization rate in homo-PP was obtained. In contrast, PP-OTMS exhibited a crystallization rate improvement of 1.6 to 1.7 times with the addition of SiO_2. Research by Taniike *et al.* showed that the addition of 5 wt% PP-grafted SiO_2 improved the crystallization rate of homo-PP by 4.6 times under 128°C isothermal crystallization conditions [22]. In the present research, the crystallization of PP functionalized on a small scale with added silica was enhanced to an almost unmeasurable extent compared to homo-PP under the same isothermal crystallization temperature. The direct grafting of the matrix PP functional groups to the silica is seen as having had a greater effect than the addition of PP-grafted SiO_2 to the matrix PP.

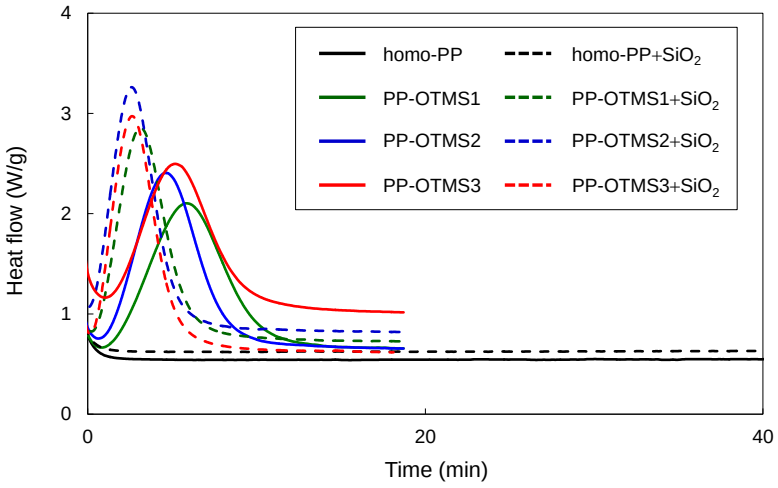

Figure 5. Exotherms of isothermal crystallization at 144°C.

Figure 6 shows the relationship between OMe content in the polymer chain before melt-mixing and the polymer crystallization rate after that process. It was observed that the more OMe groups there were in the polymer chains before melt-mixing, the greater the improvement in the crystallization rate was.

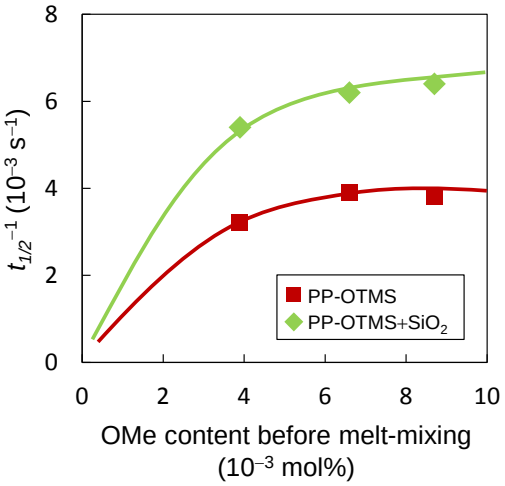

Figure 6. Effect of OMe content on crystallization rate.

The spherulites in the isothermal crystallization process at 144°C were observed by POM (Figure 7). In PP-OTMS+SiO_2, crystallization was almost complete 15 min after the start of isothermal crystallization, and an extremely high, almost uncountable number of spherulites were observed. The number of spherulites increased in the following order: PP-OTMS1+SiO_2 < PP-OTMS2+SiO_2 < PP-OTMS3+SiO_2. Conversely, in the homo-PP+SiO_2, only a few spherulites were observed even after 80 min, and crystallization did not complete. As stated in Chapter 3, a clear increase in the number of spherulites was also observed in the PP-OTMS copolymers without silica addition. An even greater number of spherulites was observed in the PP-OTMS in which silica was mixed. These observations suggest that enhanced nucleation had a considerable effect on

improving the crystallization rate during melt-mixing for systems with added silica as well. In general, it is known that nanosilica without grafted polymer chains does not exhibit a nucleation effect and that its addition to matrix PP has almost no effect on the crystallization rate [26], while nanosilica with grafted polymer does exhibit a nucleation effect and enhances matrix crystallization [22]. In this research as well, the PP-OTMS+SiO_2 crystallization rate was considerably faster than that without added silica, strongly supporting the possibility that this major improvement in the crystallization rate was due to the PP-OTMS functional groups reacting with the hydroxyl groups on the SiO_2 surface and the PP chains grafting onto the SiO_2. The greater nucleation effect observed in tandem with the increased reacted amount of the functional groups also supports the possibility that the PP chains grafted to the SiO_2 nanoparticles.

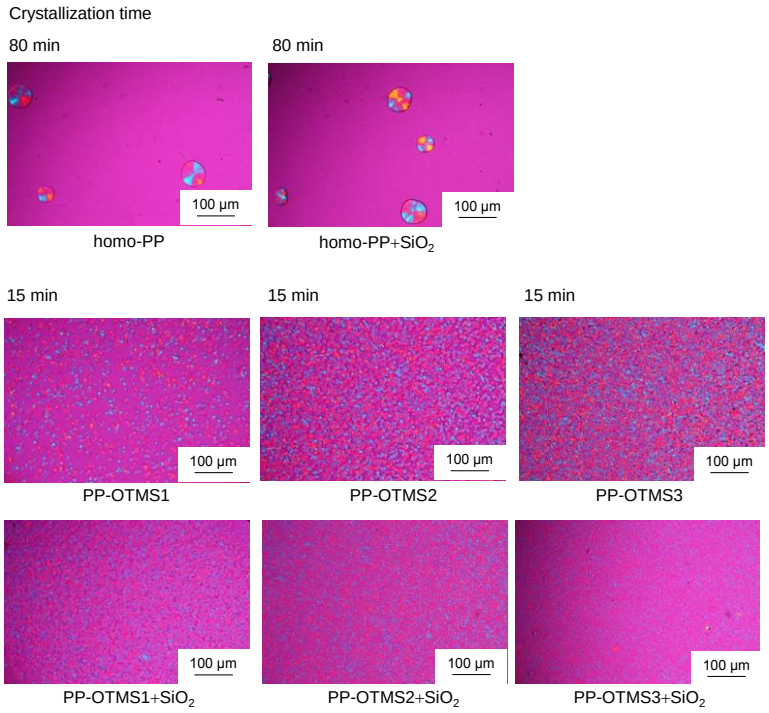

Figure 7. POM images during isothermal crystallization at 144°C.

The homo-PP+SiO_2 and PP-OTMS+SiO_2 film samples were prepared by crystallizing them at 130°C or 140°C. Observing those film samples through POM showed that, at both 130°C and 140°C, the PP-OTMS+SiO_2 spherulites became finer than those in homo-PP+SiO_2 (Figure 8). A similar PP-OTMS+SiO_2 nucleation effect was observed even at different crystallization temperatures.

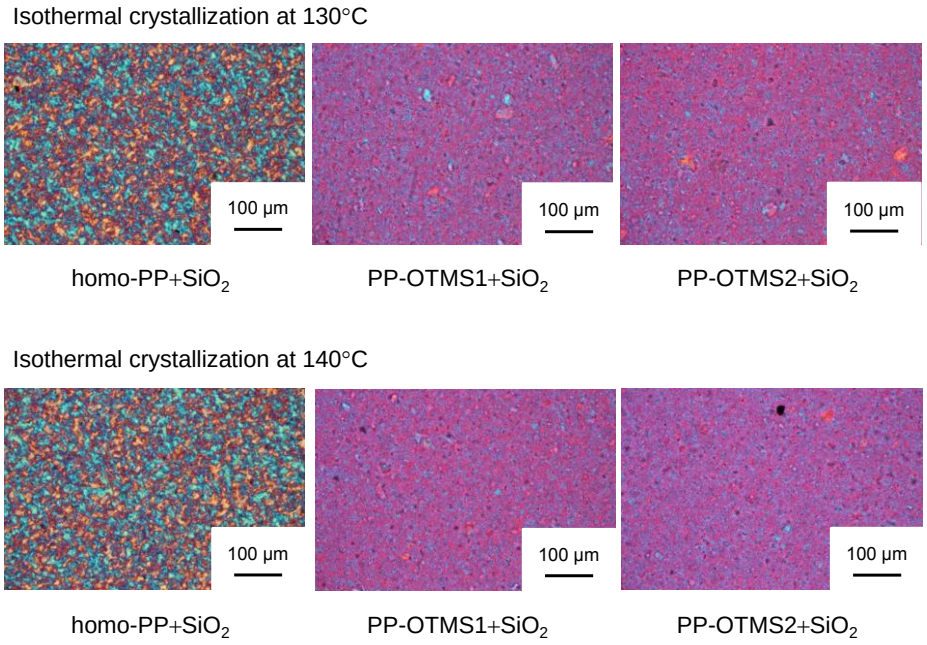

Figure 8. POM images of the isothermal crystallization samples at 130 °C, 140°C.

Tensile tests were conducted to evaluate the mechanical properties of the polymers. Young's modulus improved as the number of functional groups in the PP-OTMS increased (Figure 9 (a)). The reinforcement was greatest in the PP-OTMS3+SiO_2 sample, exhibiting a 16% improvement over homo-PP. The improvement in Young's modulus is attributed to the improved silica dispersion due to the functional groups introduced in the PP chains, as confirmed by the TEM observations. It is considered that the increase of crystallinity also improved the Young's modulus. Similarly, tensile strength also improved as the OMe content increased (Figure 9 (b)). Among the samples, tensile strength was highest in PP-OTMS3+SiO_2, exhibiting a 8% improvement over homo-PP. Various research on enhancing the physical properties of PP has been conducted, and tensile strength improvements of a maximum of 30% or more have been reported [22]. Although this research did not obtain effects as extensive as those reported in other reports, it did suggest that further improvements in physical properties could be achieved by optimizing the number of functional groups and the melt-mixing conditions.

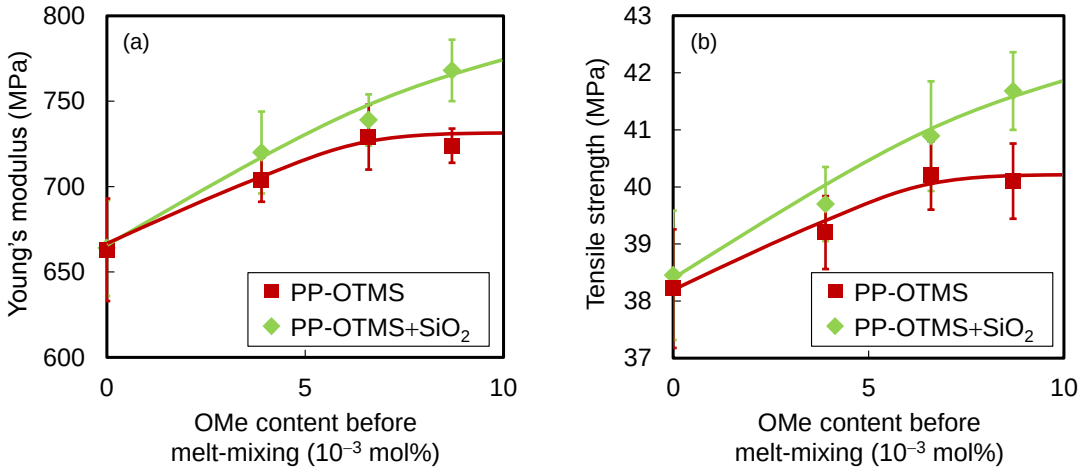

Figure 9. Effects of OMe content on (a) Young's modulus and (b) Tensile strength.

PP-OTMS in which methoxysilyl groups were introduced on a small scale as reactive functional groups were mixed with nanosilica. The results of a DSC analysis of crystallization behavior showed that the crystallization rate of the obtained PP-OTMS+SiO_2 improved over that of PP-OTMS. In addition, POM observations revealed that PP-OTMS+SiO_2 exhibited a greater nucleation effect than PP-OTMS. Tensile tests performed to evaluate mechanical properties indicated that PP-OTMS+SiO_2 had higher Young's modulus and tensile strength values than homo-PP. It is possible that these enhancements in crystallization behavior and mechanical properties resulted from the formation of silica with grafted PP chains through the reactions of the functional groups introduced in the PP chains with the surface hydroxyl groups on the nanosilica.

4-4. Conclusions

The small-scale introduction of reactive functional groups, which does not cause deterioration of the matrix PP crystallinity or physical properties, was performed through propylene copolymerization using a ZN catalyst. It is possible that, by advancing the reaction between the reactive functional groups and the hydroxyl groups on the SiO_2 surface, the PP-OTMS+SiO_2 prepared via subsequent post-polymerization led to the formation of PP-grafted SiO_2 with a PP matrix containing functional groups on a small scale. A graft reaction on the SiO_2 is strongly suggested by the significantly enhanced crystallization rate, a nucleation effect not seen when SiO_2 is added to homo-PP, and the improvements of mechanical properties such as those observed for Young's modulus and tensile strength.

References

[1] Hasegawa N, Kawasumi M, Kato M, Usuki A, Okada A. *J. Appl. Polym. Sci.*, **67**, 87 (1998).

[2] E. Pavlidou, D. Bikiaris, A. Vassiliou, M. Chiotelli, G. Karayannidis, *J. Phys.*, **10**, 190 (2005).

[3] M. Kawasumi, N. Hasegawa, M. Kato, A. Usuki, A. Okada, *Macromolecules*, **30**, 6333 (1997).

[4] O.H. Lin, H.M. Akil, *Polym. Compos*., **32**, 1568 (2011).

[5] D. Sun, R. Zhang, Z. Liu, Y. Huang, Y. Wang, J. He, B. Han, G. Yang, *Macromolecules*, **38**, 5617 (2005).

[6] S. Jain, H. Goossens, F. Picchioni, P. Magusin, B. Mezari, M. van Duin, *Polymer*, **46**, 6666 (2005).

[7] K. Adachi, T. Hirano, P.H. Kasai, K. Nakamae, H. Iwabuki, K. Murakami, *Polym. Int.*, **59**, 510 (2010).

[8] Y. Mizutani, S. Nago, *J. Appl. Polym. Sci*., **72**, 1489 (1999).

[9] Q. Dou, X. Zhu, K. Peter, D.E. Demco, M. Möller, C. Melian, *J. Sol-Gel Sci. Technol*., **48**, 51 (2008).

[10] W. Bahloul, V.B. Legare, L. David, P. Cassagnau. *J. Polym. Sci. Pol. Phys*., **48**, 1213 (2010).

[11] K. Takeuchi, M. Terano, T. Taniike, *Polymer*, **55**, 1940 (2014).

[12] K. Kaneko, N. Yadav, K. Takeuchi, B. Maira, M. Terano, T. Taniike. *Compos. Sci. Technol*., **102**, 120 (2014).

[13] L. Elias, F. Fenouillot, J.C. Majeste, P. Cassagnau, *Polymer*, **48**, 6029 (2007).

[14] Y. Liu, M. Kontopoulou, *Polymer*, **47**, 7731 (2006).

[15] M.Z. Rong, M.Q. Zhang, S.L. Pan, B. Lehmann, K. Friedrich, *Polym. Int.*, **53**, 176 (2004).

[16] D.N. Bikiaris, G.Z. Papageorgiou, E. Pavlidou, N. Vouroutzis, P. Palatzoglou, G.P. Karayannidis, *J. Appl. Polym. Sci.*, **100**, 2684, (2006).

[17] E. Pavlidou, D. Bikiaris, A. Vassiliou,M. Chiotelli,G. Karayannidis. *J. Phys*., **10**, 190 (2005).

[18] H.J. Zhou, M.Z. Rong, M.Q. Zhang, W.H. Ruan, K. Friedrich, *Polym. Eng. Sci*., **47**, 499 (2007).

[19] M.Z. Rong, M.Q. Zhang, Y.X. Zheng, H.M. Zeng, R. Walter, K. Friedrich, *Polymer*, **42**, 167 (2001).

[20] N. Xu, W. Zhou, W. Shi, *Polym. Adv. Technol*., **15**, 654 (2004).

[21] W.H. Ruan, X.B. Huang, X.H. Wang, M.Z. Rong, M.Q. Zhang, *Macromol. Rapid. Commun*., **27**, 581 (2006).

[22] T. Taniike, M. Toyonaga, M. Terano, *Polymer,* **55**, 1012 (2014).

[23] M.F. Diop, J.M. Torkelson, *Macromolecules*, **46**, 7834 (2013).

[24] L. Hongdian, H. Yuan, L. Ming, C. Zuyao, F. Weicheng, *Compos. Sci. Technol*., **66**, 3035 (2006).

[25] R. Watanabe, M. Kunioka, J. Mizukado, H. Suda, H. Hagihara, *Polymer*, **99**, 63 (2016).

[26] Y. Liu, M. Kontopoulow, *J. Vinyl. Add. Tech.*, **13**, 147 (2007).

Chapter 5

General Conclusions

This research studied the enhancement of PP physical properties through functionalization using ZN catalysts.

Chapter 2 describes the study of the synthesis of functionalized PP through propylene copolymerization using styrene and 1-allylnaphthalene as comonomers, and presents an analysis of the crystallization behavior and mechanical properties of the obtained functionalized PP. A nucleation effect was observed even with functional groups introduced on a small enough scale to avoid decreasing of melting temperature and crystallinity, which made it clear that the crystallization rate can be improved.

Chapter 3 presents the study of the physical properties of the polymers obtained by introducing reactive trimethoxysilyl group into the PP chains and performing post-treatment. The reactions between the reactive functional groups introduced into the PP chain dramatically enhanced crystallization and improved the physical properties.

Chapter 4 introduces the study of reactions involving the grafting of PP chains onto silica using PP in which trimethoxysilyl groups were introduced. The obtained silica nanocomposites exhibited an extremely large nucleation effect and a considerably enhanced crystallization rate. In addition, the nucleation effect of the obtained silica nanocomposite increased commensurately with the rise in the number of functional groups, and mechanical properties also improved.

This research demonstrated the points below.

1. Restricting functional groups to a small scale in the functionalization of PP using ZN catalysts makes it possible to enhance the crystallization rate without deteriorating the base properties of PP.
2. Even if functional groups are introduced into the PP chains on a small scale, the use of reactive functional groups allows a dramatic enhancement of the crystallization through

the reactions between reactive functional groups and fillers. Physical properties can also be improved. Consequently, reactive functional groups can be described as the most appropriate type of functional group for small-scale functionalization.

3. The small-scale functionalization method makes it possible to mitigate the decreased catalytic activity that was the drawback of functionalization processes based on conventional copolymerization. This broadens the types of functional groups that can be used.

Consequently, this research is believed to provide very beneficial to the development of industrial materials.

Achievements

＜Original paper＞

"Polypropylene Crystallization Behavior after Introducing Small Amount of Aromatic Functional Groups" by Takeshi Nagai, Patchanee Chammingkwan, Minoru Terano, Toshiaki Taniike, *Polymers*, **2016**, *submitted*.

"High-performance polypropylene-based copolymer containing a small amount of reactive functional group" by Takeshi Nagai, Patchanee Chammingkwan, Minoru Terano and Toshiaki Taniike, Current Trends in Polymer Science, **2017**, *accepted*.

＜International conference＞

"Crystallization Behavior of Polypropylene Nanocomposites Including Structure Controlled Polypropylene-Grafted Nanosilica"

International Workshop on Catalytic Olefin Polymerization and High Performance Polyolefins, Shanghai, China, Oct., 2014.

"Control of Crystallization Behavior by Introducing a Small Amount of Aryl Groups to Polypropylene"

10th International Symposium on Weatherability, Gunma, Japan, July, 2015

“Control of crystallization behavior by introducing functional groups to polypropylene”

World Polyolefin Congress 2015, Tokyo, Japan, Nov., 2015.

“Effects of functional groups on polymer properties in Ziegler-Natta catalyzed propylene polymerization”

4th Blue Sky Conference on catalytic olefin polymerization, Sorrento, Italy, June, 2016.

＜Domestic conference＞

ポリプロピレン鎖への微量フェニル基導入による結晶化挙動の制御

マテリアルライフ学会第 26 回研究発表会、群馬、2015 年、7 月

微量導入された芳香環によるポリプロピレン結晶化挙動の制御

高分子学会第 64 回高分子討論会、宮城、2015 年、9 月

Ziegler-Natta 触媒により合成された官能基化ポリプロピレンの物性評価

マテリアルライフ学会第 27 回研究発表会、滋賀、2016 年、7 月

Acknowledgement

I would like to express my sincere regards to Professor Dr. Minoru Terano for his excellent guidance and encouragement. I am deeply grateful to Associate Professor Dr. Toshiaki Taniike for his helpful discussion and many suggestion about experiments.

I would like to thank Assistant professor Dr. Chammingkwan Patchanee for her quite valuable advice and comments. I would like to thank Professor Dr. Masayuki Yamaguchi for the assistance of my research and borrowing me various experimental machines. Great acknowledgments are made to Professor Dr. Katsuhisa Tokumitsu provided valuable advices and helpful discussions for my minor research.

I would like to thank to Dr. Keisuke Goto, Dr. Masahito Toyonaga, Dr. Kengo Takeuchi, Dr. Toshiki Funako, Dr. Ikki Katada, Dr. Yanning Zeng, Dr. Kei Kaneko, Dr. Goond Hongmanee, Dr. Mingkwan Wannaborworn, Mrs. Supawadee Poonpong, Mr. Taira Tobita, Mrs. Saori Miyano and other members in Terano and Taniike laboratory. I also deeply appreciate members in Laboratory for their kind supporting the research. Sincere thanks to all the members in Terano, Taniike and Yamaguchi laboratories for their kind supports.

I am deeply grateful to my company President Yoichiro Kojima, Senior Managing Director Tsukasa Suzuki, Director Atsushi Matsumoto, Assistant General Manager Tetsuya Tadano, Section Chief Minoru Yonebayashi and Supervisor Masahiro Aoki for encouragement and supports of my study. I also thank to all the colleagues in Kojima Industries Corporation for their encouragement.

I highly appreciate my wife, children and my parents for their understanding my work and supports for my life.

副テーマ研究論文

ポリシラン添加によるポリプロピレン/ポリエチレンの融着特性改良に関する研究

永井 健

北陸先端科学技術大学院大学　マテリアルサイエンス研究科

徳満 勝久 教授

滋賀県立大学

1. 諸言

ポリオレフィンの代表であるポリエチレン (PE)、ポリプロピレン (PP) は成形加工性がよく、安価であり現在生産される熱可塑性プラスチック製品の半数以上を占めている。また、軽量であり、リサイクル性が高いことから低環境負荷材料としても注目されている。PE と PP は炭素と水素から構成され分子構造が類似しているが、PP は PE のエチレンユニットの 1 つの水素原子がメチル基に置換された構造をとることによって、その性質を大きく変えている。例えば PP は PE に比べて融点が高い。これはメチル基が存在することにより、主鎖の C-C 結合が回転し辛くなるためである。一方で、PP は熱や光により劣化しやすく、これはメチル基の結合した 3 級炭素上の水素の引き抜きが起こりやすいことが理由である。このように PE と PP は異なる特徴を持つため、我々は製品の要求する品質に合わせてこれらを使い分けている。

PE、PP は熱融着処理を必要とする製品にも数多く使用されている。例えば、PE は分子構造が柔軟であるため低温においても衝撃特性が優れ、ガス配管として利用される。一方、PP は耐熱性の要求される自動車用バッテリーケースやレトルト食品用包装材のインナーフィルムとして用いられている。近年ではフィルムに多機能性を求め、多層複合フィルムが製造されている。フィルムの複合化を行なうにあたり、最も重要な特性の 1 つとして基材接着性があるが PE や PP は基材接着性に乏しく、フィルム複合化の課題となっている。よって、PE と PP において、接着性や相容性の向上が望まれており、これまでに多くの研究がなされている。Bates 等は、PE と PP の融着において、ともにメタロセン触媒により合成された PE と PP の方がチーグラー・ナッタ触媒で合成されたそれらよりも融着強度が高いことを報告し、この理由として PE/PP 界面に存在する非晶ポリマーがチーグラー・ナッタ PE、PP の方が多く、分子鎖の絡み合いが起きにくいためと説明している[1]。また、Yamaguchi は長鎖分岐を有する低密度ポリエチレン (LDPE) と短鎖分岐を有する直鎖状低密度ポリエチレン (LLDPE) とでは、LLDPE の方が PP との融着強度が高いことを報告している[2]。

一方で、Tokumitsu 等は、PE の融着特性の向上において、低分子量ポリシランが効果的に働くことを見出している[3]。また、ポリシランが超高分子量ポリエチレン (UHMWPE) の溶融混練時におけるトルクを低下する効果があることを報告している[4]。さらに、PP と高密度ポリエチレン (HDPE) の融着においても、ポリメチルフェニルシラン (PMPS) を塗布した場合、未塗布と比較して剥離エネルギーが増加することを見出し[5]、PMPS は PP と HDPE の融着においても効果があることを明らかにしている。この研究において、剥離界面の EPMA (電子線マイクロアナライザ) による元素分析を行ない、PP と HDPE 界面に塗布された PMPS が PP よりも HDPE 側の界面に多く存在することが分かり、PMPS は PP よりも HDPE に拡散しやすいことが示唆された。また、PMPS の添加された PP の DMA (動的粘弾性) 測定の結果、PMPS を添加するこ

とで、PP の b 緩和 (Tg) のピーク温度が低下し、ピーク強度の増加が見られ、PP の非晶領域の分子運動性の向上が示唆された[6]。
本研究は、PP と PE の融着強度の向上を目的として、様々な PE を用いて PMPS の添加効果について検討を行なった。

2. 実験

2-1. 材料

本研究に用いた PE および、PP の情報を Table 1 に記載する。HDPE は Hi-zex 2200J (プライムポリマー株式会社製)、LDPE はノバテック LC602A (日本ポリエチレン株式会社製) を使用した。また、LLDPE は分子量の異なる 2 種類を用いた。ハーモレックス NF444N (Mw = 1.73 x 10^5、日本ポリエチレン株式会社製)、ハーモレックス NM744N (Mw = 2.17 x 10^5、日本ポリエチレン株式会社製) を使用した。PP はプライムポリプロ F113G (プライムポリマー株式会社製) を使用した。

Table 1. Characteristics of PE and PP

Code	Mw (g・mol^{-1})	Density (g・cm^{-3})
HDPE	9.15 x 10^5	0.964
LDPE	3.12 x 10^5	0.917
LLDPE	1.73 x 10^5	0.912
	2.17 x 10^5	0.912
PP	4.50 x 10^5	0.910

直鎖型低分子量ポリシランとして、ポリメチルフェニルシラン (オグソール SI-10-40、大阪ガスケミカル株式会社製、以下 PMPS と記載) (Figure 1)を用いた。分子量情報について、Table 2 に示す。

Table 2. Characteristics of PMPS

Code	Mw (g・mol^{-1})	Mn (g・mol-1)	n
PMPS	620	530	4-6

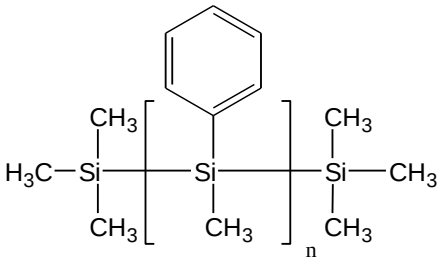

Figure 1. Chemical structure of polysilane.

2-2. PP/15wt%PMPS の調製

混練機 (株式会社東洋精機製作所製 LABO PLASTOMILL 50M) (Figure 2)を用いて PP への PMPS のブレンドを行なった。PP に PMPS を 15 wt%添加し、温度 200°C で 3 分間、10 rpm で予備混練を行なった。その後、7 分間、40 rpm で溶融混練することで PP/15wt%PMPS を調製した。

Figure 2. Melt kneading machine.

2-3. フィルム調製

井元製作所製小型加熱プレス (10t) (Figure 3) を用いて、熱プレスによって 0.3 mm 厚のフィルムの作製を行なった。PE は 160°C、PP は 180°C で 120 秒間加熱し溶融させた。30 秒間脱気を行なった後、10MPa で 180 秒間加圧した。その後、氷水を用いて 0°C での結晶化を行なった。

フィルムは 40 mm x 40 mm サイズにカットし、熱融着サンプルとした。

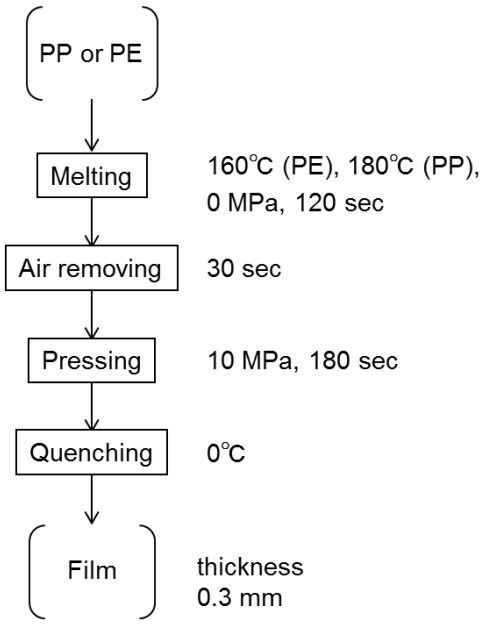

Scheme 1. Film preparation

Figure 3. Hot press machine.

2-4. 熱融着

熱融着はヒートシールテスター (テスター産業株式会社製 TP-701－B) (Figure 4) を用いて実施した。PP および 2-2. にて調製した PP/15wt%PMPS を用いて各種 PE との熱融着を行なった。また、PP/15wt%PMPS と比較して、PP、PE 界面へ PMPS を塗布したサンプルについても熱融着を行なった (Figure 5)。熱融着サンプルの半分の面積に PMPS を塗布することとし、塗布量は 1.0 g/cm^2 とした。融着温度は、160°C とし、融着時間は 60 秒、120 秒、240 秒および 420 秒を検討した。融着後は氷水を用いて 0°C での冷却を行なった。

Figure 4. Heat-seal tester.

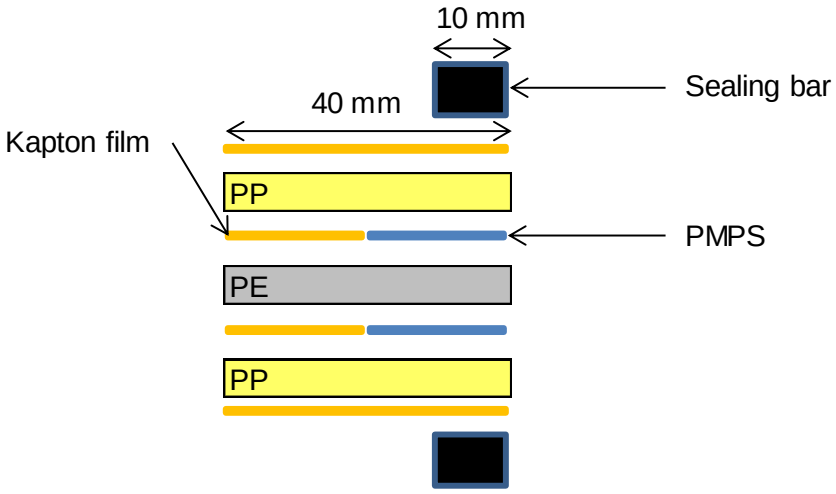

Figure 5. Image of heat fusion films.

2-5. T 型剥離試験

融着強度を測定するために、引張試験機 (株式会社島津製作所製 EZ-Test) を用いて T 型剥離試験を実施した (Figure 6)。引張速度は 10 mm/min とし、チャック間距離は 10 mm とした。試験は 3 回実施した。

剥離試験サンプルは Figure 7 のように作製した。融着部の長さが 10 mm となるように調整した。

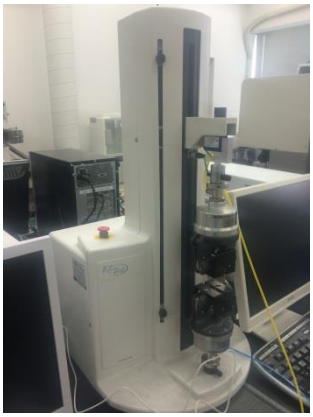

Figure 6. Tensile tester.

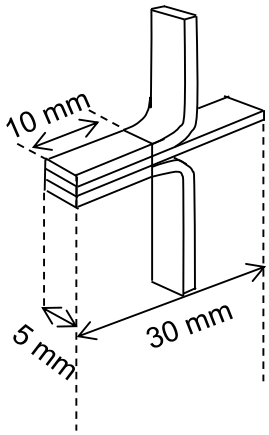

Figure 7. Sample for peeling test.

2-6. 剥離面の組成分析

剥離面の組成分析を赤外分光光度計 (FT-IR) (サーモフィッシャーサイエンティフィック株式会社製 NEXUS470) を用いて実施した (Figure 8)。測定方法は全反射法とし、ダイヤモンドプリズムを使用した。積算回数は 16 回、分解能 8 cm^{-1} とした。

Figure 8. FT-IR spectrometer.

3. 結果と考察

PP、PE の融着における融着条件の検討を行なった。融着温度は 160°C とし、融着時間の検討を行なった。また、PMPS の塗布有無について検討を実施した。
融着の結果を Table 3 に示す。

Table 3. Results of sealing

Sample of PE	Sealing time (sec)	with PMPS	without PMPS
HDPE	240	×	-
	420	×	-
LDPE	240	×	-
	420	×	-
LLDPE (Mn=57800)	240	○	○
	420	○	○
LLDPE (Mn=99500)	240	○	-
	420	○	-

○: sealing, ×: not sealing.

HDPE、LDPE においては、PMPS 塗布条件で 240 sec、420 sec ともに剥離した。一方で、LLDPE では明らかな融着が起こり、PMPS の塗布無についても融着が見られた。
この結果、PMPS を塗布した系においても、HDPE、LDPE よりも LLDPE の方が PP と融着しやすいことが分かった。HDPE は高密度で直鎖状の PE が結晶化しているため、融解後も PMPS が浸透し辛く、PMPS の効果が低かったと考えられる。LDPE は分岐構造であるため PMPS を含浸してしまい PP への効果を低下させた、もしくは PMPS が分子運動を活性化させたが、PP との分子鎖の絡み合いがやや困難であったため、この条件では融着に至らなかった可能性がある。一方、LLDPE は低密度であるため PMPS が浸透しやすく、さらに短鎖分岐であるため PP との分子鎖の絡み合いも可能であり、よって融着されたと考えられる。

次に、融着された LLDPE と PP を剥離し、剥離面の組成について分析を行なった。FT-IR スペクトルを Figure 9、Figure 10 に示す。PMPS 塗布の有無ともに、剥離面 A からは PP が検出され、剥離面 B からは PE が検出された。160°C での融着時に、PE が融解し PP 同士で融着していることが懸念されたが、そのようなことは起こっていないことが分かった。

また、PMPS を塗布したサンプルにおいて、剥離面 B から PE 以外の付着物のピークが検出された。850-1250 cm^{-1} にピークが検出され、PMPS 由来であると考えられる。よって、PMPS は PP と比較して LLDPE 側に移行しやすいことが分かった。160°C では LLDPE は融解しているが、PP は融解していないため PMPS が LLDPE 側に移行しやすいと考えられるが、融着後 LLDPE が結晶化した後にも PP の非晶部に入るよりも LLDPE 側に存在しているため、PMPS は PP と比較して PE との親和性が高いと考えられる。

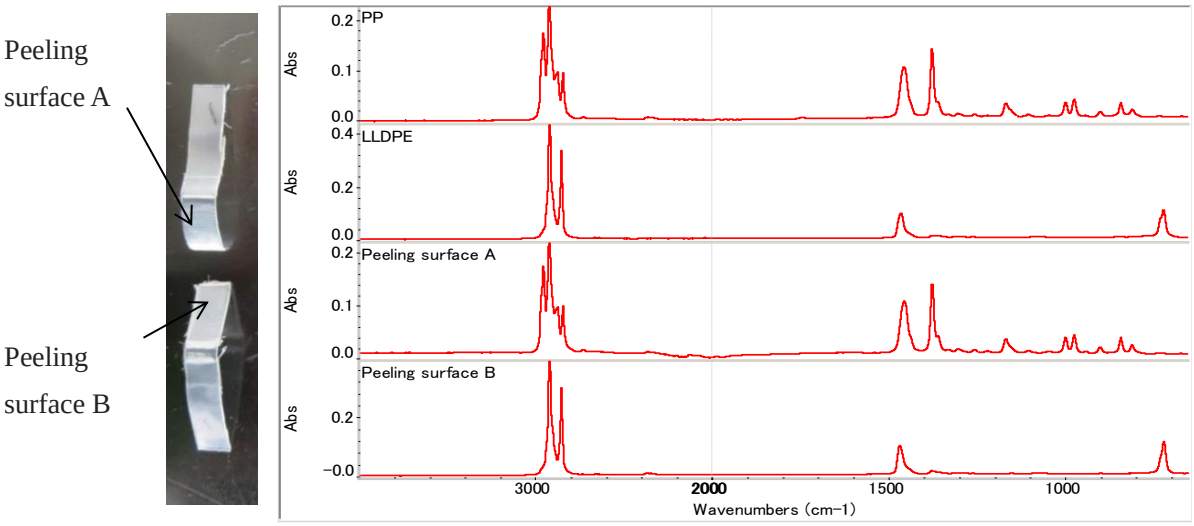

Figure 9.　FT-IR spectra of peeling surface (PP/LLDPE without PMPS).

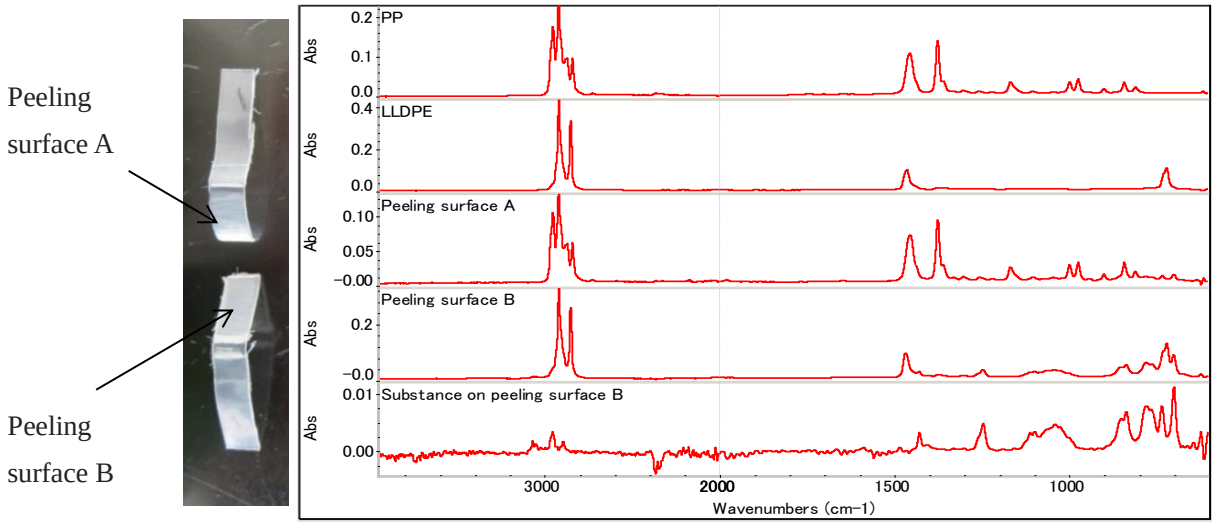

Figure 10. FT-IR spectra of peeling surface (PP/LLDPE with PMPS).

LLDPE と PP の融着において、PMPS が LLDPE 側に存在することが分かった。よって、PP に対して予め PMPS を溶融混練によりブレンドしたサンプル PP/15wt%PMPS を調製し、これを用いてフィルムの熱融着を行なった。
また、240 秒、420 秒での融着では PE 層が押し出されているように見えたため、融着時間を 60 秒、120 秒とした。
剥離エネルギーは、式 (1) を用いて算出した。算出した剥離エネルギーを Table 4、Figure 11 に示す。

$$P\ (\mathrm{J/cm^2}) = \Sigma \frac{F\ (\mathrm{N}) \times S\ (\mathrm{mm})}{A\ (\mathrm{cm^2})} \qquad (1)$$

P : Peeling energy, F : Force (N), S : Stroke of chacking, A : Area of cross section ($\mathrm{cm^2}$)

Table 4. Results of peeling test

Sample	Sealing time (sec)	Peeling energy ($\mathrm{J/cm^2}$)
PP	60	11.0±0.8
	120	24.0±3.0
PP/15wt%PMPS	60	46.6±2.7
	120	65.7±3.4

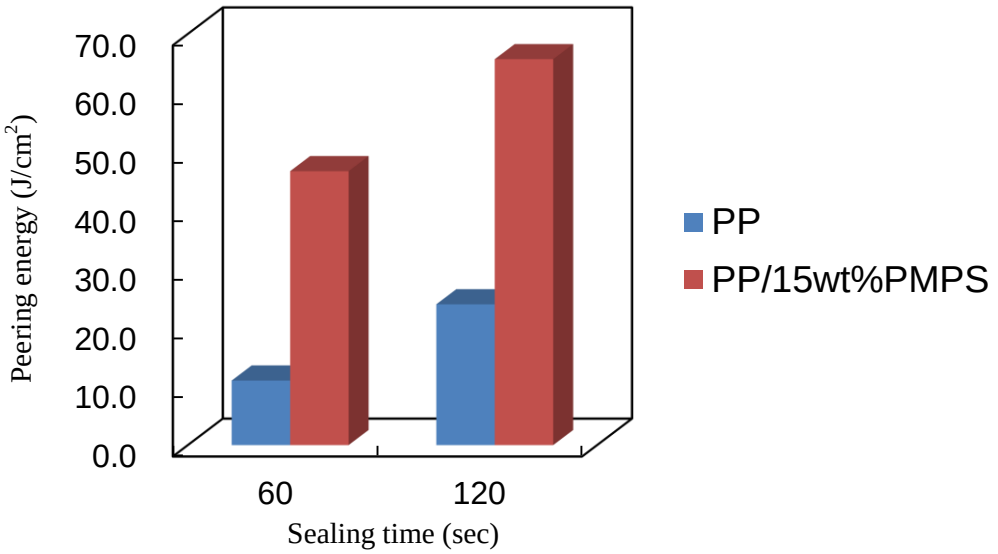

Figure 11. Peeling energy of PP and PP/15wt%PMPS.

剥離試験の結果、PP と LLDPE の融着において、融着時間を長くすることで融着強度が向上した。また、PP へ PMPS をブレンドした PP/15wt%PMPS を用いることで、融着強度が大きく向上した。PMPS のブレンドによって、LLDPE と PP の融着強度を向上させることが可能であることが分かった。PP 中に含まれる PMPS が PP の非晶部の分子運動性を高め、さらに LLDPE へと移行する際に、LLDPE の分子鎖と PP の分子鎖の絡み合いを促進させたと考えられる。

4. 結論

PP と PE の熱融着において、PMPS を塗布した場合においても HDPE や LDPE よりも LLDPE との融着強度が高いことが示された。
また、PP へ PMPS をブレンドすることによって、短時間の融着時間においても PP と LLDPE の融着強度が大きく向上した。PP 中にブレンドされた PMPS が PP の非晶部の分子運動性を高めたことによって、LLDPE 分子鎖と多くの絡み合いを形成したと考えられる。

5. 参考文献

[1] K. A. Chaffin, J. S. Knutsen, P. Brant, F. S. Bates, *Science* **2000**, *288*, 2187-2190.
[2] M. Yamaguchi, *J. App. Polym. Sci* . **1998**, *70*, 457-463.
[3] K. Tokumitsu, M. Yamada, M. Nakamura, K. Kobori, *J. Appl. Polym. Sci.* **2012**, *126*, E188-E194.
[4] Katsuhisa, T. A. Iguchi, S. Nakamura, M. Yamada, M. Nakamura, K. Kobori, *J. Appl. Polym. Sci.* **2012**, *126*, 403-409.
[5] 今里ふくみ：修士論文 滋賀県立大学 (**2010**)
[6] 徳満 勝久, 次世代ポリオレフィン総合研究 **2014**, *8*, 92-96.

6. 謝辞

本副テーマ研究を遂行するにあたり、終始暖かくご指導、ご鞭撻を頂きました滋賀県大学 工学部 材料科学科 有機複合材料研究室 徳満勝久教授に心より感謝申し上げます。
また、貴重なご指導とご助言、暖かいお言葉を頂きました同研究室 竹下宏樹 准教授、山下義裕講師、駒井茂様に心より感謝申し上げます。
実験を行なうにあたり、多くのご指導を頂きました同研究室の学生の皆様に心より感謝申し上げます。

平成 28 年 3 月 24 日

北陸先端科学技術大学院大学
マテリアルサイエンス研究科
永井健